RISK NEUTRAL AND RISK AVERSE APPROACHES TO MULTISTAGE STOCHASTIC PROGRAMMING WITH APPLICATIONS TO HYDROTHERMAL OPERATION PLANNING PROBLEMS

A Thesis
Presented to
The Academic Faculty

by

Wajdi Tekaya

In Partial Fulfillment
of the Requirements for the Degree
Doctor of Philosophy in the
School of Industrial and Systems Engineering

Georgia Institute of Technology
May 2013

RISK NEUTRAL AND RISK AVERSE APPROACHES TO MULTISTAGE STOCHASTIC PROGRAMMING WITH APPLICATIONS TO HYDROTHERMAL OPERATION PLANNING PROBLEMS

Approved by:

Professor Alexander Shapiro, Advisor
School of Industrial and Systems Engineering
Georgia Institute of Technology

Professor Arkadi Nemirovski
School of Industrial and Systems Engineering
Georgia Institute of Technology

Professor Shabbir Ahmed
School of Industrial and Systems Engineering
Georgia Institute of Technology

Professor Santiago Grijalva
School of Electrical and Computer Engineering
Georgia Institute of Technology

Professor Shijie Deng
School of Industrial and Systems Engineering
Georgia Institute of Technology

Date Approved: / /

DEDICATION

To my family

ACKNOWLEDGEMENTS

My most sincere and deepest gratitude goes to my advisor Prof. Alexander Shapiro. Without his continuous guidance, support and availability, this thesis would not exist. I learned a lot from his motivation, critical thinking and dedication for research and academic achievement. I owe him a debt of gratitude far beyond the scope of any words I can say here.

It is a great debt that I owe to all the professors that taught me at ISyE and those with whom I worked. I would like to thank Prof. Arkadi Nemirosvski for his numerous insightful comments, ideas and valuable advice. I'm grateful to Prof. Jim Dai and Prof. Shabbir Ahmed for the great classes, encouragements and advice. I would like to thank all the committee members for their time and valuable feedback.

I'm indebted to Vinod Cheriyan, Haiyue Yu and Ola Batarseh for their stimulating and helpful discussions and thought journeys. I would like to express special thanks to Wonki Kim, Min Kyu Sim and Camilo Ortiz Diaz for the great friendship and challenging squash games. I'm grateful to all my friends and colleagues at ISyE for their consideration and company. Thank you Chinmay Dubey, Tugce Isik, Abraham Panjikaran, Fangfang Xiao and many others whom I shouldn't have forgotten.

I would like to express my sincere thanks to my family. Without their support and encouragements through the good and bad times, I would not be at this point. My friends back home were always of a great advice and company. Many thanks go to Brahim, Ghazi, Khaled, Majdi, Mehdi and many others whom I shouldn't have forgotten.

I would like to thank ONS for their financial support. The numerous fruitful discussions with Joari Paulo da Costa and Murilo Pereira Soares were crucial for the

success of this research project.

TABLE OF CONTENTS

LIST OF TABLES

LIST OF FIGURES

SUMMARY

The main objective of this thesis is to investigate risk neutral and risk averse approaches to multistage stochastic programming with applications to hydrothermal operation planning problems. The purpose of hydrothermal system operation planning is to define an operation strategy which, for each stage of the planning period, given the system state at the beginning of the stage, produces generation targets for each plant. This problem can be formulated as a large scale multistage stochastic linear programming problem. The energy rationing that took place in Brazil in the period 2001/2002 raised the question of whether a policy that is based on a criterion of minimizing the expected cost (i.e. risk neutral approach) is a valid one when it comes to meet the day-to-day supply requirements and taking into account severe weather conditions that may occur. The risk averse methodology provides a suitable framework to remedy these deficiencies. This thesis attempts to provide a better understanding of the risk averse methodology from the practice perspective and suggests further possible alternatives using robust optimization techniques. The questions investigated and the contributions of this thesis are as follows.

First, we suggest a multiplicative autoregressive time series model for the energy inflows that can be embedded into the optimization problem that we investigate. Then, computational aspects related to the stochastic dual dynamic programming (SDDP) algorithm are discussed. We investigate the stopping criteria of the algorithm and provide a framework for assessing the quality of the policy. The SDDP method works reasonably well when the number of state variables is relatively small while the number of stages can be large. However, as the number of state variables increases the

convergence of the SDDP algorithm can become very slow. Afterwards, performance improvement techniques of the algorithm are discussed. We suggest a subroutine to eliminate the redundant cutting planes in the future cost functions description which allows a considerable speed up factor. Also, a design using high performance computing techniques is discussed. Moreover, an analysis of the obtained policy is outlined with focus on specific aspects of the long term operation planning problem. In the risk neutral framework, extreme events can occur and might cause considerable social costs. These costs can translate into blackouts or forced rationing similarly to what happened in 2001/2002 crisis. Finally, issues related to variability of the SAA problems and sensitivity to initial conditions are studied. No significant variability of the SAA problems is observed.

Second, we analyze the risk averse approach and its application to the hydrothermal operation planning problem. A review of the methodology is suggested and a generic description of the SDDP method for coherent risk measures is presented. A detailed study of the risk averse policy is outlined for the hydrothermal operation planning problem using different risk measures. The adaptive risk averse approach is discussed under two different perspectives: one through the mean-AV@R and the other through the mean-upper-semideviation risk measures. Computational aspects for the hydrothermal system operation planning problem of the Brazilian interconnected power system are discussed and the contributions of the risk averse methodology when compared to the risk neutral approach are presented. We have seen that the risk averse approach ensures a reduction in the high quantile values of the individual stage costs. This protection comes with an increase of the average policy value - the price of risk aversion. Furthermore, both of the risk averse approaches come with practically no extra computational effort and, similarly to the risk neutral method, there was no significant variability of the SAA problems.

Finally, a methodology that combines robust and stochastic programming approaches is investigated. In many situations, such as the operation planning problem, the involved uncertain parameters can be naturally divided into two groups, for one group the robust approach makes sense while for the other the stochastic programming approach is more appropriate. The basic ideas are discussed in the multistage setting and a formulation with the corresponding dynamic programming equations is presented. A variant of the SDDP algorithm for solving this class of problems is suggested. The contributions of this methodology are illustrated with computational experiments of the hydrothermal operation planning problem and a comparison with the risk neutral and risk averse approaches is presented. The worst-case-expectation approach constructs a policy that is less sensitive to unexpected demand increase with a reasonable loss on average when compared to the risk neutral method. Also, we comp are the suggested method with a risk averse approach based on coherent risk measures. On the one hand, the idea behind the risk averse method is to allow a trade off between loss on average and immunity against unexpected extreme scenarios. On the other hand, the worst-case-expectation approach consists in a trade off between a loss on average and immunity against unanticipated demand increase. In some sense, there is a certain equivalence between the policies constructed using each of these methods.

CHAPTER I

INTRODUCTION

More than half a century ago, Beale [3] and Dantzig [10] discussed the notion of uncertainty in linear optimization problems. Since that time, a significant amount of literature has been written on that topic. This research comes within this general framework with a focus on the practical aspects of the methodology. In this thesis we investigate risk neutral and risk averse approaches for multistage stochastic programming with applications to hydrothermal operation planning problems.

This introduction is organized as follows. In section 1.1, we present the motivation behind this research. In the following section, a brief overview of the existing literature is presented. Finally, in section 1.3, we suggest an outline of this thesis.

1.1 Motivation

The Brazilian power system is a large scale system planned and operated to achieve cost reduction and reliability in power supply. By December 2010, about eight-tenths of Brazil's power came from hydroelectric plants.

On May 2001, the Brazilian government imposed emergency rationing for eight months after a dry rainy season that left water levels of hydroelectricity reservoirs at record lows. At that time, about nine-tenths of Brazil's power came from hydroelectric plants. During the rationing period, the population was forced to reduce consumption by an average of 20 percent. This decision had a negative impact on the economy (cf [23]: "Economic growth cooled from a projected 4 percent to just 2.5 percent last year. Consumers stopped buying new appliances and electronic goods, and manufacturers cut back production."), worsened social tensions and put in front regional hostilities (cf. [25]). This incident raised several questions about the possible solutions to this

problem. Methodological aspects of the power system operation planning were among the points that were questioned. Up to this point, the standard risk neutral approach (i.e. minimizing costs on average) was implemented for planning of the Brazilian power system.

The energy rationing that took place in Brazil in the period 2001/2002 raised the question of whether a policy that is based on a criterion of minimizing the expected cost is a valid one when it comes to meet the day-to-day supply requirements and taking into account severe weather conditions that may occur. The risk averse methodology provides a suitable framework to remedy these deficiencies. As a consequence, a shift towards a risk averse approach is underway, so as to enforce the continuity of load supply. This thesis attempts to provide a better understanding of the risk averse methodology from the practice perspective and suggests further possible alternatives.

1.2 Related research

In this section, we give a brief overview of the related works in the literature.

On the modelling level, the hydrothermal operation planning problem was discussed in early works (e.g. [19],[38]).

As far as two stage problems are concerned, Wets discussed in [42] properties of the two stage linear problems where only the right hand side is random and provided an equivalent convex problem formulation. In [40] and [41], Walkup and Wets presented further properties and the results are extended to the general case where the second stage data and the first stage objective are random. On the algorithmic level, the cutting plane method for convex problems was first introduced by Kelley [15]. Benders suggested, in [5], a cutting plane algorithm to solve a general class of problems with mixed variable types. In the two stage problems setting, Van Slyke and Wets suggested another cutting plane based approach in [39]. Birge and Louveaux

proposed an extension with multiple cuts strategy in [8]. An extensive literature exists related to the class of decomposition methods. Birge and Louveaux [7] and Ruszczyski [26] give an overview of such methods and their related bibliography.

Among the initial contributions to multistage problems, we can mention Louveaux's work in [17] where he suggested an algorithm for solving multistage problems with quadratic objective function and linear inequality constraints.The key idea is the equivalence of the extended problem to a nested sequence of piecewise quadratic programs. Birge suggested in [6], an extension to the multistage problems for the L-shaped method suggested by Van Slyke and Wets in [39].

The SDDP algorithm was introduced in [19], [20] and became a popular method for scheduling of hydro-thermal electricity systems. Analysis and several extensions for this algorithm were suggested in literature (cf. [9],[11],[16]). The SDDP method utilizes convexity of linear multistage stochastic programs and stagewise independence of the stochastic data process. It is based on building piecewise linear outer approximations of the cost-to-go functions and can be viewed as a variant of the approximate dynamic programming techniques. The distinguishing feature of the SDDP approach is random sampling from the set of scenarios in the forward step of the algorithm. Almost sure convergence of the SDDP algorithm was proved in Philpott and Guan [22] under mild regularity conditions (see also [34, Proposition 3.1]).

Several risk averse approaches to multistage stochastic programming were suggested in recent literature. Eichhorn and Römisch [12] developed techniques based on the so-called polyhedral risk measures. This approach was extended further in Guigues and Römisch [13] to incorporate the SDDP method in order to approximate the corresponding risk averse recourse functions. Theoretical foundations for a risk averse approach based on conditional risk mappings were developed in Ruszczyński and Shapiro [27] (see also [30, Chapter 6]). For risk measures given by convex combinations of the expectation and Average Value-at-Risk, it was shown in [34] how

to incorporate this approach into the SDDP algorithm with a little additional effort. This was implemented in an extensive numerical study in Philpott and de Matos [21].

1.3 Overview of the thesis

This thesis is organized as follows. In Chapter 2, the hydrothermal operation planning problem is presented along with the numerical instance that we consider. Furthermore, we suggest a first order autoregressive multiplicative time series model for the energy inflows that will be used throughout this thesis.

Chapter 3 tackles the risk neutral approach. First, a statement of the risk neutral approach for the multistage stochastic linear programming problem in the general setting along with the considered assumptions are outlined. Methodological aspects are also suggested. Second, a generic description of the SDDP algorithm in the risk neutral framework is presented. Third, several aspects of the stopping criteria are discussed. Then, some performance improvement techniques of the algorithm are suggested. Finally, an analysis of the constructed solution (i.e. policy) is presented along with a study of the variability of the Sample Average Approximation problems and the sensitivity to the initial conditions.

In chapter 4, we investigate the risk averse methodology. A brief overview of some mathematical notions such as coherent and conditional risk mappings is presented. Then, basic assumptions and the general problem statement are put forth. An overview of the different formulations for linear multistage stochastic problems with coherent risk measures is given. A generic description of the SDDP algorithm to solve such problems is presented. Some examples of risk measures are considered, namely the mean-AV@R and the mean-upper-semideviation risk measures. An extensive numerical study of the risk averse methodology is suggested and the contributions of the approach when compared with the classical risk neutral method are outlined. The computational results are illustrated on the long term hydrothermal operation

planning problem for the Brazilian power system.

A methodology that combines robust and stochastic programming approaches is investigated in chapter 5. First, the general problem statement along with the considered assumptions is presented. Second, a variant of the SDDP method is to solve such class of problem is discussed. Finally, this framework is illustrated through an extensive numerical study on the long term operation planning problem for the Brazilian power system. A comparison with the risk neutral method and the risk averse approach is performed.

CHAPTER II

HYDROTHERMAL OPERATION PLANNING PROBLEM

2.1 Introduction

The purpose of this chapter is to introduce the long term hydrothermal operation planning problem and to suggest a time series model for the energy inflows that will be used throughout this thesis. The aggregate system model that we consider for the Brazilian power system was proposed in [2]. The hydrothermal operation planning problem was discussed in early works such that [19] and [38]. Several modelling aspects related to physical constraints on variables like limits on the capacity of the equivalent reservoir, hydro and thermal generation, transmission capacity were discussed in [38] and [19]. The content of this chapter is available in [36] and [31].

This chapter is organized as follows. Section 2.2 contains a brief introduction of the Brazilian power system and a presentation of the Hydrothermal operation planning problem along its mathematical formulation. In section 2.3, an analysis of historical data was performed and a multiplicative first order time series model for the energy inflows is suggested and validated. Finally, in section 2.4, numerical data of the considered instance and computations parameters are presented.

2.2 Hydrothermal operation planning problem

2.2.1 Presentation of the Brazilian power system

The Brazilian interconnected power system is a large scale system planned and constructed considering the integrated utilization of the generation and transmission resources of all agents and the use of inter-regional energy interchanges, in order to achieve cost reduction and reliability in power supply.

The main transmission grid is operated and expanded in order to achieve safety

of supply and system optimization. The inter-regional and inter-basin transmission links allow interchanges of large blocks of energy between areas making it possible to take advantage of the hydrological diversity between river basins.

As of December 2010, the installed capacity of hydro plants corresponds to 79.1% total installed capacity, but its relative position should diminish to 71.0% in 2020.

2.2.2 Problem statement

The purpose of hydrothermal system operation planning is to define an operation strategy which, for each stage of the planning period, given the system state at the beginning of the stage, produces generation targets for each plant. The usual objective is to minimize the expected value of the total cost along the planning period, so as to meet requirements on the continuity of energy supply subject to feasibility constraints. The operation costs comprise fuel costs, purchases from neighboring systems and penalties for failure in load supply.

The hydrothermal operation planning problem is a decision problem under uncertainty because of unknown variables such as future inflows, demand, fuel costs and equipment availability. It is a multistage optimization problem where in the Brazilian case it is usual to consider a planning horizon of 5 years on a monthly basis.

In summary, the Brazilian hydro power operation planning problem is a multistage (60 stages) and large scale (more than 200 power plants, of which 141 are hydro plants), stochastic optimization problem. This setting far exceeds the computer capacity to solve it with adequate accuracy in reasonable time frame. The standard approach to solve this problem is to resort to a chain of models considering long, mid and short term planning horizon in order to be able to tackle the problem in a reasonable time. For the long-term problem, it is usual to consider an approximate representation of the system, the so-called aggregate system model, a composite representation of a multireservoir hydroelectric power system, proposed by [2], that

aggregates all hydro power plants belonging to a homogeneous hydrological region into a single equivalent energy reservoir, and solves the resulting problem.

For the Brazilian interconnected power system, the aggregate representation is composed of four energy equivalent reservoirs, one in each one of the four interconnected main regions: Southeast (SE), South (S), Northeast (NE) and North (N). The resulting policy obtained with the aggregate representation can then be further refined, so as to provide decisions for each of the hydro and thermal power plants. This can be done by solving the mid-term problem, considering a planning horizon up to a few months and individual representation of the hydro plants with boundary conditions (the expected cost-to-go functions) given by the solution of the long-term problem. This is the approach nowadays used for solving the long and mid term hydrothermal power planning in the Brazilian interconnected power system.

Considering the aggregate representation of the hydroplants, the energy conservation equation for each equivalent energy reservoir $n = 1, \ldots, 4$ can be written as

$$\mathrm{SE}_{t,n} = \mathrm{SE}_{t-1,n} + \mathrm{CE}_{t,n} - \mathrm{GH}_{t,n} - \mathrm{SP}_{t,n}. \tag{1}$$

That is, the stored energy (SE) at the end of each stage is equal to the initial stored energy plus a random energy inflow (CE) minus total hydro generated energy (GH) and losses (SP) due to spillage, evaporation, etc.

At each stage, the load L has to be met by the total hydro, the sum of all thermal generation belonging to system n, given by the set NT_n, and the net interconnection energy flow (NF) to each subsystem. In other words, the energy balance equation for system n is

$$\mathrm{GH}_{t,n} + \sum_{j \in \mathrm{NT}_n} \mathrm{GT}_{t,j} + \mathrm{NF}_{t,n} = L_{t,n}. \tag{2}$$

where (GT) denotes the thermal generation. Note that this equation is always feasible (i.e., the problem has complete recourse) due to the inclusion of a dummy thermal plant with generation capacity equal to the demand and operation cost that reflects

the social cost of not meeting the energy demand (deficit cost). The hydroelectric generation costs are assumed to be zero. Physical constraints on variables like limits on the capacity of the equivalent reservoir, hydro and thermal generation, transmission capacity and so on are taken into account. More details can be found in [38] and [19].

2.2.3 Mathematical formulation

The risk neutral version of the operation planning problem can be formulated as a (linear) large scale multistage stochastic programming problems which in a generic form (nested formulation) can be written as

$$\underset{\substack{A_1x_1=b_1\\ x_1\geq 0}}{\text{Min}}\; c_1^{\intercal}x_1 + \mathbb{E}\left[\min_{\substack{B_2x_1+A_2x_2=b_2\\ x_2\geq 0}} c_2^{\intercal}x_2 + \mathbb{E}_{|\xi_{[2]}}\Big[\cdots + \mathbb{E}_{|\xi_{[T-1]}}\Big[\min_{\substack{B_Tx_{T-1}+A_Tx_T=b_T\\ x_T\geq 0}} c_T^{\intercal}x_T\Big]\Big]\right] \tag{3}$$

In general setting, components of vectors c_t, b_t and matrices A_t, B_t can be modeled as random variables forming the stochastic data process $\xi_t = (c_t, A_t, B_t, b_t)$, $t = 2, ..., T$, with $\xi_1 = (c_1, A_1, b_1)$ being deterministic. In the particular case of the operation planning problem, only the right hand side (b_t) , $t = 2, ..., T$ is considered random. By $\xi_{[t]} = (\xi_1, ..., \xi_t)$ we denote the history of the data process up to time t.

In terms of the previous section notation, the problem translates to:

$$x_t = (\text{SE}, \text{GH}, \text{GT}, \text{SP}, \text{NF})_t^{\top}, \;\; b_t = (\text{CE}, \text{L})_t^{\top}, \;\; c_t = (0, 0, \text{CT}, 0, 0)_t^{\top},$$

$$A_t = \begin{pmatrix} I & I & 0 & I & 0 \\ 0 & I & \Delta & 0 & I \end{pmatrix}, \;\; B_t = \begin{pmatrix} -I & 0 & 0 & 0 & 0 \\ 0 & 0 & 0 & 0 & 0 \end{pmatrix},$$

where $\Delta = \{\delta_{n,j} = 1 \text{ for all } j \in \text{NT}_n \text{ and zero else}\}$, I and 0 are identity and null matrices, respectively, of appropriate dimensions and the components of CT are the unit operation cost of each thermal plant and penalty for failure in load supply. Note that hydroelectric generation costs are assumed to be zero.

Table 1 summarizes the different dimensions of the problem that we consider in this thesis. Note that the effective dimension of the variables needed at stage t from stage $t-1$ is 8 when the first order autoregressive time series model suggested in the following section is used. Also, we slightly abuse the notation in this counts to include in (GT) and (L) the inequalities for the capacity constraints.

Table 1: Problem dimensions

Variable/data	Dimension
SE (V)	4
GH (V)	4
GT (V)	95
SP (V)	4
NF (V)	10
CE (D)	4
L (D)	4
Capacity constraints	152

2.3 Time series model for the energy inflows

In this section, we present a multiplicative first order time series model for the energy inflows that will be used throughout this thesis.

2.3.1 The historical data

The historical data is composed of 79 observations of the natural monthly energy inflow (from year 1931 to 2009) for each of the four systems. Let X_t, $t = 1, \ldots, 948$ denote a time series of monthly inflows for one of the regions. Figure 1 shows the histograms for the historical observations for each of the 4 systems in the aggregated model. X_t is non negative and highly skewed to the right for each of the 4 systems. This observation motivates considering $Y_t = \log(X_t)$ for analysis in order to obtain a more symmetric distribution.

Figure 2 shows the histograms for Y_t - the logarithm of historical observations for each of the 4 systems. After taking the logarithm, the histograms become more

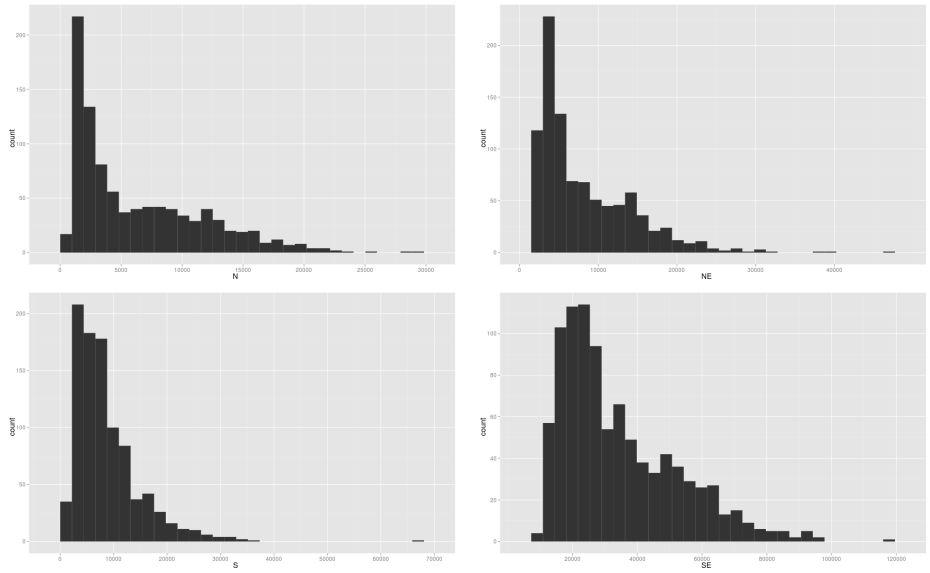

Figure 1: Histograms of the historical observations

symmetric.

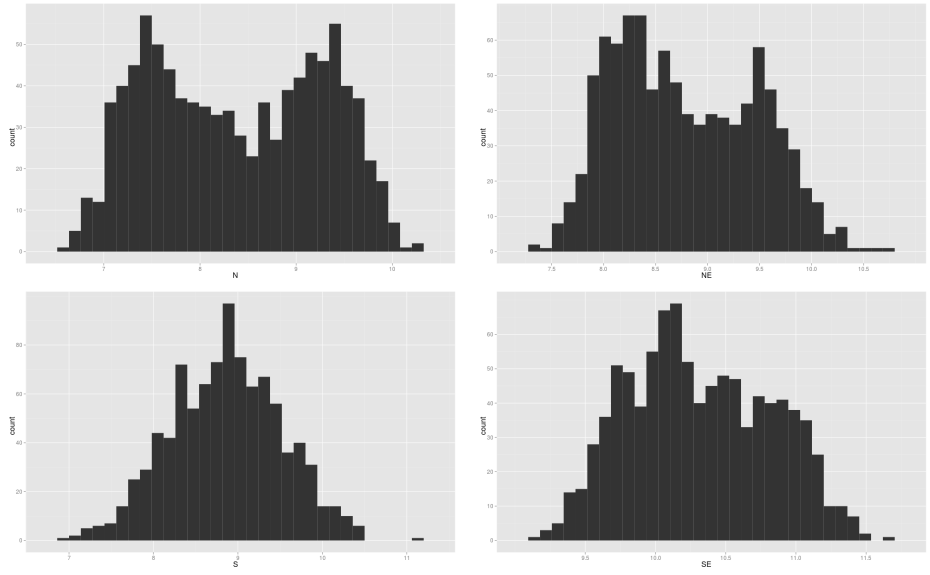

Figure 2: Histograms of the log-observations

Figure 3 shows monthly box plots of regions inflows. It could be seen that inflows of the (N), (NE) and (SE) systems have a clear seasonal behavior, while for the (S) system it is not obvious.

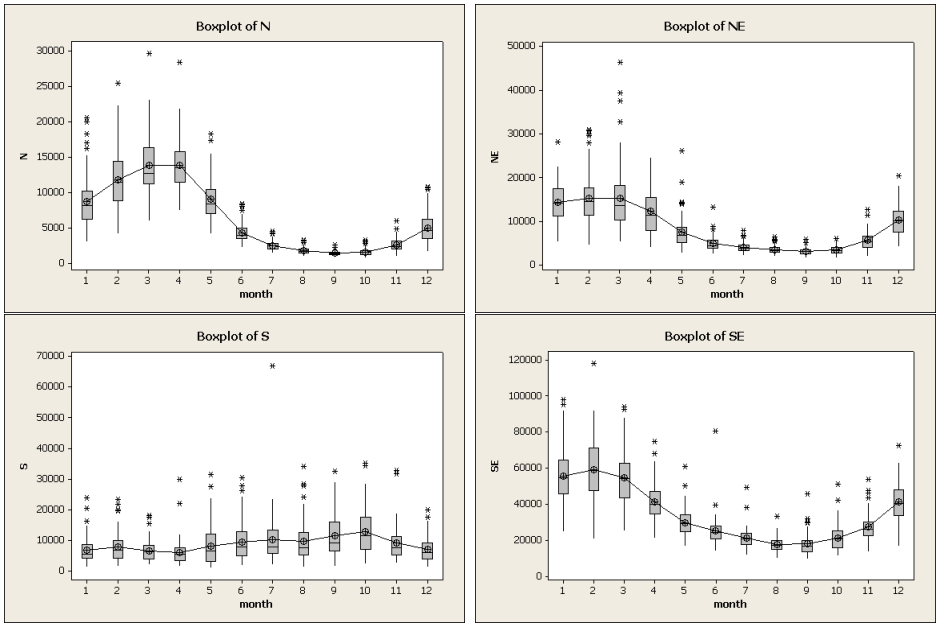

Figure 3: Box plot of the inflows for each system

2.3.2 Time series analysis

As an example we give below analysis of the time series X_t of the (SE) data points. Analysis of the other 3 regions were carried out in a similar way. Figure 4 shows box plots of monthly inflows of the log-observations $Y_t = \log(X_t)$ of (SE) inflows. One can clearly note the seasonal behavior of the series, suggesting that a periodic monthly model could be a reasonable framework for this series.

Let $\hat{\mu}_t = \hat{\mu}_{t+12}$ be the monthly averages of Y_t and $Z_t = Y_t - \hat{\mu}_t$ be the corresponding residuals. Figure 5 shows the partial autocorrelation of the Z_t time series. High value at lag 1 and insignificant values for larger lags suggest the first order $AR(1)$ autoregressive time series model for Z_t:

$$Z_t = \alpha + \phi Z_{t-1} + \epsilon_t. \tag{4}$$

For the adjusted model, the estimate for the constant term α resulted is highly insignificant and could be removed from the model. This is not surprising since values Z_t by themselves are already residuals. Trying second order $AR(2)$ model for Z_t didn't

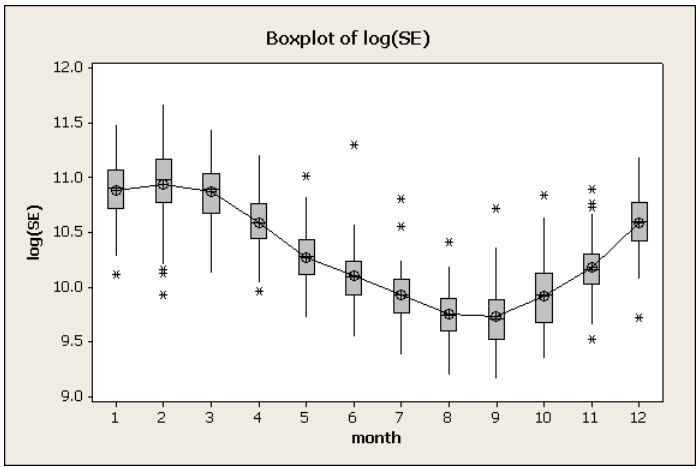

Figure 4: Box plot of the log-observations of (SE) inflows

give a significant improvement of the fit.

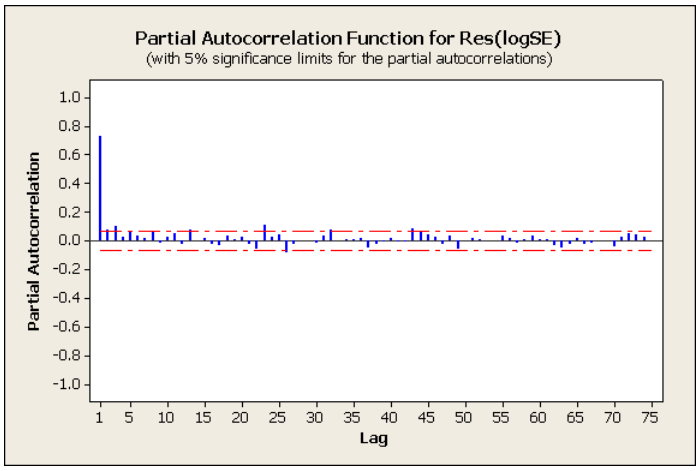

Figure 5: Partial autocorrelation of the residuals of the log-observations of (SE) inflows

Similar results were obtained for the other three subsystems. Therefore, we consider AR(1) model for all subsystems in the subsequent analysis.

2.3.3 Model description

The analysis of the previous section suggests the following model for the time series Y_t for a given month

$$Y_t - \hat{\mu}_t = \phi(Y_{t-1} - \hat{\mu}_{t-1}) + \epsilon_t, \tag{5}$$

where ϵ_t is iid sequence having normal distribution $N(0, \sigma^2)$. For the original times series X_t this gives

$$X_t = e^{\epsilon_t} e^{\hat{\mu}_t - \phi\hat{\mu}_{t-1}} X_{t-1}^{\phi}. \tag{6}$$

Unfortunately this model is not linear in X_t and would result in a nonlinear multistage program. Therefore we proceed by using the following (first order) approximation of the function $y = x^{\phi}$ at $e^{\hat{\mu}_{t-1}}$

$$x^{\phi} \approx (e^{\hat{\mu}_{t-1}})^{\phi} + \phi(e^{\hat{\mu}_{t-1}})^{\phi-1}(x - e^{\hat{\mu}_{t-1}}),$$

which leads to the following approximation of the model (6)

$$X_t = e^{\epsilon_t} \left[e^{\hat{\mu}_t} + \phi e^{\hat{\mu}_t - \hat{\mu}_{t-1}} (X_{t-1} - e^{\hat{\mu}_{t-1}}) \right]. \tag{7}$$

We allow, further, the constant ϕ to depend on the month, and hence to consider the following time series model

$$X_t = e^{\epsilon_t} \left[e^{\hat{\mu}_t} + \gamma_t e^{\hat{\mu}_t - \hat{\mu}_{t-1}} (X_{t-1} - e^{\hat{\mu}_{t-1}}) \right] \tag{8}$$

with $\gamma_t = \gamma_{t+12}$.

We estimate the parameters of model (8) directly from the data.

- Denote by $R_t = \frac{X_t - e^{\hat{\mu}_t}}{e^{\hat{\mu}_t}}$. If the error term ϵ_t is set to zero, i.e., the multiplicative error term e^{ϵ_t} is set to one, (8) can be written as:

  $$R_t = \gamma_t R_{t-1} \tag{9}$$

  For each month, we perform a least square fit to the R_t sequence to obtain the monthly values for γ_t, assuming that $\gamma_t = \gamma_{t+12}$.

- The errors ϵ_t are modelled as a component of multivariate normal distribution $N(0, \widehat{\Sigma}_t)$, where $\widehat{\Sigma}_t$ is the sample covariance matrix for

  $$\log\left(\frac{X_t}{[e^{\hat{\mu}_t} + \gamma_t e^{\hat{\mu}_t - \hat{\mu}_{t-1}} (X_{t-1} - e^{\hat{\mu}_{t-1}})]} \right)$$

  on a *monthly basis*, i.e., $\widehat{\Sigma}_{t+12} = \widehat{\Sigma}_t$.

2.3.4 Model validation

In this experiment we compute the one step ahead predictions and compare the obtained results against real realizations for the past 2 years of the available historical data. At each time step we compute the predicted value $\widehat{X}_t$ using the corresponding realization X_{t-1}, from the historical values, by employing the constructed model

$$\widehat{X}_t = e^{\hat{\mu}_t} + \gamma_t e^{\hat{\mu}_t - \hat{\mu}_{t-1}}(X_{t-1} - e^{\hat{\mu}_{t-1}}). \tag{10}$$

Consequently we compare the predicted value $\widehat{X}_t$ with the real realization X_t. Figure 6 shows the obtained results for the past 2 years of the available historical data. The model exhibits a good fit for systems (N), (NE) and (SE). For system (S) the model gives sometimes lower peaks than the real realizations.

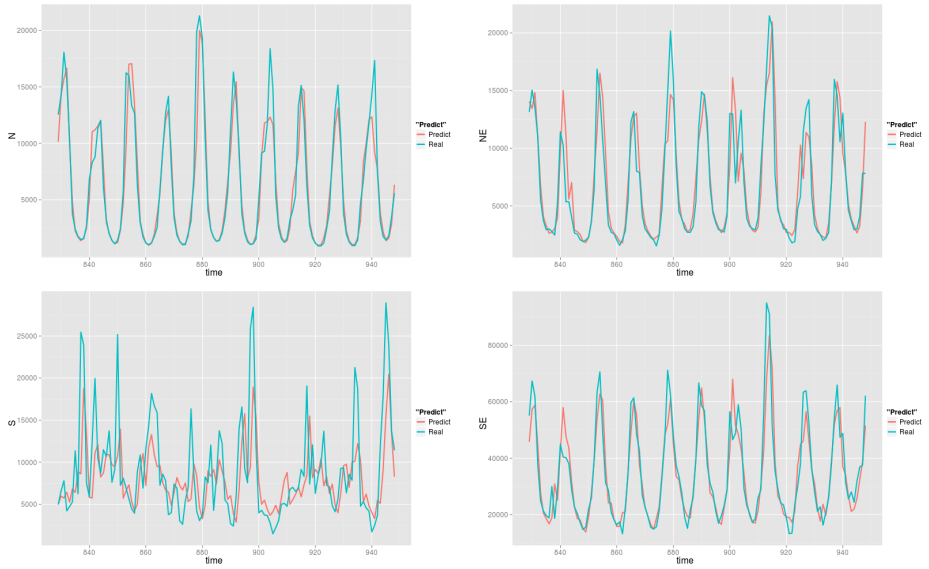

Figure 6: One step ahead prediction

We generate 200 scenarios using the model (8). Each scenario contains 948 points (similar length as the historical data). For each scenario, the mean and standard deviation is computed for each one of the 4 systems starting from the observation 121. We start from observation 121 to eliminate the initial value effect. The obtained

values are then compared to the historical data values. Figures 7 and 8 show the box plots for the obtained means against the historical data realizations (red segments).

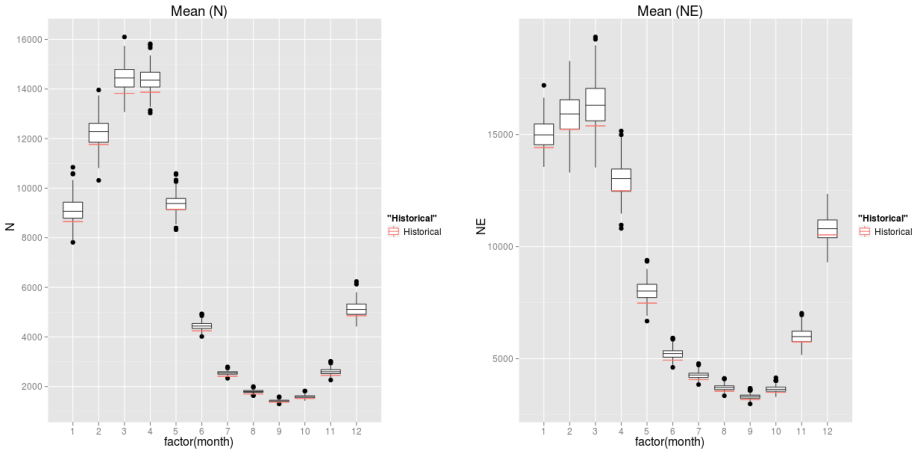

Figure 7: Monthly means boxplot: (N) and (NE)

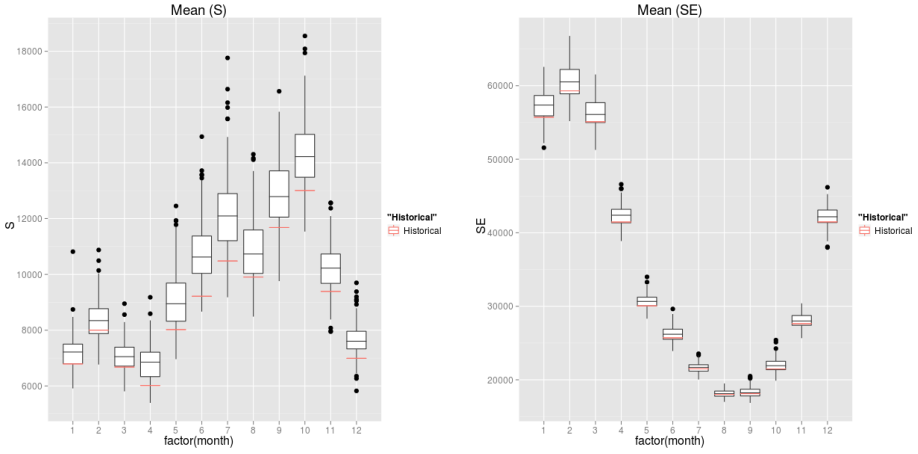

Figure 8: Monthly means boxplot: (S) and (SE)

The average values, obtained for all systems, are relatively close to the historical values in most of the cases.

Figures 9 and 10 illustrate the box plots for standard deviations against the historical data realizations (red segments). The suggested model also gives a reasonably good fit to variability when compared to the historical data values.

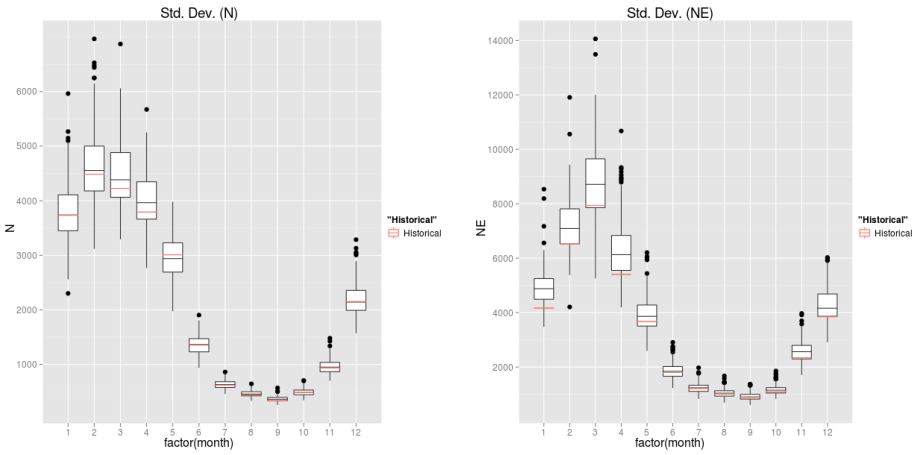

Figure 9: Monthly standard deviations boxplot: (N) and (NE)

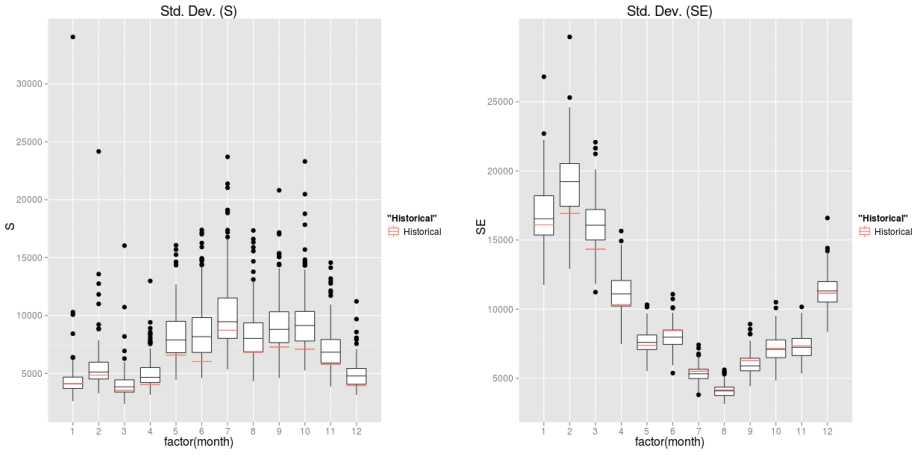

Figure 10: Monthly standard deviations boxplot: (S) and (SE)

2.4 Case study description

The numerical experiments in this thesis are carried out considering instances of multi-stage linear stochastic problems based on an aggregate representation of the Brazilian Interconnected Power System long-term operation planning problem, as of January 2012, which can be represented by a graph with four generation nodes - comprising sub-systems Southeast (SE), South (S), Northeast (NE) and North (N) – and one (Imperatriz, IM) transshipment node (cf. Figure 11).

The load of each area must be supplied by local hydro and thermal plants or

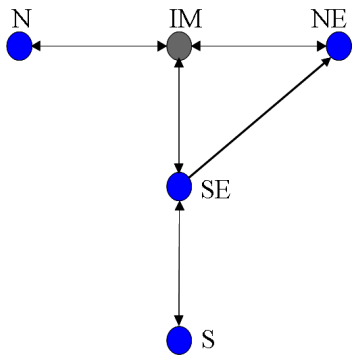

Figure 11: Case-study interconnected power system

Table 2: Deficit costs and depths

	% of total load curtailment	Cost
1	0 – 5	1206.38
2	5 – 10	2602.56
3	10 – 20	5439.12
4	20 – 100	6180.26

by power flows among the interconnected areas. A slack thermal generator of high cost that increases with the amount of load curtailment accounts for load shortage at each area (cf. Table 2). Interconnection limits between areas may differ depending on the flow direction, as shown in Table 3. The energy balance equation for each sub-system has to be satisfied for each stage and scenario. There are bounds on stored and generated energy for each sub-system aggregate reservoir and on thermal generations.

The long-term planning horizon for the Brazilian case comprises 60 months. In

Table 3: Interconnection limits between systems

		to				
		SE	S	NE	N	IM
from	SE	–	7700	1000	0	4000
	S	5670	–	0	0	0
	NE	600	0	–	0	3000
	N	0	0	0	–	–
	IM	2854	0	3960	3149	–

order to obtain a reasonable cost-to-go function that represents the continuity of the energy supply after these first 60 stages, 60 more stages are added to the problem and consider a zero cost-to-go function at the end of the 120^{th} stage. There is no definitive answer for how to remedy the end of horizon effect. Empirically, we could observe that with 60 additional stages this effect is dissipated (cf. section 3.7.3). The first stage corresponds to January. Hence, the objective function of the planning problem is to minimize the expected cost of the operation along the 120 months planning horizon, while supplying the area loads and obeying technical constraints. In the case of the risk neutral approach, the objective function is the minimization of the expected value along the planning horizon of thermal generation costs plus a penalty term that reflects energy shortage.

The case's general data, such as hydro and thermal plant data and interconnection capacities were taken as static values through time. The demand for each system and the energy inflows in each reservoir were taken as time varying. The units for the energy inflows are in Mega Watts month (MWm) and the costs are in Brazilian real.

The algorithms presented in this thesis were implemented in C++ using GUROBI 5.0 solver. The sequential codes were run on 1 core of a quad-core Intel E5520 Xeons @ 2.26GHz, and 24GB RAM machine. The parallel codes were run using multiple core of the same machine.

The scenario tree (cf. 3.3) generated in the numerical experiments has 100 realizations per stage with the total number of scenarios $1 \times 100 \times \cdots \times 100 = 100^{119}$.

2.5 Conclusion

In this chapter, we introduced, in section 2.2, the Brazilian power system and presented the long term hydrothermal operation planning problem along its mathematical formulation. In section 2.3, historical data of the energy inflows was analyzed and

a multiplicative first order time series model for the energy inflows was suggested. Finally, numerical data of the instance that we consider in this thesis and computations parameters were presented.

CHAPTER III

RISK NEUTRAL APPROACH

3.1 Introduction

In this chapter we discuss the risk neutral approach to multistage linear stochastic programming problems based on the Stochastic Dual Dynamic Programming (SDDP) method. We give a general description of the algorithm and present computational studies related to the long term operation planning of the Brazilian interconnected power system. The SDDP algorithm was introduced in [19, 20]. It became a popular method for scheduling of hydro-thermal electricity systems. The method is based on building piecewise linear outer approximations of the cost-to-go functions and can be viewed as a variant of the approximate dynamic programming techniques. The distinguishing feature of the SDDP approach is random sampling from the set of scenarios in the forward step of the algorithm. Almost sure convergence of the SDDP algorithm was proved in [22] under mild regularity conditions (see also [34, Proposition 3.1]). However, little is known about rates of convergence and computational complexity of the SDDP method. In [34] and [36], the risk neutral SDDP method was analyzed. The first 2 sections of this chapter are along the same lines. The content of this chapter is available in [32] and [36].

This chapter is organized as follows. In section 3.2, we present the risk neutral formulation of multistage linear stochastic programming problems, the considered assumptions and the methodology that we follow. In the next section, the SDDP method for the risk neutral approach is outlined and a generic algorithmic description is presented. In section 3.5, we discuss the stopping criteria of the algorithm

and provide a framework to assess the quality of the policy. Several aspects of performance improvements of the algorithm are discussed in section 3.6 and a design using high performance computing techniques is discussed. Finally, we conclude this chapter with an analysis of the obtained solution and an investigation of the problem variability and its sensitivity to the initial conditions.

3.2 General problem statement and assumptions

3.2.1 Problem statement

In general, the risk neutral (i.e. when optimization is performed on average) formulation for the multistage linear stochastic programming problems can be written in the following form

$$\begin{array}{ll} \min_{x_1, x_2(\cdot), \ldots, x_T(\cdot)} & \mathbb{E}\left[c_1^{\mathsf{T}} x_1 + c_2^{\mathsf{T}} x_2(\xi_{[2]}) + \cdots + c_T^{\mathsf{T}} x_T(\xi_{[T]})\right] \\ s.t. & A_1 x_1 = b_1, x_1 \geq 0 \\ & x_t(\xi_{[t]}) \in \chi_t(x_{t-1}(\xi_{[t-1]}), \xi_t), t = 2, \ldots, T, \end{array} \tag{11}$$

where $\chi_t(x_{t-1}, \xi_t) = \{x_t : B_t x_{t-1} + A_t x_t = b_t, x_t \geq 0\}$, $t = 2, \ldots, T$, $\xi_1 = (c_1, A_1, b_1)$ is deterministic and $\xi_t = (c_t, A_t, B_t, b_t)$, $t = 2, ..., T$ denotes the stochastic data process formed by the vectors c_t, b_t and matrices A_t, B_t. We denote by $\xi_{[t]} = (\xi_1, ..., \xi_t)$ the history of the data process up to time t.

In the extensive form (11), the optimization is performed over feasible policies or decision rules. A policy is defined as a sequence of measurable functions $x_t(\xi_{[t]}), t = 1, \ldots, T$. The nonanticipativity property is guaranteed by $x_t(\cdot)$ being function of the data process up to time t (i.e. $\xi_{[t]}$). Feasibility means that the constraints are satisfied almost surely, i.e.,

$$x_t(\xi_{[t]}) \in \chi_t(x_{t-1}(\xi_{[t-1]}), \xi_t) \text{ w.p. } 1, \ t = 2, \ldots, T \tag{12}$$

Equivalently, this problem can be written in the nested form

$$\min_{\substack{A_1x_1=b_1\\x_1\geq 0}} c_1^{\mathsf{T}}x_1 + \mathbb{E}\left[\min_{\substack{B_2x_1+A_2x_2=b_2\\x_2\geq 0}} c_2^{\mathsf{T}}x_2 + \mathbb{E}_{|\xi_{[2]}}\left[\cdots + \mathbb{E}_{|\xi_{[T-1]}}\left[\min_{\substack{B_Tx_{T-1}+A_Tx_T=b_T\\x_T\geq 0}} c_T^{\mathsf{T}}x_T\right]\right]\right] \tag{13}$$

The equivalence between the extensive form (11) and the nested form (13) is justified by the decomposition property of the expectation operator (i.e. $\mathbb{E}[X] = \mathbb{E}[\mathbb{E}[X|Y]]$ where X, Y are random variables) and the interchangeability of minimization and expectation (c.f. [24, Theorem 14.60]).

The nested form (13) allows writing the dynamical programming equations, for $t = T, \ldots, 2$, as follows

$$Q_t(x_{t-1}, \xi_{[t]}) = \min_{\substack{B_tx_{t-1}+A_tx_t=b_t\\x_t\geq 0}} \left\{c_t^{\mathsf{T}}x_t + \mathcal{Q}_{t+1}(x_t, \xi_{[t]})\right\} \tag{14}$$

where

$$\mathcal{Q}_{t+1}(x_t, \xi_{[t]}) := \mathbb{E}\left[Q_{t+1}(x_t, \xi_{[t+1]})|\xi_{[t]}\right] \tag{15}$$

with $\mathcal{Q}_{T+1}(\cdot) \equiv 0$. The functions $\mathcal{Q}_t(\cdot), t = 2, \ldots, T$ are called cost-to-go (or value) functions. In the first stage, the following problem has to be solved

$$\min_{\substack{A_1x_1=b_1\\x_1\geq 0}} c_1^{\mathsf{T}}x_1 + \mathcal{Q}_2(x_1, \xi_2) \tag{16}$$

The optimal value of this problem gives the optimal value of the multistage problem.

Proposition 3.2.1. *The cost-to-go functions $\mathcal{Q}_t(x_{t-1}, \xi_{[t-1]}), t = 2, \ldots, T$ are convex in x_{t-1}. Furthermore, if the data process has finite realizations, then the cost-to-go functions are convex piecewise linear.*

Theorem 3.2.1. *(Optimal policy) A feasible policy $\left\{x_t^*(\xi_{[t]})\right\}_{t=1,\ldots,T}$ is optimal if x_1^* is an optimal solution for the first stage and for $t = 2, \ldots, T$,*

$$x_t^*(\xi_{[t]}) \in \operatorname*{arg\,min}_{\substack{B_tx_{t-1}+A_tx_t=b_t\\x_t\geq 0}} \left\{c_t^{\mathsf{T}}x_t + \mathcal{Q}_{t+1}(x_t, \xi_{[t]})\right\} \ \textit{w.p. 1} \tag{17}$$

3.2.2 Assumptions

First, we assume that at each stage $t = 1, \ldots, T-1$ the problem has relatively complete recourse (cf. section 2.4).

Second, we make the basic assumption that the random data process is stagewise independent, i.e., random vector ξ_{t+1} is independent of $\xi_{[t]} = (\xi_1, ..., \xi_t)$ for $t = 1, ..., T-1$. Under the stagewise independence assumption, the cost-to-go function $\mathcal{Q}_t(x_{t-1}, \xi_{[t-1]})$, for $t = T, \ldots, 2$, is independent of $\xi_{[t-1]}$. Thus, the dynamical programming equations can be written in the form

$$Q_t(x_{t-1}, \xi_t) = \min_{\substack{B_t x_{t-1} + A_t x_t = b_t \\ x_t \geq 0}} \left\{ c_t^{\mathsf{T}} x_t + \mathcal{Q}_{t+1}(x_t) \right\} \tag{18}$$

where

$$\mathcal{Q}_{t+1}(x_t) := \mathbb{E}\left[Q_{t+1}(x_t, \xi_{t+1}) \right] \tag{19}$$

with $\mathcal{Q}_{T+1}(\cdot) \equiv 0$.

In some cases across stages dependence can be dealt with by adding state variables to the model. In particular, the following construction is relevant for the considered applications. Suppose that only the right hand side vectors b_t are across stage dependent, while other parameters of the problem form a stagewise independent process (in particular, they could be deterministic). We are interested in cases where, for physical reasons, components of vectors b_t cannot be negative. Suppose that random vectors b_t follow p-th order autoregressive process with multiplicative error terms:

$$b_t = \varepsilon_t \bullet (\mu + \phi_1 b_{t-1} + ... + \phi_p b_{t-p}), \;\; t = 2, ..., T, \tag{20}$$

where vector μ and matrices $\phi_1, ..., \phi_p$ are estimated from the data. Here $\varepsilon_2, ..., \varepsilon_T$ are independent of each other error vectors and such that with probability one their components are nonnegative and have expected value one, and $a \bullet b$ denotes the term by term (Hadamard) product of two vectors. The *multiplicative* error term model

is considered to ensure that realizations of the random process b_t have nonnegative values.

The autoregressive process (20) can be formulated as a first order autoregressive process

$$\begin{bmatrix} b_t \\ b_{t-1} \\ b_{t-2} \\ \cdots \\ b_{t-p+1} \end{bmatrix} = \begin{bmatrix} \varepsilon_t \\ \mathbf{1} \\ \mathbf{1} \\ \cdots \\ \mathbf{1} \end{bmatrix} \bullet \left(\begin{bmatrix} \mu \\ 0 \\ 0 \\ \cdots \\ 0 \end{bmatrix} + \begin{bmatrix} \phi_1 & \phi_2 & \cdots & \phi_{p-1} & \phi_p \\ I & 0 & \cdots & 0 & 0 \\ 0 & I & \cdots & 0 & 0 \\ & & \cdots & & \\ 0 & 0 & \cdots & I & 0 \end{bmatrix} \begin{bmatrix} b_{t-1} \\ b_{t-2} \\ b_{t-3} \\ \cdots \\ b_{t-p} \end{bmatrix} \right), \quad (21)$$

where $\mathbf{1}$ is vector of ones and I is the identity matrix of an appropriate dimension. Denote by z_t the column vector in the left hand side of (21), and by ϵ_t, M and Φ the respective terms in the right hand side of (21). Then (21) can be written as

$$z_t = \epsilon_t \bullet (M + \Phi z_{t-1}),\ t = 2, ..., T. \quad (22)$$

Consequently the feasibility equations of problem (13) can be written as

$$z_t - \epsilon_t \bullet \Phi z_{t-1} = \epsilon_t \bullet M,\ B_t x_{t-1} + A_t x_t = b_t,\ x_t \geq 0,\ \ t = 2, ..., T. \quad (23)$$

Therefore by replacing x_t with (x_t, z_t), and considering the corresponding data process ξ_t formed by random elements of c_t, A_t, B_t and error vectors ε_t, $t = 2, ..., T$, we transform the problem to the stagewise independent case. The obtained problem is still linear with respect to the decision variables x_t and z_t.

3.2.3 Methodology

We consider the following approach to solving the multistage problem (13). First, a (finite) scenario tree is generated by randomly sampling from the original distribution and then the constructed problem is solved by the *Stochastic Dual Dynamic Programming* (SDDP) algorithm. There are three levels of approximations in that

setting. The first level is modelling. The inflows are viewed as seasonal time series and modelled as a multiplicative auto-regressive process. Any such modelling involves inaccuracies - autoregressive parameters should be estimated, errors distributions are not precise, etc. We will refer to an optimization problem based on a current time series model as the *"true"* problem.

The "true" model involves data process ξ_t, $t = 1, ..., T$, having *continuous* distributions. Since the corresponding expectations (multidimensional integrals) cannot be computed in a closed form, one needs to make a discretization of the data process ξ_t. So a sample $\tilde{\xi}_t^1, ..., \tilde{\xi}_t^{N_t}$, of size N_t, from the distribution of the random vector ξ_t, $t = 2, ..., T$, is generated. These samples generate a scenario tree with the total number of scenarios $N = \prod_{t=2}^{T} N_t$, each with equal probability $1/N$. Consequently the true problem is approximated by the so-called *Sample Average Approximation* (SAA) problem associated with this scenario tree (cf. section 3.3). This corresponds to the second level of approximation in the current system.

Even with a moderate number of scenarios per stage, say each $N_t = 100$, the total number of scenarios N quickly becomes astronomically large with increase of the number of stages. Therefore the constructed SAA problem can be solved only approximately. The SDDP method suggests a computationally tractable approach to solving SAA, and hence the "true", problems, and can be viewed as the third level of approximation in this methodology.

3.3 The SAA Method

We refer the reader for an overview of the Sample Average Approximation (SAA) method to [30][Chapter 5] and its related bibliography section. Based on this reference, the key idea of the SAA method will be summarized in this section.

Assume we have the following stochastic programming problem:

$$\operatorname*{Min}_{x \in \mathcal{X}} \{f(x) := \mathbb{E}\left[F(x, \xi)\right]\} \tag{24}$$

where $\mathcal{X}$ is non empty closed subset of $\mathbb{R}^n$, ξ is a random vector with a probability distribution supported on $\Xi \subset \mathbb{R}^d$ and $F : X \times \Xi \to \mathbb{R}$. We assume that the expectation is well defined and finite valued for all $x \in \mathcal{X}$.

Suppose that we have a sample $\xi^1, \ldots, \xi^N$ of N realizations of ξ. This sample can be generated by Monte Carlo Sampling techniques or viewed as historical data of ξ. The Sample Average Approximation (SAA) of the "true" problem (24) is constructed as follows.

$$\operatorname*{Min}_{x \in \mathcal{X}} \left\{ \hat{f}_N(x) := \frac{1}{N} \sum_{j=1}^{N} F(x, \xi^j) \right\} \tag{25}$$

In other words, for a given sample, the SAA problem (25) can be considered as a stochastic programming with respective scenarios $\xi^1, \ldots, \xi^N$, each taken with probability $1/N$.

If we consider the multistage stochastic linear problem formulation (13) under the stagewise independence assumption, the construction of the scenario tree for the SAA of the "true" problem proceeds as follows. At each stage t, random samples $\xi_t^1, \ldots, \xi_t^{N_t}$ of ξ_t are generated independently of each other. The tree is obtained by connecting each node at stage t to the same set of nodes at stage $t+1$.

If we measure the computational complexity, of the true problem, in terms of the number of scenarios required to approximate the true distribution of the random data process with a reasonable accuracy, the conclusion is rather pessimistic. In order for the optimal value and solutions of the SAA problem to converge to their true counterparts all sample sizes $N_2, ..., N_T$ should tend to infinity. Furthermore, available estimates of the sample sizes N_t required for a first stage solution of the SAA problem to be ε-optimal for the true problem, with a given confidence (probability), sums up to a total number of scenarios N which grows as $O(\varepsilon^{-2(T-1)})$ with decrease of the error level $\varepsilon > 0$ (cf., [30, section 5.8.2]). This indicates that from the point of view of the number of scenarios, complexity of multistage programming problems grows exponentially with increase of the number of stages.

3.4 Description of the SDDP algorithm

We present the SDDP algorithm when applied to the SAA problem. Suppose that N_t, $t = 2, ..., T$, points are generated at every stage of the process. We assume that first stage data are known, i.e., ξ_1 is deterministic and hence $N_1 = 1$ (no sampling at the first stage). Let

$$\xi_t^j = (c_{tj}, A_{tj}, B_{tj}, b_{tj}), \quad j = 1, .., N_t, \ t = 2, ..., T, \tag{26}$$

be the generated points. As it was already mentioned the total number of scenarios of the SAA problem is $N = \prod_{t=1}^{T} N_t$ and can be very large. In this section we deal only with the SAA problem, i.e., we only consider scenarios corresponding to points in (26).

3.4.1 Backward step of the algorithm

Let $\bar{x}_t$, $t = 1, ..., T-1$, be trial points (we can use more than one trial point at every stage of the backward step, an extension to that will be straightforward). Let $\mathcal{Q}_t(\cdot)$ be the cost-to-go functions of dynamic programming equations (19) associated with the considered multistage problem, and $\mathfrak{Q}_t(\cdot)$ be a current approximation of $\mathcal{Q}_t(\cdot)$ given by the maximum of a collection of *cutting* planes

$$\mathfrak{Q}_t(x_{t-1}) = \max_{k \in \mathcal{I}_t} \left\{ \alpha_{tk} + \beta_{tk}^{\mathsf{T}} x_{t-1} \right\}, \ t = 1, ..., T-1. \tag{27}$$

At stage $t = T$ we solve the following problems

$$\operatorname*{Min}_{x_T \in \mathbb{R}^{n_T}} c_{Tj}^{\mathsf{T}} x_T \ \text{ s.t. } B_{Tj} \bar{x}_{T-1} + A_{Tj} x_T = b_{Tj}, \ x_T \geq 0, \ j = 1, ..., N_T. \tag{28}$$

Recall that $Q_{Tj}(\bar{x}_{T-1})$ is equal to the optimal value of problem (28) and that subgradients of $Q_{Tj}(\cdot)$ at $\bar{x}_{T-1}$ are given by $-B_{Tj}^{\mathsf{T}} \pi_{Tj}$, where π_{Tj} is a solution of the dual of (28). Therefore for the cost-to-go function $\mathcal{Q}_T(x_{T-1})$ we can compute its value and a subgradient at the point $\bar{x}_{T-1}$ by averaging the optimal values of (28) and the

corresponding subgradients. Consequently we can construct a supporting plane to $\mathcal{Q}_T(\cdot)$ and add it to the current collection of supporting planes of $\mathfrak{Q}_T(\cdot)$.

Now going one stage back let us recall that $Q_{T-1,j}(\bar{x}_{T-2})$ is equal to the optimal value of problem

$$\underset{x_{T-1}\in\mathbb{R}^{n_{T-1}}}{\text{Min}} c_{T-1,j}^{\mathsf{T}} x_{T-1} + \mathcal{Q}_T(x_{T-1}) \text{ s.t. } B_{T-1,j}\bar{x}_{T-2} + A_{T-1,j}x_{T-1} = b_{T-1,j},\ x_{T-1} \geq 0. \tag{29}$$

However, function $\mathcal{Q}_T(\cdot)$ is not available. Therefore we replace it by $\mathfrak{Q}_T(\cdot)$ and hence consider problem

$$\underset{x_{T-1}\in\mathbb{R}^{n_{T-1}}}{\text{Min}} c_{T-1,j}^{\mathsf{T}} x_{T-1} + \mathfrak{Q}_T(x_{T-1}) \text{ s.t. } B_{T-1,j}\bar{x}_{T-2} + A_{T-1,j}x_{T-1} = b_{T-1,j},\ x_{T-1} \geq 0. \tag{30}$$

Recall that $\mathfrak{Q}_T(\cdot)$ is given by maximum of affine functions (see (27)). Therefore we can write problem (30) in the form

$$\begin{array}{ll} \underset{x_{T-1}\in\mathbb{R}^{n_{T-1}},\theta\in\mathbb{R}}{\text{Min}} & c_{T-1,j}^{\mathsf{T}} x_{T-1} + \theta \\ \text{s.t.} & B_{T-1,j}\bar{x}_{T-2} + A_{T-1,j}x_{T-1} = b_{T-1,j},\ x_{T-1} \geq 0 \\ & \theta \geq \alpha_{Tk} + \beta_{Tk}^{\mathsf{T}} x_{T-1},\ k \in \mathcal{I}_T. \end{array} \tag{31}$$

Consider the optimal value, denoted $\underline{Q}_{T-1,j}(\bar{x}_{T-2})$, of problem (31), and let $\pi_{T-1,j}$ be the partial vector of an optimal solution of the dual of problem (31) corresponding to the constraint $B_{T-1,j}\bar{x}_{T-2} + A_{T-1,j}x_{T-1} = b_{T-1,j}$, and let

$$\underline{\mathcal{Q}}_{T-1}(\bar{x}_{T-2}) := \frac{1}{N_{T-1}} \sum_{j=1}^{N_{T-1}} \underline{Q}_{T-1,j}(\bar{x}_{T-2})$$

and

$$g_{T-1} = -\frac{1}{N_{T-1}} \sum_{j=1}^{N_{T-1}} B_{T-1,j}^{\mathsf{T}} \pi_{T-1,j}.$$

Consequently we add the corresponding affine function to collection of $\mathfrak{Q}_{T-1}(\cdot)$. And so on going backward in t. Note that the (last stage) cost-to-go function $\mathcal{Q}_T(\cdot)$ is not available for computations. What do we have is its lower approximation $\mathfrak{Q}_T(\cdot)$, i.e.,

$\mathcal{Q}_T(\cdot) \geq \mathfrak{Q}_T(\cdot)$ (this inequality could, and usually will, be strict). This is why problem (29) is replaced by problem (30) at this stage of the backward step procedure. The constructed affine function is a supporting plane of $\underline{\mathcal{Q}}_{T-1}(\cdot)$. Since $\underline{\mathcal{Q}}_{T-1}(\cdot)$ could be *strictly* smaller than $\mathcal{Q}_{T-1}(\cdot)$, the constructed affine function could be only a cutting plane of $\mathcal{Q}_{T-1}(\cdot)$.

The computed approximations $\mathfrak{Q}_2(\cdot), ..., \mathfrak{Q}_T(\cdot)$ (with $\mathfrak{Q}_{T+1}(\cdot) \equiv 0$ by definition) and a feasible first stage solution $\bar{x}_1$ can be used for constructing an implementable policy as follows.

For a realization

$$\xi_t = (c_t, A_t, B_t, b_t),\ t = 2, ..., T,$$

of the data process, decisions $\bar{x}_t$, $t = 1, ..., T$, are computed recursively going forward with $\bar{x}_1$ being the chosen feasible solution of the first stage problem, and $\bar{x}_t$ being an optimal solution of

$$\operatorname*{Min}_{x_t} c_t^{\mathsf{T}} x_t + \mathfrak{Q}_{t+1}(x_t) \ \text{ s.t. } A_t x_t = b_t - B_t \bar{x}_{t-1},\ x_t \geq 0, \tag{32}$$

for $t = 2, ..., T$. These optimal solutions can be used as trial decisions in the backward step of the algorithm. Note that $\bar{x}_t$ is a function of $\bar{x}_{t-1}$ and ξ_t, i.e., $\bar{x}_t$ is a function of $\xi_{[t]} = (\xi_1, ..., \xi_t)$, for $t = 2, ..., T$. That is, policy $\bar{x}_t = \bar{x}_t(\xi_{[t]})$ is nonanticipative and by the construction satisfies the feasibility constraints for every realization of the data process.

Thus the computed approximations $\mathfrak{Q}_2(\cdot), ..., \mathfrak{Q}_T(\cdot)$ (i.e., the cuts stored in the computer memory) and the first stage solution define an implementable and feasible policy for both – the true and SAA problems. That is, if we restrict the data process to the generated sample, i.e., we consider only realizations $\xi_2, ..., \xi_T$ of the data process drawn from scenarios of the SAA problem, then $\bar{x}_t = \bar{x}_t(\xi_{[t]})$ becomes an implementable and feasible policy for the corresponding SAA problem. On the other hand, if we consider realizations $\xi_2, ..., \xi_T$ of the true problem, then this gives

an implementable and feasible policy for the true problem.

Since the policy $\bar{x}_t = \bar{x}_t(\xi_{[t]})$ is feasible, the expectation

$$\mathbb{E}\left[\sum_{t=1}^{T} c_t^{\mathsf{T}} \bar{x}_t(\xi_{[t]})\right] \tag{33}$$

gives an upper bound for the optimal value of the corresponding multistage problem. If we take this expectation over the true probability distribution of the random data process, then the above expectation (33) gives an upper bound for the optimal value of the true problem. On the other hand, if we restrict the data process to scenarios of the SAA problem, each with equal probability $1/N$, then the expectation (33) gives an upper bound for the optimal value of the SAA problem conditional on the sample used in construction of the SAA problem.

3.4.2 Forward step of the algorithm

The *forward* step of the SDDP algorithm consists in generating M random realizations (scenarios) of the data process and computing the respective optimal values

$$\vartheta_i := \sum_{t=1}^{T} c_{ti}^{\mathsf{T}} \bar{x}_{ti}, \quad i = 1, ..., M.$$

That is, ϑ_i is the value of the corresponding policy for the realization $\xi_1, \xi_2^i, ..., \xi_T^i$ of the data process. As such ϑ_i is an unbiased estimate of expected value of that policy, i.e., $\mathbb{E}[\vartheta_i] = \mathbb{E}\left[\sum_{t=1}^{T} c_t^{\mathsf{T}} \bar{x}_t(\xi_{[t]})\right]$.

The forward step has two functions. First, some (all) of computed solutions $\bar{x}_{ti}$ can be used as trial points in the next iteration of the backward step of the algorithm. Second, these solutions can be employed for constructing a statistical upper bound for the optimal value of the corresponding multistage program (true or SAA depending on from what distribution the sample scenarios were generated).

Consider the average (sample mean) $\tilde{\vartheta}_M := M^{-1} \sum_{i=1}^{M} \vartheta_i$ and standard error

$$\tilde{\sigma}_M := \sqrt{\frac{1}{M-1} \sum_{i=1}^{M} (\vartheta_i - \tilde{\vartheta}_M)^2}$$

of the computed values ϑ_i. Since ϑ_i is an unbiased estimate of the expected value of the constructed policy, we have that $\tilde{\vartheta}_M$ is also an unbiased estimate of the expected value of that policy. By invoking the Central Limit Theorem we can say that $\tilde{\vartheta}_M$ has an approximately normal distribution provided that M is reasonably large. This leads to the following (approximate) $(1-\alpha)$-confidence *upper* bound for the value of that policy

$$\tilde{\vartheta}_M + z_\alpha \frac{\tilde{\sigma}_M}{\sqrt{M}}. \tag{34}$$

The corresponding $(1-\alpha)$-confidence *lower* bound is

$$\tilde{\vartheta}_M - z_\alpha \frac{\tilde{\sigma}_M}{\sqrt{M}}, \tag{35}$$

and the $(1-\alpha)$-two-sided confidence interval is

$$\left[\tilde{\vartheta}_M - z_{\alpha/2} \frac{\tilde{\sigma}_M}{\sqrt{M}}, \tilde{\vartheta}_M + z_{\alpha/2} \frac{\tilde{\sigma}_M}{\sqrt{M}}\right]. \tag{36}$$

Here $1-\alpha \in (0,1)$ is a chosen confidence level and $z_\alpha = \Phi^{-1}(1-\alpha)$, where $\Phi(\cdot)$ is the cdf of standard normal distribution. For example, for $\alpha = 0.05$ the corresponding critical value $z_{0.05} = 1.64$. That is, with probability approximately $1-\alpha$ the expected value of the constructed policy is less than the upper bound. Since the expected value (33) of the constructed policy is bigger than or equal to the optimal value of the considered multistage problem, we have that it also gives an upper bound for the optimal value of the multistage problem with confidence at least $1-\alpha$. Note that the *upper* bound can be used for the SAA or the true problem depending on from what distribution the sampled scenarios were generated.

Since $\mathfrak{Q}_t(\cdot)$ is the maximum of cutting planes of the cost-to-go function $\mathcal{Q}_t(\cdot)$ we have that

$$\mathcal{Q}_t(\cdot) \geq \mathfrak{Q}_t(\cdot), \ t = 2, ..., T. \tag{37}$$

Therefore the optimal value computed at a backward step of the algorithm, gives a lower bound for the considered SAA problem. This lower bound is deterministic (i.e.,

is not based on sampling) if applied to the corresponding SAA problem. On the other hand, the upper bound is a function of generated scenarios and thus is stochastic even for considered (fixed) SAA problem. This upper bound may vary for different sets of random samples, in particular from one iteration to the next of the forward step of the algorithm.

3.4.3 Generic description of the risk neutral SDDP

An algorithmic description of the SDDP method for the risk neutral approach is presented in Algorithm 1.

3.5 Stopping criteria and validation of the optimality gap

The procedure for stopping the algorithm suggested in [20] is when the lower bound (i.e. line 24 in Algorithm 1) falls in the $100(1-\alpha)\%$ confidence interval (36), computed in the forward step procedure of the algorithm. This criteria was discussed in [34] as follows. This stopping criterion depends on the number of scenarios used in the forward step and the chosen confidence level $100(1-\alpha)\%$. Reducing the number of scenarios results in increasing the standard deviation of the corresponding estimate and hence making the lower end of the confidence interval smaller. Also increasing the confidence level makes the confidence interval larger, i.e., decreases its lower end. This indicates that for sufficiently large confidence level the algorithm could be stopped at any iteration and this stopping criterion does not give any reasonable guarantee for quality of the obtained solution and could result in a premature stop of the iteration procedure.

Figure 12 illustrates the bounds behaviour for the SDDP algorithm where the upper bound is equal to the lower end of $100(1-\alpha)\%$ confidence interval (36). In this experiment, the upper bound was computed using 50 and 100 observations. Also, we consider $\alpha = 0.05$ and run the algorithm with 1 trial solution per iteration. As discussed previously, we can see how this stopping criterion depends on the number

Algorithm 1 Risk neutral SDDP algorithm

Require: $\left\{\mathfrak{Q}_t^0\right\}_{t=2,\ldots,T+1}$(Init. Lower approx.) and $\epsilon > 0$(accuracy)

Initialize: $i \leftarrow 0$, $\bar{z} = \infty$ (Upper bound), $\underline{z} = -\infty$ (Lower bound)
while $\bar{z} - \underline{z} > \epsilon$ **do**
    Sample M scenarios: $\left\{\{c_{tk}, A_{tk}, B_{tk}, b_{tk}\}_{2\leq t\leq T}\right\}_{1\leq k\leq M}$

    (Forward step)
    for $k = 1 \rightarrow M$ **do**
        for $t = 1 \rightarrow T$ **do**
            $\bar{x}_t^k \leftarrow \arg\min_{x_t\in\mathbb{R}^{n_t}} \left\{ \begin{array}{l} c_{tk}^\top x_t + \mathfrak{Q}_{t+1}^i(x_t) : \\ B_{tk}x_{t-1} + A_{tk}x_t = b_{tk}, x_t \geq 0 \end{array} \right\}$
        end for
        $\vartheta_k \leftarrow \sum_{t=1}^T c_{tk}^\mathsf{T}\bar{x}_t^k$
    end for

    (Upper bound update)
    $\overline{z} \leftarrow \tilde{\vartheta}_M + z_\alpha \frac{\tilde{\sigma}_M}{\sqrt{M}}$

    (Backward step)
    for $k = 1 \rightarrow M$ **do**
        for $t = T \rightarrow 2$ **do**
            for $j = 1 \rightarrow N_t$ **do**
                $\left[\widetilde{Q}_{tj}(\bar{x}_{t-1}^k), \widetilde{\pi}_{tj}^k\right] \leftarrow \min_{x_t\in\mathbb{R}^{n_t}} \left\{ \begin{array}{l} c_{tj}^\top x_t + \mathfrak{Q}_{t+1}^i(x_t) : \\ B_{tj}\bar{x}_{t-1} + A_{tj}x_t = b_{tj}, x_t \geq 0 \end{array} \right\}$
            end for
            $\widetilde{\mathcal{Q}}_t(\bar{x}_{t-1}^k) := \frac{1}{N_t}\sum_{j=1}^{N_t} \widetilde{Q}_{t,j}(\bar{x}_{t-1}^k)$; $\tilde{g}_t^k := -\frac{1}{N_t}\sum_{j=1}^{N_t} \tilde{\pi}_{tj}^k \widetilde{B}_{t,j}$
            $\mathfrak{Q}_t^{i+1} \leftarrow \{x_{t-1} \in \mathfrak{Q}_t^i : -\tilde{g}_t^k x_{t-1} \geq \widetilde{\mathcal{Q}}_t(\bar{x}_{t-1}^k) - \tilde{g}_t^k \bar{x}_{t-1}^k\}$
        end for
    end for

    (Lower bound update)
    $\underline{z} \leftarrow \min_{x_1\in\mathbb{R}^{n_1}} \left\{c_1^\top x_1 + \mathfrak{Q}_2(x_1) : A_1x_1 = b_1, x_1 \geq 0\right\}$

    $i \leftarrow i + 1$
end while

of scenarios used in the forward step: reducing the number of scenarios from 100 to 50 results in an earlier stopping time (i.e. at iteration 3155 for 100 scenarios and at iteration 1362 for 50 scenarios).

It was suggested, in [34] and [36], to use the $(1-\alpha)$%-confidence upper bound, i.e., use the upper bound (34). The upper end of the confidence interval gives an upper bound for the optimal value of the SAA problem with confidence (probability)

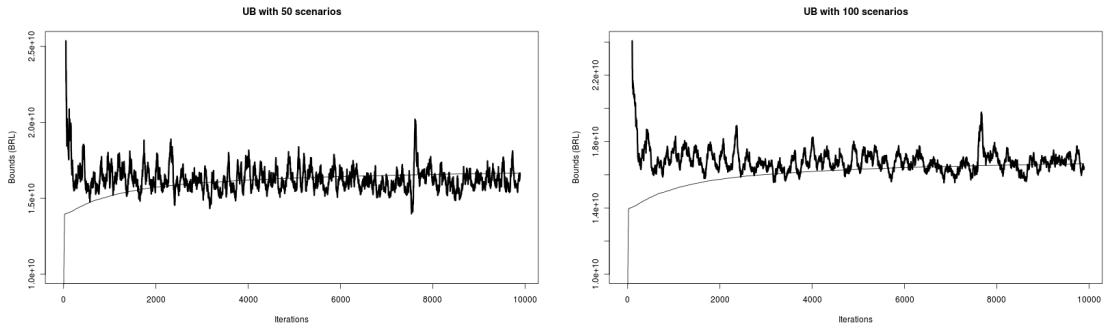

Figure 12: Risk neutral approach: SDDP bounds with UB as suggested in [20]

$100(1-\alpha)\%$. At the same time the backward step gives a lower bound for the optimal value of the SAA problem (this lower bound is based on all scenarios of the SAA problem and does not involve sampling of the tree of the SAA problem). The difference between these two bounds gives an estimate, with confidence $100(1-\alpha)\%$, of the optimality gap of the corresponding policy. If this difference is smaller than a specified accuracy level $\varepsilon > 0$, then the procedure could be stopped.

Figure 13 illustrates the bounds behaviour for the SDDP algorithm where the upper bound is equal to the $(1-\alpha)\%$-confidence upper end (34). In this experiment, the upper bound was computed using 50 and 100 observations. Also, we consider $\alpha = 0.05$ and run the algorithm with 1 trial solution per iteration.

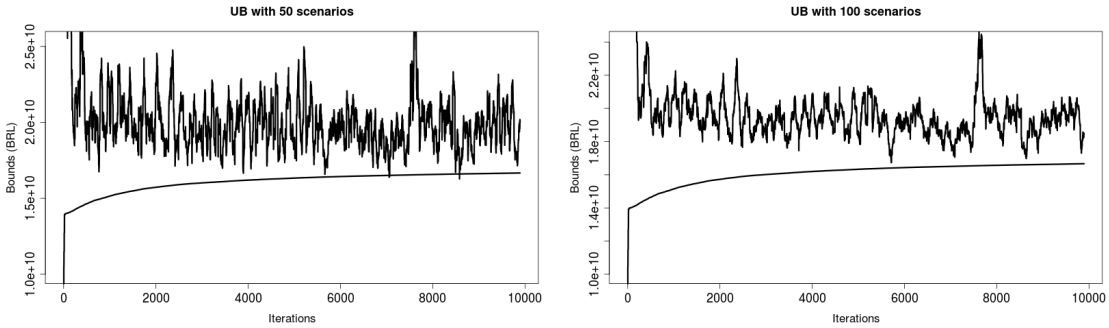

Figure 13: Risk neutral approach: SDDP bounds with UB as suggested in (34)

3.5.1 Gap based stopping criterion

We consider the relative gap between the upper bound defined by (34) and the lower bound computed in backward steps of the algorithm, that is $(ub - lb)/lb$. Figure 14 illustrates the evolution of the gap across iterations. The plot on the left shows the gap as defined above (i.e. $(ub - lb)/lb$) and the plot on the right shows a simple moving average of the gap using 500 observations. In both cases the upper bound was computed using a sample size of 100 observations.

In our experiments we estimate the upper bound at each iteration by taking the past 100 observations over iterations. This allows us to approximate the gap without the significant computational effort of running at each iteration a large number of forward sample paths. The underlying justification is that in later stages (after iteration 2000) the lower bound does not improve significantly (i.e. the constructed policy does not change significantly the cost of the decision at the first stage).

A significant decrease in the gap value occurs during the first 2000 iterations. Furthermore, due to the statistical nature of the upper bound the gap is not monotonic and, at some iterations, sudden changes are observed.

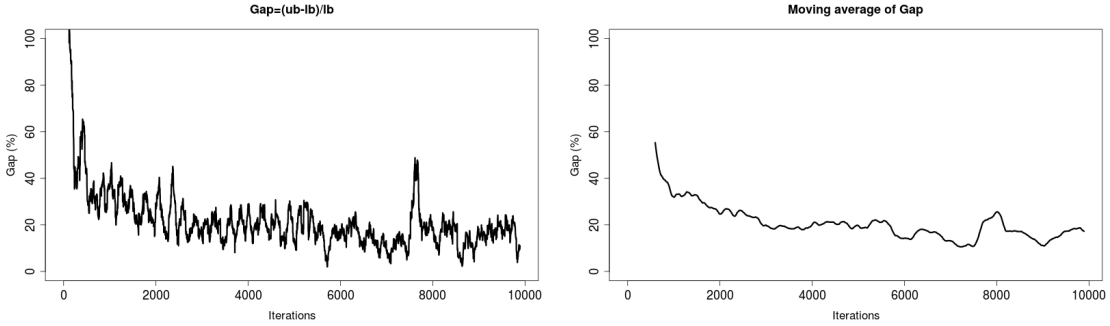

Figure 14: Risk neutral approach: SDDP gap

Table 4 summarizes the CPU time needed to achieve a certain number of iterations for the risk neutral SDDP method. Clearly, using the sequential implementation and given a reasonable amount of time, it does not make sense to consider *zero gap* as a

stopping criterion.

Table 4: Risk neutral approach: CPU time

iteration	CPU time (dd:hh:mm)
2000	00:11:34
3000	01:04:15
4000	02:06:12
5000	03:18:40

Figure 15 shows the evolution of the CPU time per iteration required by the SDDP method across iterations. We can observe a linear trend accompanied with noise at some iterations. This noise is mainly due to the shared computing environment in which the computations were performed.

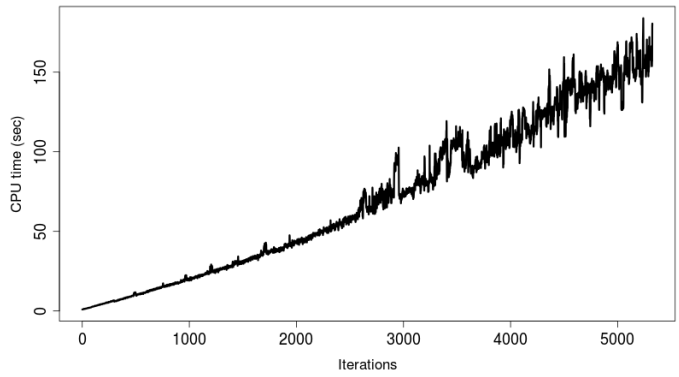

Figure 15: Risk neutral approach: CPU time per iteration

3.5.2 Policy value and validation of optimality gap

Assume that we have 2 policies and we would like to know if they are significantly different. One of the possible approaches is to use a t-test by proceeding as follows. We generate a set of sample scenarios which will be considered as a reference sample. For each scenario of the reference sample, we compute the value for the 2 policies. We perform a paired sample t-test on the obtained values. The null hypothesis is the means of two normally distributed populations are equal. The result of the test is a

rejection of the null hypothesis at the 5% significance level if the p-value is less than 5%.

This approach can be used in the SDDP context as follows. First ,we generate a reference sample of scenarios. Assume that we would like to know whether the policy changes significantly after iteration 3000. Then, at each specified number of iterations, we evaluate the policy and compare it to the one computed at iteration 3000. We perform this experiment with a reference scenario sample of size 1000 and we evaluate the policy each 100 iterations. Figure 16 gives the evolution of the p-value as function of iterations. The dashed line represents the 5% significance level.

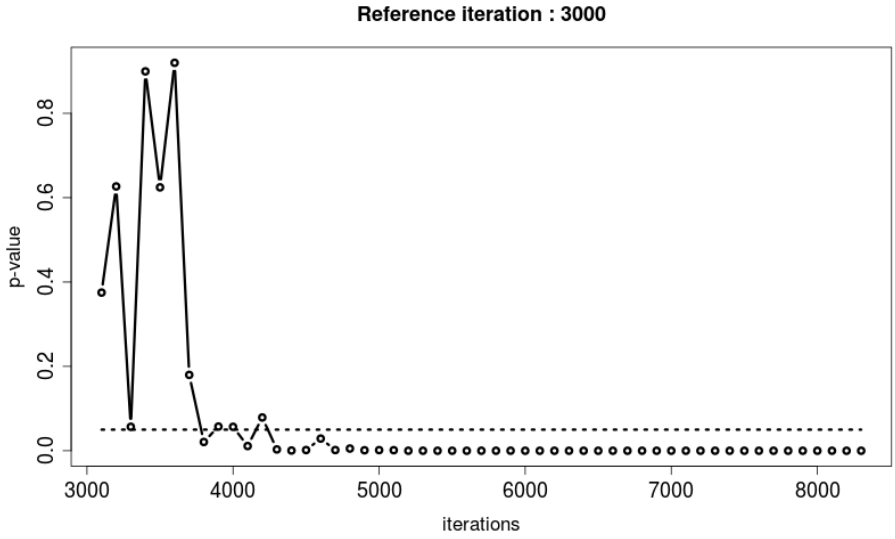

Figure 16: Risk neutral approach: p-value evolution with reference iteration 3000

Starting from iteration 4300, the null hypothesis (i.e. the means of two normally distributed populations are equal) is rejected at the 5% significance level. In other words, the policy obtained at iteration 4300 onward is significantly different than the one constructed at iteration 3000.

Figure 17 gives the evolution of the p-value as function of iterations for a sample size of 5000. The dashed line represents the 5% significance level. Starting from iteration 7000, the policy obtained at iteration 7000 onward is significantly different

than the one constructed at iteration 5000. This is equivalent to at least 3 days of run time for the sequential code.

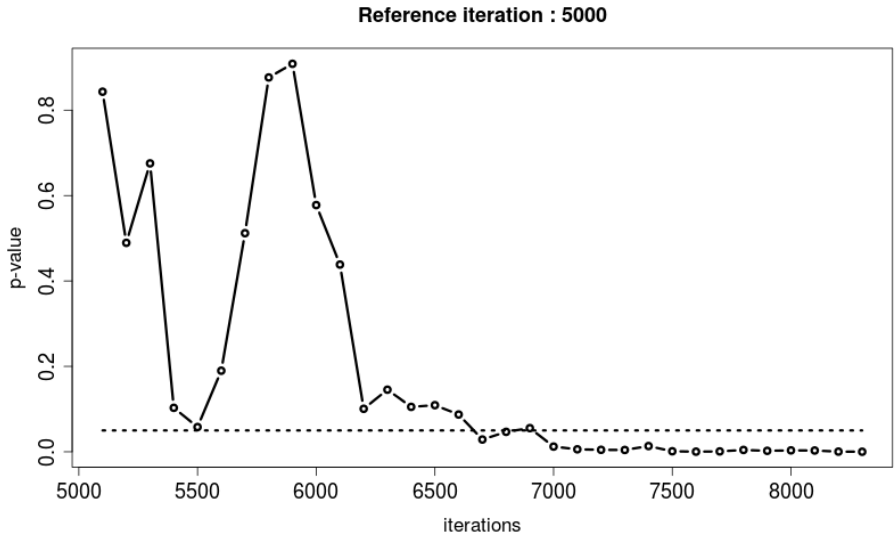

Figure 17: Risk neutral approach: p-value evolution with reference iteration 5000

3.6 Performance improvements

3.6.1 Redundant cutting planes elimination

Typically, a significant number of cutting planes added by the SDDP method in the backward step becomes at some point not necessary for the description of the cost-to-go functions approximations and could be eliminated. In this section we present a subroutine that identifies these redundant cutting planes. This subroutine allows a significant speed up of any SDDP type algorithm in general while preserving the statistical properties of the constructed policy.

First, we start by presenting the problem setting. At each stage, the cost-to-go function of dynamic programming equations are approximated by $\mathfrak{Q}(\cdot)$ given by the maximum of a collection of cutting planes in the following manner:

$$\mathfrak{Q}(x) = \max_{k \in \mathcal{I}} \left\{ \alpha_k + \beta_k^{\mathsf{T}} x \right\} \tag{38}$$

for $x \in \Gamma$ where Γ is a compact set.

An example of a redundant cutting plane is illustrated in Figure 18. In this figure, we assume that all the hyperplanes define half spaces in the non negative orthant and $\Gamma = [0, 4]$.

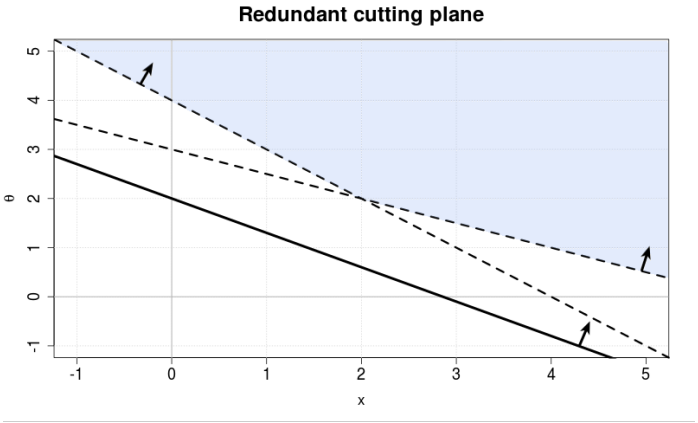

Figure 18: Illustration of a redundant cutting planes

The cutting plane in bold line is redundant since it can never be active in describing $\mathfrak{Q}(.)$ over Γ. Thus, it can be safely discarded. Empirical evidence (cf. Figure 19) shows that the SDDP method tends to generate a significant number of such cutting planes especially in initial stages.

Without loss of generality, assume that we want to check if $\alpha_1 + \beta_1^\mathsf{T} x$ is redundant. By checking the feasibility of the linear system described in (39) we can answer this question.

$$\begin{cases} \theta \leq \alpha_1 + \beta_1^\mathsf{T} x \\ \theta \geq \alpha_k + \beta_k^\mathsf{T} x, \forall k \in \mathcal{I} \setminus \{1\} \\ x \in \Gamma \end{cases} \tag{39}$$

where (θ, x) are variables and $(\alpha_k, \beta_k)_{k \in \mathcal{I}}$ are known data.

If problem (39) is infeasible, then $\alpha_1 + \beta_1^\mathsf{T} x$ is redundant (as illustrated in Figure 18) and could be removed. Otherwise, the constraint should be maintained.

Algorithmic description of the redundant cutting planes elimination subroutine is

presented in Algorithm 2.

Algorithm 2 Redundant cutting planes elimination subroutine

Require: $\mathfrak{Q}(x) = \max_{k\in\mathcal{I}} \left\{\alpha_k + \beta_k^\intercal x\right\}$

1: **for** $j \in \mathcal{I}$ **do**
2: Check feasibility of the polyhedron $\mathbf{P} = \left\{ (\theta, x) : \begin{array}{l} \theta \leq \alpha_j + \beta_j^\intercal x \\ \theta \geq \alpha_k + \beta_k^\intercal x, \forall k \in \mathcal{I}\setminus\{j\} \\ x \in \Gamma \end{array} \right\}$
3: **if** $\mathbf{P} = \emptyset$ **then**
4: Discard $(\alpha_j + \beta_j^\intercal x)$ from $\mathbf{P}$
5: **end if**
6: **end for**

First, we investigate the question of how frequently should this subroutine be used. We run 3000 iterations of the SDDP method with 1 trial point per iteration on the risk neutral case. We run several experiments where we use different constant cycle lengths (i.e. a cycle length of 50 means that we run the subroutine each 50 iterations). The ∞ denotes the case where we don't use the subroutine.

Cycle length	SDDP run time (dd:hh:mm)	subroutine run time (dd:hh:mm)	Total CPU time (dd:hh:mm)
50	00:09:59	00:04:10	00:14:09
100	00:10:18	00:02:06	00:12:24
200	00:11:21	00:01:06	00:12:27
400	00:13:19	00:00:43	00:14:02
∞	01:04:54	-	01:04:54

Table 5: Risk neutral approach: CPU time (SDDP with subroutine)

Over the 3000 iterations, a speed up factor of at least 2 times is recorded with a cycle length of 100 or 200 when compared to experiment without running the subroutine. It is clear that the use of the subroutine significantly improves the method performance. Clearly, a tradeoff between the time spent in removing redundant cutting planes and performing SDDP iterations has to be made. On the one hand, with a cycle length of 50, the lowest SDDP run time is obtained. However, a significant amount of time is spent in running the subroutine. On the other hand, with a cycle

length of 400, the lowest time spent on running the subroutine is achieved. Nevertheless, a longer time to run the SDDP method is recorded. Furthermore, subroutines runs become more expensive as the number of cutting planes increases. A better strategy consists in changing the cycle length throughout the experiment as function of how costly it is to run the subroutine compared to performing further SDDP iterations.

For instance, we implement the following strategy (denoted S1). We consider an initial cycle of length 100 and the length is doubled each 1500 iterations (i.e. 1-1500: cycle of 100, 1500-3000: cycle of 200,...). Table 6 shows the CPU time required to run 5000 iterations of the SDDP algorithm with strategy S1 and without it. The total CPU time went from 90 hours down to 29 hours with this simple strategy. The choice of 1500 iterations threshold was done following the argument outlined in the previous paragraph. Clearly, more elaborate strategies can be constructed using this subroutine.

Cycle length	SDDP run time (dd:hh:mm)	subroutine run time (dd:hh:mm)	Total CPU time (dd:hh:mm)
S1	01:05:35	00:03:10	01:08:45
∞	03:18:40	-	03:18:40

Table 6: Risk neutral approach: CPU time (SDDP with subroutine strategy)

This subroutine allows to have some measure of the cutting planes efficiency at each stage. Figure 19 plots the percentage of redundant cutting planes compared to the total number of cuts added per stage for the risk neutral approach. Performing 3000 iterations with 1 trial point per iteration generates 3000 cutting planes at each stage $t \geq 2$. It can be seen that the proportion of redundant cutting planes is higher for earlier stages with more than 70% in the first 60 stages. This can be explained by the continuous refinement of the cost-to-go function approximations for the first stages. In addition, the lower error accumulation in the cost-to-go function approximation for later stages explains the lower proportion of redundant cutting

planes.

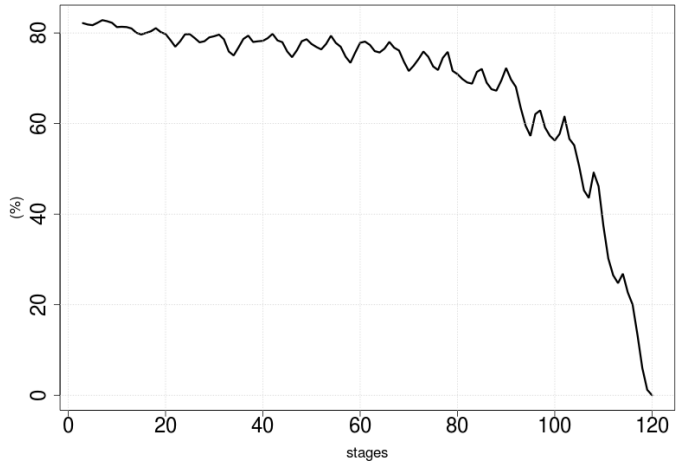

Figure 19: Risk neutral approach: Percentage of redundant cutting planes

3.6.2 Parallel implementation

The simplest design for an SDDP parallel implementation is with an evenly distributed computation load between processors. The idea is that at the end of each iteration, the processors share the cutting planes of the cost-to-go functions that they compute. At the beginning of each iteration, each processor starts with the same model for the cost-to-go function at each stage. Each processor performs a forward step different than the others in order to select different locations where the model is going to be improved. In the backward step, each processor computes 1 cutting plane at each stage. At the end of the backward step, each processor shares with all the others the computed cut. It is basically an all-to-all communication framework. The parallel architecture was implemented using OpenMPI 1.6.1. For the operation planning problem that we consider, each processor will send a message of size $9 \times 8 = 72$ bytes to every other processor (where 8 is the size in bytes to store a double precision floating-point type and 9 is the number of the cutting plane coefficients plus the right hand side). Let P denote the total number of processors.

Figure 20 illustrates the CPU time (in hours) needed to add 5000 cutting planes per stage as function of the number of processors used. A speed up factor of more than 4 times (when compared with the sequential code) is obtained for $P = 10$ to perform 5000 iterations. The experiment with 40 processors (i.e. $P = 40$) less than 5 hours to complete. The SDDP algorithm is, by construction, very adequate to the use of parallel architecture.

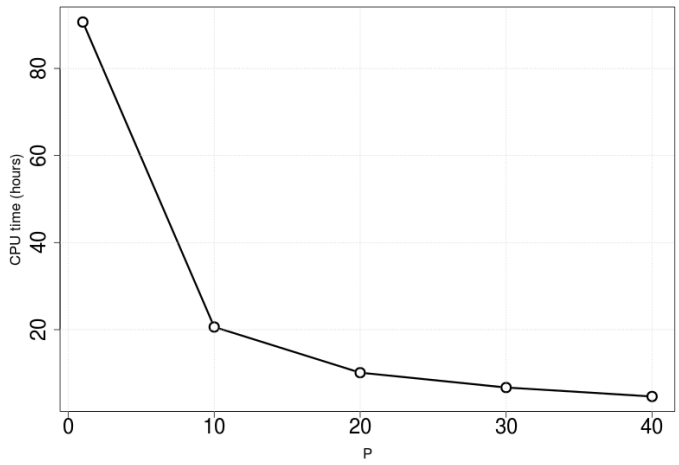

Figure 20: Risk neutral approach: CPU time as function of the number of processors

When a parallel implementation of the algorithm is used, a different strategy is used for the construction of the policy (similar to the case when multiple trial points are used at each iteration in the sequential setting). Indeed, when 1 processor is used, the algorithm decides at each stage one location where to approximate the cost-to-go functions. Then, it updates the model and computes the next point. When multiple processors are used (or equivalently multiple trial solutions per iteration in the sequential code), several different points are computed using the same model approximation at each iteration. One question that we can ask is which strategy is better? In what follows, we try to investigate this issue.

Table 7 summarizes the lower bound and average policy value obtained for experiments using different number of processors. Increasing the number of processors improves the lower bound (i.e. higher value) and the quality of the constructed policy (i.e. lower average policy value).

Table 7: Risk neutral approach: LB and average policy value as function of P

P	1	10	20	30	40
Lower bound	24.036	24.212	24.321	24.412	24.489
Average policy	28.206	28.126	27.950	27.880	27.857

Figure 21 plots the percentage of redundant cutting planes for $P = 1$ (i.e. sequential code) and for $P = 40$. Both of the algorithms were run for 5000 iterations. The parallel implementation has considerably fewer number of redundant cutting planes when compared to the sequential version, especially in the initial stages.

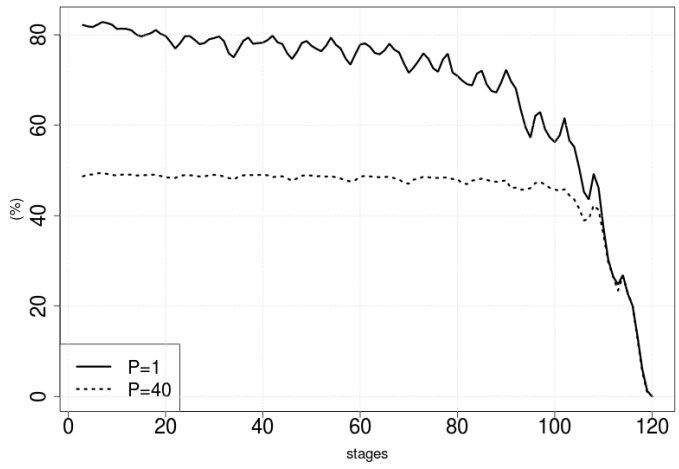

Figure 21: Risk neutral approach: percentage of redundant cutting planes as function of P

All the results presented in this section did not use the subroutine suggested in the previous section. It is worth noting that a combination of the parallel computing technique with the cutting plane elimination subroutine yields a significant performance improvement. A possible implementation could be the following. At some

iteration (chosen according to the argument suggested in the previous section), each processor will run the redundant cutting planes elimination subroutine on a certain set of stages divided evenly among all the processors. For instance, if we have 2 processors, then the first one will run the subroutine on stages 1 to 60 and the other will run it on stages 61 to 120. Once the subroutine has completed running, each processor shares the indices of the redundant cutting planes with the others.

3.7 Discussion

We run the SDDP algorithm for 5000 iterations. Table 8 shows the bounds status and the 95% confidence interval for the policy value. The latter is estimated using 2000 scenarios. The achieved gap is 19.57 %.

Table 8: Risk neutral approach: Bounds and total discounted cost for 120 stages ($\times 10^9$)

		Policy value		
Lower bound	Upper bound	95% C.I. left	Average	95% C.I. right
24.036	28.740	27.557	28.200	28.843

3.7.1 Interpretation of the results

In this section, we analyze the constructed policy. As it was discussed in the previous chapter, the study horizon of the hydro thermal operation planning problem is 60 stages (i.e. 5 years). Table 9 shows the 95% confidence interval for the discounted 60 stage total cost.

Table 9: Risk neutral approach: Total discounted cost for 60 stages ($\times 10^9$)

95% C.I. left	Average	95% C.I. right
16.276	16.806	17.336

Figure 22 plots the average and 99% quantile of individual stage costs for 120 stages. We can observe the seasonal behaviour of the costs. High costs correspond

to dry seasons where thermal generators are used (i.e. costs incur) to compensate for the supply shortage of the hydro plants. Low costs coincide with rainy seasons where the hydro plants deliver more of the load. The relatively high values observed in the peaks of the 99% quantile of the costs are equivalent to extreme scenarios occurring. The occurrence of such scenarios in reality has lead to the 2001/2002 energy crisis in Brazil. In later chapters of this thesis, we will suggest solutions to remedy this problem.

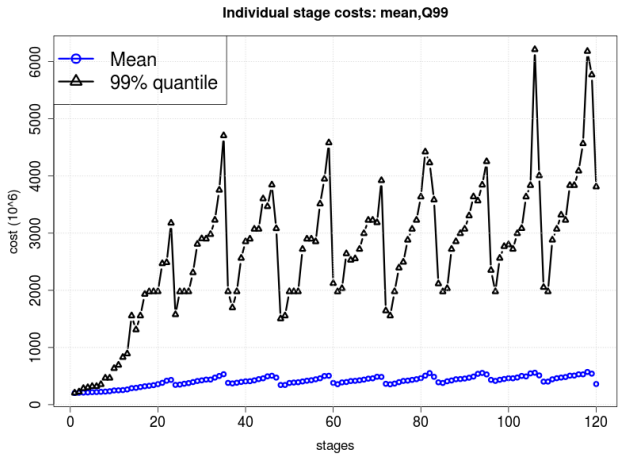

Figure 22: Risk neutral approach: Average and 99% quantile of individual stage costs

Figure 23 plots the boxplot of individual stage costs for 120 stages. For each stage, the thick line within the white box is the median cost for that stage. The lower end of the white box is the 25% quantile and the upper end of the white box is the 75% quantile. Finally, the lower end of the dotted line is the minimum individual stage cost and the upper end of the dotted line is the maximum individual stage cost. The purpose of such plot is to look at the cost distribution at each stage. First, we can notice the deterministic cost at the first stage. Typically, during the rainy season, the extreme high values are lower and there is less variability of the costs when compared to the dry season.

Figure 24 plots the average of individual stage deficit for each of the 4 systems.

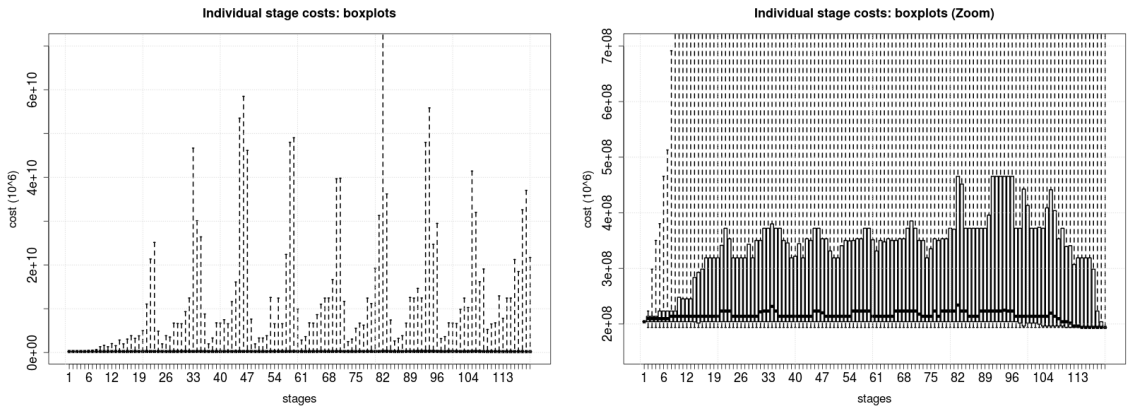

Figure 23: Risk neutral approach: boxplot of individual stage costs

Similarly to the costs, we can notice the seasonality in the deficit. Indeed, most of the incurred cost is coming from the deficit (modelled as fictitious thermal plant as described in the previous chapter). During the initial stages, the incurred deficits are the lowest when compared to future deficits for all systems. This is mainly due to the favourable initial conditions that we consider in our instance (approximately 50% of the reservoirs' total capacity). The (N) system (smallest in capacity) has relatively more recurring deficits. For most of the regions, the energy inflows are higher during December to April (cf. Figure 3). Typically, the deficits (and consequently the costs) attain its peak just prior to these periods.

Figure 25 plots the average, 5% and 95% quantiles of individual stage spillage in MWm for each of the 4 systems. Typically, the spillage occurs during rainy seasons (i.e. December to April). Higher spillage occur in the (SE) system (system with the largest capacity).

Figure 26 plots the average, 5% and 95% quantiles of individual stage storage energy in MWm for each of the 4 systems.

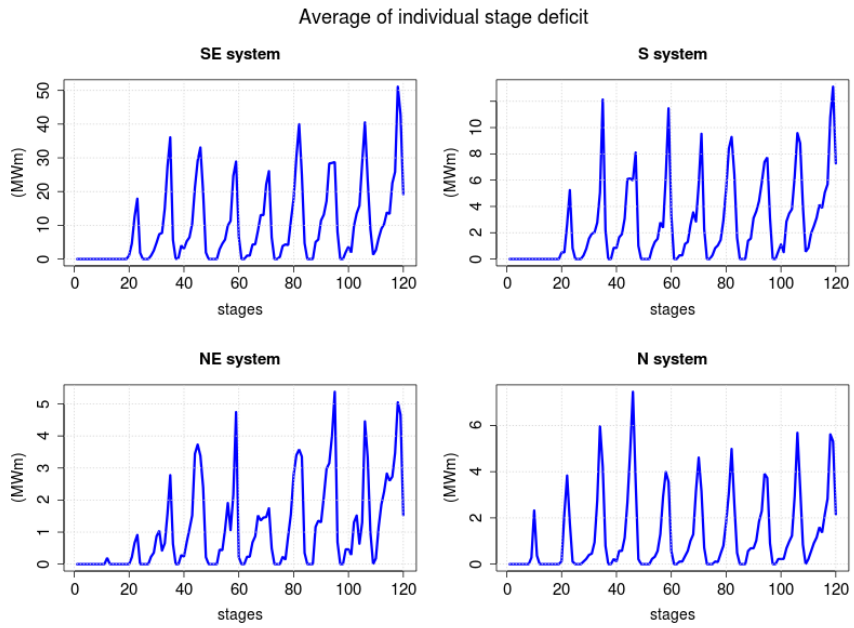

Figure 24: Risk neutral approach: Average of individual stage deficit

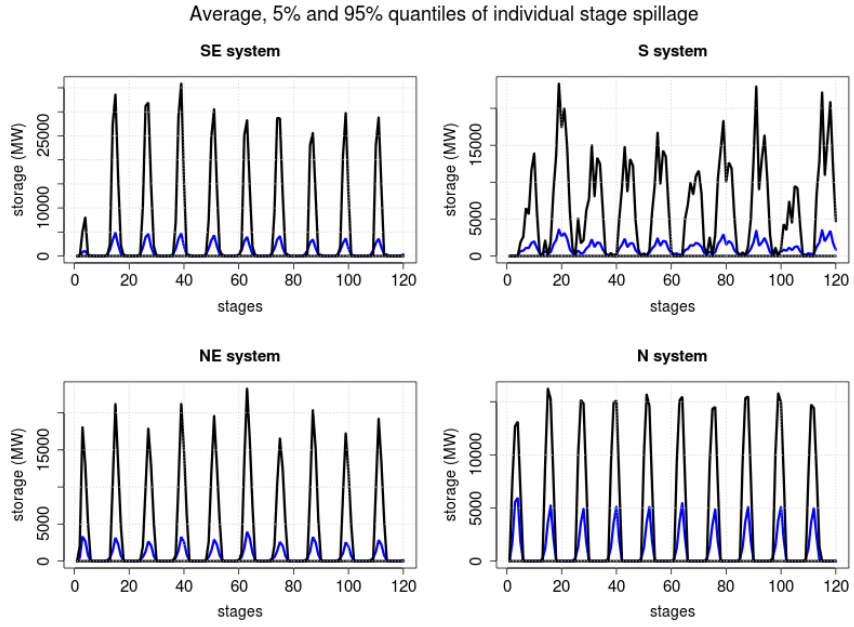

Figure 25: Risk neutral approach: Average, 5% and 95% quantiles of individual stage spillage

3.7.2 Variability of SAA problems

In this section we discuss variability of the bounds of optimal values of the SAA problems. Recall that an SAA problem is based on a randomly generated sample,

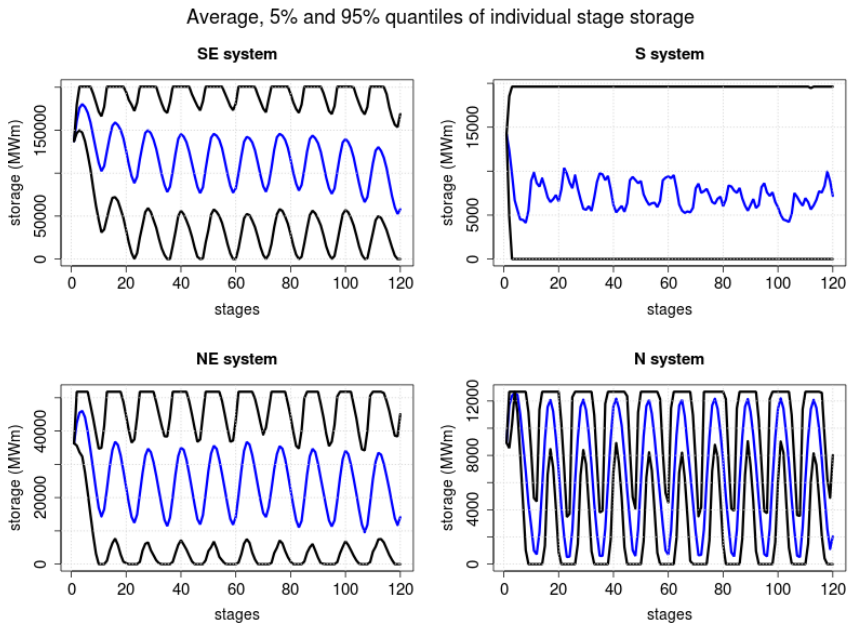

Figure 26: Risk neutral approach: Average, 5% and 95% quantiles of individual stage storage

and consequently is subject to random perturbations, and in itself is an approximation of the "true" problem.

In this experiment we generate twenty SAA problems where each one having $1 \times 100 \times \cdots \times 100 = 100^{119}$ scenarios. Then we run 5000 iterations of the SDDP algorithm for the risk neutral approach. At the last iteration, we perform a forward step to evaluate the obtained policy with 2000 scenarios and compute the average policy value.

Table 10 shows the 95% confidence interval for the lower bound and average policy value at iteration 3000 over a sample of 20 SAA problems. The policy value statistics were computed using a sample of 2000 scenarios. The last 2 columns of the table shows the range divided by the average of the lower bound (where the range is the difference between the maximum and minimum observation) and the standard deviation divided by the average value. This problem has relatively low variability (approx. 4%) for both of the lower bound and the average policy value.

Table 10: Risk neutral approach: SAA variability

	95% C.I. left ($\times 10^9$)	Average ($\times 10^9$)	95% C.I. right ($\times 10^9$)	range/mean	sdev./mean
Lower bound	22.290	22.695	23.100	15.92%	4.07%
Average policy	27.333	27.836	28.339	17.05%	4.12%

3.7.3 Sensitivity to initial conditions and total number of stages

The purpose of this experiment is to investigate the impact of changing initial conditions on the distribution of the individual stage costs. Table 11 shows the initial conditions used in all of the experiments and the maximum storage value for each system.

Table 11: Initial conditions and maximum storage capacity

	SE	S	NE	N
Maximum storage	200,717.6	19,617.2	51,806.1	12,744.9
Reservoir level	119,428.8	11,535.09	29,548.19	6649.39
% of Maximum capacity	56.5 %	58.8%	57.03%	52.17%

We consider the following 2 initial levels: 25% and 75% of the maximum storage capacity in each system. Figure 27 shows the individual stage costs for the risk neutral approach in two cases: all the reservoirs start at 25% or at 75% of the maximum capacity.

When we start with 25% of the maximum capacity in all reservoirs, high costs occur for the first stages which reflects the recourse to the expensive thermal generation to satisfy the demand. Similarly, when we start with 75% of the maximum capacity in all reservoirs low costs occur in the first stages. In both cases the costs become identical starting from 60^{th} stage. This observation support the argument in favour of extending the study horizon (i.e. 60 stages) by an extra 60 stages to take into account the end of horizon effect.

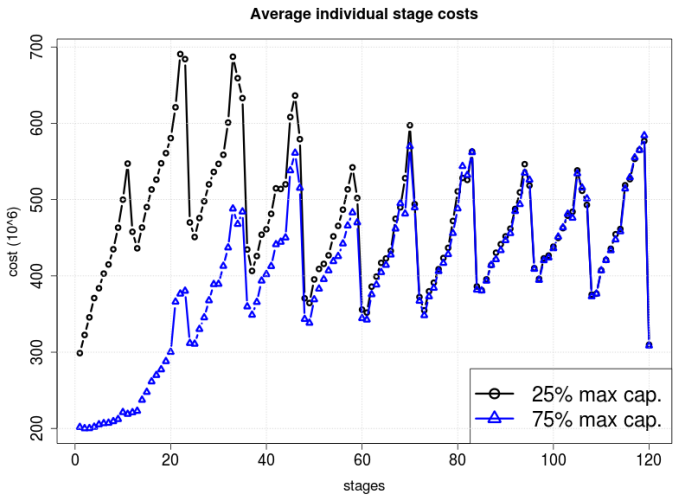

Figure 27: Risk neutral approach: Sensitivity to initial conditions

3.8 Conclusion

In this chapter we investigated the risk neutral approach to multistage stochastic linear programming problems. In section 3.2, we presented the risk neutral formulation of multistage linear stochastic programming problems, the considered assumptions and the methodology that we follow. A generic description of the SDDP algorithm was suggested in section 3.4. In section 3.5, we discussed the stopping criteria of the algorithm and provided a framework for assessing the policy quality. It appears that the SDDP method works reasonably well when the number of state variables is relatively small while the number of stages can be large. However, as the number of state variables increases the convergence of the SDDP algorithm can become very slow. Several aspects of performance improvements of the algorithm were discussed in section 3.6. We suggested a subroutine to eliminate the redundant cutting planes in the future cost functions description which allowed a considerable speed up factor. Also, a design using high performance computing techniques was discussed. Moreover, an analysis of the obtained policy was outlined with focus on specific aspects of the long term operation planning problem in section 3.7. In the risk neutral framework,

extreme events can occur and might cause considerable social costs. These costs can translate into blackouts or forced rationing similarly to what happened in 2001/2002 crisis. In the coming chapters, we will suggest solutions to this problem. Finally, issues related to variability of the SAA problems and sensitivity to initial conditions were studied.

CHAPTER IV

RISK AVERSE APPROACH

4.1 Introduction

Up to this point, the standard risk neutral approach was implemented for planning of the Brazilian power system. The energy rationing that took place in Brazil in the beginning of the last decade raised the question of whether a policy that is based on a criterion of minimizing the expected cost is a valid one when it comes to meet the day-to-day supply requirements. As a consequence, a shift towards a risk averse criterion is underway, so as to enforce the continuity of load supply.

Several risk averse approaches to multistage stochastic programming were suggested in recent literature. Eichhorn and Römisch [12] developed techniques based on polyhedral risk measures. This approach was extended further in Guigues and Römisch [13] to incorporate the SDDP method in order to approximate the corresponding risk averse recourse functions. Theoretical foundations for a risk averse approach based on conditional risk mappings were developed in Ruszczyński and Shapiro [27] (see also [30, Chapter 6]). For risk measures given by convex combinations of the expectation and Average Value-at-Risk, it was shown in [34] how to incorporate this approach into the SDDP algorithm with a little additional effort. This was implemented in an extensive numerical study in Philpott and de Matos [21]. Most of the content of this chapter was published in [36].

This chapter is organized as follows. In section 4.2, we present an overview of some mathematical notions that we will be used in later sections such as coherent and conditional risk measures. A general problem statement and the considered assumptions are put forth, in section 4.3. A generic description of the risk averse SDDP

algorithm is outlined in section 4.4. Finally, computational aspects are analyzed and the contributions of the risk averse methodology when compared to the risk neutral approach are outlined.

4.2 Mathematical background

In this section, we summarize some elements of the mathematical background that needed for this chapter. We refer the reader to [30] and [29] for a detailed treatment and further references.

We consider the following notation. Let $(\Omega, \mathcal{F}, P)$ denotes a probability space. A random variable Z is a measurable function $Z : \Omega \to \mathbb{R}$. $Z \succeq Z'$ is equivalent to $Z(\omega) \geq Z'(\omega)$ for a.e. $\omega \in \Omega$. $\mathcal{L}_p(\Omega, \mathcal{F}, P)$ denotes the space of random variables $Z(\omega)$ with finite p^{th} order moment :

$$\mathbb{E}\left[|Z|^p\right] = \int_\Omega |Z(\omega)|^p dP(\omega) < \infty$$

where $p \in [1, \infty)$. $\mathcal{L}_\infty(\Omega, \mathcal{F}, P)$ denotes the space of random variables $Z(\omega)$ with finite sup-norm (i.e. $\|Z\|_\infty := \operatorname{ess\,sup} |Z| < \infty$) where:

$$\operatorname{ess\,sup}(Z) = \inf \left\{ \sup_{\omega \in \Omega} Z'(\omega) : Z'(\omega) = Z(\omega) \text{ a.e. } \omega \in \Omega \right\}$$

4.2.1 Coherent risk measures

A risk measure is a real valued function $\rho : \mathcal{L}_p(\Omega, \mathcal{F}, P) \to \mathbb{R}$, for some $p \in [1, \infty]$. A risk measure ρ is called law invariant if for any $Z, Z' \in \mathcal{L}_p(\Omega, \mathcal{F}, P)$ such that $Z \overset{d}{=} Z'$, then $\rho(Z) = \rho(Z')$.

Example 1. *An example of a risk measure is the Value-at-risk measure defined as follows*

$$\mathsf{V@R}_\alpha(Z) := \inf \{t : P(Z \leq t) \geq 1 - \alpha\} \tag{40}$$

where $\alpha \in (0,1)$. *In other words,* $\mathsf{V@R}_\alpha(Z)$ *is the left* $(1-\alpha)$ *quantile of the distribution of* Z. *One important observation is that* $\mathsf{V@R}_\alpha$ *is not subadditive (i.e.* $\exists Z, Z' \in \mathcal{L}_p(\Omega, \mathcal{F}, P)$ *such that* $\mathsf{V@R}_\alpha(Z+Z') > \mathsf{V@R}_\alpha(Z) + \mathsf{V@R}_\alpha(Z')$*).*

A coherent risk measure (cf. [1]) is a risk measure that satisfies the following properties (P1)-(P4).

(P1) Monotonicity : if $Z, Z' \in \mathcal{L}_p(\Omega, \mathcal{F}, P)$ and $Z \succeq Z'$, then $\rho(Z) \geq \rho(Z')$

(P2) Convexity : $\forall Z, Z' \in \mathcal{L}_p(\Omega, \mathcal{F}, P)$ and $t \in [0,1]$, we have:

$$\rho(tZ + (1-t)Z') \leq t\rho(Z) + (1-t)\rho(Z')$$

(P3) Translation equivariance : If $a \in \mathbb{R}$ and $Z \in \mathcal{L}_p(\Omega, \mathcal{F}, P)$, then $\rho(Z+a) = \rho(Z) + a$

(P4) Positive homogeneity : If $t \geq 0$ and $Z \in \mathcal{L}_p(\Omega, \mathcal{F}, P)$, then $\rho(tZ) = t\rho(Z)$

It is worth mentioning that

$$(P2) \Leftrightarrow (P4) \text{ and } (P5)$$

where $(P5)$ denotes the subadditivity property:

(P5) Subadditivity : $\forall Z, Z' \in \mathcal{L}_p(\Omega, \mathcal{F}, P)$, we have:

$$\rho(Z+Z') \leq \rho(Z) + \rho(Z')$$

Example 2. *One of the important examples of a coherent risk measure is the Average Value-at-Risk measure defined as follows for* $Z \in \mathcal{L}_1(\Omega, \mathcal{F}, P)$

$$\mathsf{AV@R}_\alpha(Z) := \frac{1}{\alpha}\int_0^\alpha \mathsf{V@R}_\theta(Z)d\theta = \inf_{t\in\mathbb{R}}\left\{t + \frac{1}{\alpha}\mathbb{E}\left[Z-t\right]_+\right\} \tag{41}$$

where $\alpha \in (0,1)$. *It can be shown that* $\mathsf{V@R}_\alpha(Z)$ *is a minimizer of the right hand side of (41). Thus, we have*

$$\mathsf{AV@R}_\alpha(Z) = \mathsf{V@R}_\alpha(Z) + \frac{1}{\alpha}\mathbb{E}\left[Z - \mathsf{V@R}_\alpha(Z)\right]_+$$

Note that $\mathsf{AV@R}_1(Z) = \mathbb{E}[Z]$. *Also, it can be shown that*

$$\lim_{\alpha \to 0} \mathsf{AV@R}_\alpha(Z) = \operatorname{ess\,sup}(Z)$$

It is possible to show that in a certain sense $\mathsf{AV@R}_\alpha(\cdot)$ *gives a best possible upper convex bound for* $\mathsf{V@R}_\alpha(\cdot)$, *(cf. [18]).*

Example 3. *Another important example of a coherent risk measure is the mean-upper-semideviation risk measure defined as follows for* $Z \in \mathcal{L}_p(\Omega, \mathcal{F}, P)$

$$\rho(Z) := \mathbb{E}[Z] + \lambda \left(\mathbb{E}\left[[Z - \mathbb{E}[Z]]_+^p \right] \right)^{1/p} \tag{42}$$

where $p \in [1, \infty)$ *and* $\lambda \in [0, 1]$.

Similarly to expectation (cf. [24, Theorem 14.60]), it was shown in [30, section 6.4] that the interchangeability property holds for monotone risk measures and consequently for coherent risk measures.

4.2.2 Conditional risk measures

In this section, we introduce the notion of conditional risk measure. We refer the reader to [30, Chapter 6] for a discussion of optimization problems involving coherent risk measures.

Let $\mathcal{F}_1$ and $\mathcal{F}_2$ two sigma algebras of Ω such that $\mathcal{F}_1 \subset \mathcal{F}_2$. P is a probability measure on $(\Omega, \mathcal{F}_2)$. A mapping $\rho : \mathcal{L}_p(\Omega, \mathcal{F}_2, P) \to \mathcal{L}_p(\Omega, \mathcal{F}_1, P)$ is a conditional risk mapping if it satisfies the following properties:

(P'1) Monotonicity : if $Z, Z' \in \mathcal{L}_p(\Omega, \mathcal{F}_2, P)$ and $Z \succeq Z'$, then $\rho(Z) \geq \rho(Z')$

(P'2) Convexity : $\forall Z, Z' \in \mathcal{L}_p(\Omega, \mathcal{F}_2, P)$ and $t \in [0, 1]$, we have:

$$\rho(tZ + (1-t)Z') \leq t\rho(Z) + (1-t)\rho(Z')$$

(P'3) Translation equivariance : If $Y \in \mathcal{L}_p(\Omega, \mathcal{F}_1, P)$ and $Z \in \mathcal{L}_p(\Omega, \mathcal{F}_2, P)$, then $\rho(Z + Y) = \rho(Z) + Y$

(P'4) Positive homogeneity : If $t \geq 0$ and $Z \in \mathcal{L}_p(\Omega, \mathcal{F}_2, P)$, then $\rho(tZ) = t\rho(Z)$

Conditional counterpart for the previously considered examples are as follows.

Example 4. *The conditional Value-at-risk measure is defined as follows for* $Z \in \mathcal{L}_1(\Omega, \mathcal{F}_2, P)$ *and* $Y \in \mathcal{L}_p(\Omega, \mathcal{F}_1, P)$

$$\mathsf{V@R}_{\alpha|Y}(Z) := \inf \{t : P(Z \leq t|Y) \geq 1 - \alpha\} \tag{43}$$

where $\alpha \in (0, 1)$. *In other words,* $\mathsf{V@R}_{\alpha|Y}(Z)$ *is the* $(1-\alpha)$ *quantile of the conditional distribution of* Z *given* Y.

Example 5. *The conditional Average Value-at-Risk measure defined as follows for* $Z \in \mathcal{L}_1(\Omega, \mathcal{F}_2, P)$ *and* $Y \in \mathcal{L}_1(\Omega, \mathcal{F}_1, P)$

$$\mathsf{AV@R}_{\alpha|Y}(Z) := \inf_{T \in \mathcal{L}_1(\Omega, \mathcal{F}_1, P)} \left\{ T + \frac{1}{\alpha} \mathbb{E}_{|Y} \left[Z - T \right]_+ \right\} \tag{44}$$

where $\alpha \in (0, 1)$. $\mathsf{V@R}_{\alpha|Y}(Z)$ *is one of the minimizers of the right hand side of (44). We have*

$$\mathsf{AV@R}_{\alpha|Y}(Z) = \mathsf{V@R}_{\alpha|Y}(Z) + \frac{1}{\alpha} \mathbb{E}_{|Y} \left[Z - \mathsf{V@R}_{\alpha|Y}(Z) \right]_+$$

Example 6. *The conditional mean-upper-semideviation risk measure is defined as follows for* $Z \in \mathcal{L}_p(\Omega, \mathcal{F}_2, P)$ *and* $Y \in \mathcal{L}_p(\Omega, \mathcal{F}_1, P)$

$$\rho_{|Y}(Z) := \mathbb{E}_{|Y} \left[Z \right] + \kappa \left(\mathbb{E}_{|Y} \left[\left[Z - \mathbb{E}_{|Y}[Z] \right]_+^p \right] \right)^{1/p} \tag{45}$$

where $p \in [1, \infty)$ *and* $\kappa \in [0, 1]$.

One key aspect for multistage risk averse problems is the composition $\rho \circ \rho_{|Y}$. This composition is in general a delicate issue (cf. [27, section 5]). The tower property (46) is a very attractive feature for a risk measure since it allows, combined the interchange with minimization, to establish the equivalence between the extensive and nested formulation in the case of expectation.

$$\rho \circ \rho_{|Y} = \rho \tag{46}$$

It can be shown that the tower property (46) holds for $\rho(\cdot) = \mathbb{E}[\cdot]$ and $\rho(\cdot) = \operatorname{ess\,sup}(\cdot)$. Furthermore, this property holds for any conditional risk measure where Z and Y are independent (i.e. $\rho \circ \rho_{|Y}(Z) = \rho(Z)$). This property is not true in general for the Average Value-at-Risk (with $\alpha \in (0, 1)$) and Mean-Upper-Semideviation (with $\lambda \in (0, 1]$) risk measures.

4.3 General problem statement and assumptions

4.3.1 Problem statement

In the risk neutral formulation, the total cost is minimized on average subject to the feasibility constraints. Since the costs are functions of the random data process, they are random and hence are subject to random perturbations. For a particular realization of the data process these costs could be much bigger than their expectation. The goal of a risk averse approach is to avoid large values of the costs for some possible realizations of the data process at every stage of the considered time horizon. There are several approaches to tackle this problem.

One such approach will be to maintain constraints $c_t^\mathsf{T} x_t \leq \theta_t$, $t = 1, ..., T$, for chosen upper levels θ_t and all possible realizations of the data process. However, trying to enforce these upper limits under any circumstances could be infeasible. So we can consider penalization approaches instead. That is, at every stage the cost is penalized while exceeding a specified upper limit. In a simple form this leads to a risk averse formulation where costs $c_t^\mathsf{T} x_t$ are penalized by $\phi_t[c_t^\mathsf{T} x_t - \theta_t]_+$, with θ_t and $\phi_t \geq 0$, $t = 2, ..., T$, being chosen constants. That is, the costs $c_t^\mathsf{T} x_t$ are replaced by functions $f_t(x_t) = c_t^\mathsf{T} x_t + \phi_t[c_t^\mathsf{T} x_t - \theta_t]_+$ in the objective of the risk neutral problem (i.e. (3)). With such methodology, the upper limits θ_t are fixed and not adapted to a current realization of the random process.

Another possible approach will be through using coherent risk measures. The nested formulation for the risk averse multistage problem (cf., [27]) is as follows.

$$\underset{\substack{A_1x_1=b_1\\x_1\geq 0}}{\text{Min}} c_1^{\mathsf{T}}x_1 + \rho_{2|\xi_1}\left[\min_{\substack{B_2x_1+A_2x_2=b_2\\x_2\geq 0}} c_2^{\mathsf{T}}x_2 + \cdots + \rho_{T|\xi_{[T-1]}}\Big[\min_{\substack{B_Tx_{T-1}+A_Tx_T=b_T\\x_T\geq 0}} c_T^{\mathsf{T}}x_T\Big]\right] \quad (47)$$

where $\xi_2, ..., \xi_T$ is the random process (formed by the random elements of the data c_t, A_t, B_t, b_t) and $\rho_{2|\xi_1}, \ldots, \rho_{T|\xi_{[T-1]}}$ is a sequence of conditional coherent risk measures with $\rho_{t|\xi_{[t-1]}} : \mathcal{L}_p(\Omega, \mathcal{F}_t, P) \to \mathcal{L}_p(\Omega, \mathcal{F}_{t-1}, P)$, $t = 2, \ldots, T$ and $\mathcal{F}_1 \subset \cdots \subset \mathcal{F}_T$ is a sequence of sigma algebras generated by the data process $\xi_2, ..., \xi_T$ with $\mathcal{F}_1 = \{\emptyset, \Omega\}$.

Some examples for such conditional coherent risk mappings are :

- Mean-$\mathsf{AV@R}$ risk measure:

$$\rho_{t|\xi_{[t-1]}}[Z] = (1-\lambda_t)\mathbb{E}\left[Z|\xi_{[t-1]}\right] + \lambda_t \mathsf{AV@R}_{\alpha_t}\left[Z|\xi_{[t-1]}\right], \quad (48)$$

  with $\lambda_t \in [0,1]$ and $\alpha_t \in (0,1)$ being chosen parameters.

- Mean-Upper-Semideviation risk measure:

$$\rho_{t|\xi_{[t-1]}}(Z) := \mathbb{E}\left[Z|\xi_{[t-1]}\right] + \kappa\left(\mathbb{E}\left[\left[Z - \mathbb{E}[Z|\xi_{[t-1]}]\right]_+^p |\xi_{[t-1]}\right]\right)^{1/p} \quad (49)$$

  where $p \in [1, \infty)$ and $\kappa \in [0,1]$.

A possible interpretation of the adaptive risk averse formulation using the Mean-$\mathsf{AV@R}$ risk measure (48) is as follows. We have seen in the previous section that $\mathsf{AV@R}_\alpha[Z] \geq \mathsf{V@R}_\alpha(Z)$. Therefore $\rho_{t|\xi_{[t-1]}}[Z] \geq \varrho_{t|\xi_{[t-1]}}[Z]$, where

$$\varrho_{t|\xi_{[t-1]}}[Z] = (1-\lambda_t)\mathbb{E}\left[Z|\xi_{[t-1]}\right] + \lambda_t \mathsf{V@R}_{\alpha_t}\left[Z|\xi_{[t-1]}\right]. \quad (50)$$

If we replace $\rho_{t|\xi_{[t-1]}}[Z]$ in the risk averse formulation (47) by $\varrho_{t|\xi_{[t-1]}}[Z]$, we will be minimizing the weighted average of means and $(1-\alpha)$-quantiles, which will be a natural way of dealing with the involved risk. Unfortunately such formulation will lead to a nonconvex and computationally intractable problem. This is one of the

main reasons for using $\mathsf{AV@R}_\alpha$ instead of $\mathsf{V@R}_\alpha$ in the corresponding risk averse formulations.

Note that the nested formulation (47) with $\rho_{t|\xi_{[t-1]}}(\cdot) = \mathbb{E}(\cdot|\xi_{[t-1]})$ is exactly the same as the nested formulation of the risk neutral case (13). In the risk neutral approach, an equivalence between the nested formulation (13) and an extensive formulation (11) was pointed in Chapter 1. So, what about the extensive formulation for the risk averse approach?

Using the interchangeability property between the minimization and risk measures (cf., [28, Theorem 7.1]), the nested formulation (47) can be written as follows.

$$\begin{array}{ll} \text{Min}_{x_1, x_2(\cdot), \ldots, x_T(\cdot)} & c_1^\mathsf{T} x_1 + \rho_{2|\xi_1}\left[c_2^\mathsf{T} x_2(\xi_{[2]}) + \cdots + \rho_{T|\xi_{[T-1]}}\left[c_T^\mathsf{T} x_T(\xi_{[T]})\right]\right] \\ s.t. & A_1 x_1 = b_1, x_1 \geq 0 \\ & x_t(\xi_{[t]}) \in \chi_t(x_{t-1}(\xi_{[t-1]}), \xi_t), t = 2, \ldots, T \end{array} \tag{51}$$

where $\chi_t(x_{t-1}, \xi_t) = \{x_t : B_t x_{t-1} + A_t x_t = b_t, x_t \geq 0\}$, $t = 2, \ldots, T$. $\xi_1 = (c_1, A_1, b_1)$ is deterministic and $\xi_t = (c_t, A_t, B_t, b_t)$, $t = 2, ..., T$ denotes the stochastic data process formed by the vectors c_t, b_t and matrices A_t, B_t.

The translation equivariance property (i.e. property (P'3)) allows to write (51) in the following manner.

$$\begin{array}{ll} \text{Min}_{x_1, x_2(\cdot), \ldots, x_T(\cdot)} & \widehat{\rho}\left[c_1^\mathsf{T} x_1 + c_2^\mathsf{T} x_2(\xi_{[2]}) + \cdots + c_T^\mathsf{T} x_T(\xi_{[T]})\right] \\ s.t. & A_1 x_1 = b_1, x_1 \geq 0 \\ & x_t(\xi_{[t]}) \in \chi_t(x_{t-1}(\xi_{[t-1]}), \xi_t), t = 2, \ldots, T \end{array} \tag{52}$$

where $\widehat{\rho}(\cdot) = \rho_{2|\xi_1} \circ \cdots \circ \rho_{T|\xi_{[T-1]}}(\cdot)$. $\widehat{\rho}(\cdot)$ is also a coherent risk measure. Although it is tempting to write that $\widehat{\rho}(\cdot) = \rho(\cdot)$, this is not true in general (it is true for expectation, leading the extensive formulation (13) of the risk neutral case). Regrettably, there is no easy way to find a closed form formulation for $\widehat{\rho}(\cdot)$ in general (cf., [27]).

However, the good news is that the nested formulation (47) allows to write the

following dynamic programming equations.

$$Q_t\left(x_{t-1}, \xi_{[t]}\right) = \underset{x_t \in \mathbb{R}^{n_t}}{\text{Min}} \left\{ c_t^{\mathsf{T}} x_t + \mathcal{Q}_{t+1}(x_t, \xi_{[t]}) : B_t x_{t-1} + A_t x_t = b_t,\ x_t \geq 0 \right\}, \tag{53}$$

with

$$\mathcal{Q}_{t+1}\left(x_t, \xi_{[t]}\right) := \rho_{t+1|\xi_{[t]}}\left[Q_{t+1}\left(x_t, \xi_{[t+1]}\right)\right]. \tag{54}$$

At the first stage, problem

$$\underset{x_1 \in \mathbb{R}^{n_1}}{\text{Min}}\ c_1^{\mathsf{T}} x_1 + \mathcal{Q}_2(x_1, \xi_1)\ \text{ s.t. } A_1 x_1 = b_1,\ x_1 \geq 0, \tag{55}$$

should be solved.

4.3.2 Assumptions

First, we assume that at each stage $t = 1, \ldots, T-1$ the problem has relatively complete recourse (cf. section 2.4).

Similarly to the risk neutral case, we make the assumption that the random data process is stagewise independent, i.e., random vector ξ_{t+1} is independent of $\xi_{[t]} = (\xi_1, ..., \xi_t)$ for $t = 1, ..., T-1$. Under the stagewise independence assumption, the cost-to-go function $\mathcal{Q}_t(x_{t-1}, \xi_{[t-1]})$, for $t = T, \ldots, 2$, is independent of $\xi_{[t-1]}$. Thus, the dynamical programming equations can be written in the form

$$Q_t(x_{t-1}, \xi_t) = \min_{\substack{B_t x_{t-1} + A_t x_t = b_t \\ x_t \geq 0}} \left\{ c_t^{\mathsf{T}} x_t + \mathcal{Q}_{t+1}(x_t) \right\} \tag{56}$$

where

$$\mathcal{Q}_{t+1}(x_t) := \rho_{t+1}\left[Q_{t+1}(x_t, \xi_{t+1}) \right] \tag{57}$$

with $\mathcal{Q}_{T+1}(\cdot) \equiv 0$. Note that because of the stagewise independence, the cost-to-go functions $\mathcal{Q}_{t+1}\big(x_t\big)$ and the risk measures ρ_{t+1} in (54) do not depend on the data process. Note also that since the considered risk measures are convex and monotone, the cost-to-go functions $\mathcal{Q}_{t+1}\big(x_t\big)$ are convex (cf., [30, section 6.7.3]).

4.4 Description of the risk averse algorithm

With a relatively simple additional effort the SDDP algorithm can be applied to risk averse problems of the form (47).

4.4.1 Backward step for mean-upper-semideviation risk measures

For risk measures of the form (49), the dynamic programming equations of the SAA problem take the form

$$Q_{tj}(x_{t-1}) = \inf_{x_t \in \mathbb{R}^{n_t}} \left\{ c_{tj}^{\mathsf{T}} x_t + \mathcal{Q}_{t+1}(x_t) : B_{tj} x_{t-1} + A_{tj} x_t = b_{tj},\ x_t \geq 0 \right\}, \tag{58}$$

for $j = 1, ..., N_{t-1}$, with

$$\mathcal{Q}_{t+1}(x_t) = \widehat{Q}_{t+1}(x_t) + \kappa_t \left(\frac{1}{N_t} \sum_{j=1}^{N_t} \left[Q_{t+1,j}(x_t) - \widehat{Q}_{t+1}(x_t) \right]_+^p \right)^{1/p}, \tag{59}$$

$t = T, ..., 2$ and $Q_{T+1}(\cdot) \equiv 0$, where

$$\widehat{Q}_{t+1}(x_t) = \frac{1}{N_t} \sum_{j=1}^{N_t} Q_{t+1,j}(x_t).$$

The optimal value of the SAA problem is given by the optimal value of the first stage problem

$$\operatorname*{Min}_{x_1 \in \mathbb{R}^{n_1}} c_1^{\mathsf{T}} x_1 + \mathcal{Q}_2(x_1) \ \text{ s.t. } A_1 x_1 = b_1,\ x_1 \geq 0. \tag{60}$$

In order to apply the backward step of the SDDP algorithm we need to know how to compute subgradients of the right hand side of (59). Let us consider first the case of $p = 1$. Then (59) becomes

$$\mathcal{Q}_{t+1}(x_t) = \widehat{Q}_{t+1}(x_t) + \frac{\kappa_t}{N_t} \sum_{j=1}^{N_t} \left[Q_{t+1,j}(x_t) - \widehat{Q}_{t+1}(x_t) \right]_+. \tag{61}$$

Let $\gamma_{t+1,j}$ be a subgradient of $Q_{t+1,j}(x_t)$, $j = 1, ..., N_t$, at the considered point x_t. In principle it could happen that $Q_{t+1,j}(\,\cdot\,)$ is not differentiable at x_t, in which case it will have more than one subgradient at that point. Fortunately we need just one (any one) of its subgradients.

Then the corresponding subgradient of $\widehat{Q}_{t+1}(x_t)$ is

$$\widehat{\gamma}_{t+1} = \frac{1}{N_t}\sum_{j=1}^{N_t} \gamma_{t+1,j}, \tag{62}$$

and the subgradient of $\left[Q_{t+1,j}(x_t) - \widehat{Q}_{t+1}(x_t)\right]_+$ is

$$\nu_{t+1,j} = \begin{cases} 0 & \text{if} \quad Q_{t+1,j}(x_t) - \widehat{Q}_{t+1}(x_t) < 0, \\ \gamma_{t+1,j} - \widehat{\gamma}_{t+1} & \text{if} \quad Q_{t+1,j}(x_t) - \widehat{Q}_{t+1}(x_t) > 0, \end{cases} \tag{63}$$

and hence the subgradient of $\mathcal{Q}_{t+1}(x_t)$ is

$$g_{t+1} = \widehat{\gamma}_{t+1} + \frac{\kappa_t}{N_t}\sum_{j=1}^{N_t} \nu_{t+1,j}. \tag{64}$$

In the backward step of the SDDP algorithm the above formulas are applied to the piecewise linear lower approximations $\mathfrak{Q}_{t+1}(\cdot)$ exactly in the same way as in the risk neutral case.

Let us consider now the case of $p > 1$. Note that then the cost-to-go functions of the SAA problem are no longer piecewise linear. Nevertheless the lower approximations $\mathfrak{Q}_{t+1}(\cdot)$ are still constructed by using cutting planes and are convex piecewise linear. Similar to (64) the corresponding subgradient of $\mathcal{Q}_{t+1}(x_t)$ is (by the chain rule)

$$g_{t+1} = \widehat{\gamma}_{t+1} + p^{-1}\kappa_t q^{p^{-1}-1}\frac{1}{N_t}\sum_{j=1}^{N_t} \eta_{t+1,j}, \tag{65}$$

where $q = \frac{1}{N_t}\sum_{j=1}^{N_t}\left[Q_{t+1,j}(x_t) - \widehat{Q}_{t+1}(x_t)\right]_+^p$ and

$$\eta_{t+1,j} = \begin{cases} 0 & \text{if} \quad Q_{t+1,j}(x_t) - \widehat{Q}_{t+1}(x_t) < 0, \\ p[Q_{t+1,j}(x_t) - \widehat{Q}_{t+1}(x_t)]^{p-1}(\gamma_{t+1,j} - \widehat{\gamma}_{t+1}) & \text{if} \quad Q_{t+1,j}(x_t) - \widehat{Q}_{t+1}(x_t) > 0. \end{cases} \tag{66}$$

4.4.2 Backward step for mean-AV@R risk measures

Let us consider risk measures of the form (48), i.e.,

$$\rho_t(Z) = (1-\lambda_t)\mathbb{E}[Z] + \lambda_t \mathsf{AV@R}_{\alpha_t}[Z]. \tag{67}$$

The cost-to-go functions of the corresponding SAA problem are

$$\mathcal{Q}_{t+1}\big(x_t\big) = (1-\lambda_t)\widehat{Q}_{t+1}\big(x_t\big)+\lambda_t \left(Q_{t+1,\iota}\big(x_t\big) + \frac{1}{\alpha_t N_t}\sum_{j=1}^{N_t} \big[Q_{t+1,j}\big(x_t\big) - Q_{t+1,\iota}\big(x_t\big)\big]_+ \right), \tag{68}$$

where $\iota \in \{1,...,N_t\}$ corresponds to the $(1-\alpha_t)$ sample quantile, i.e., numbers $Q_{t+1,j}\big(x_t\big)$, $j = 1,...,N_t$, are arranged in the increasing order $Q_{t+1,\pi(1)}\big(x_t\big) \leq ... \leq Q_{t+1,\pi(N_t)}\big(x_t\big)$ and $\iota = \hat{j}$ such that $\pi(\hat{j})$ is the smallest integer such that $\pi(\hat{j}) \geq (1-\alpha_t)N_t$. Note that if $(1-\alpha_t)N_t$ is not an integer, then ι remains the same for small perturbations of x_t.

The corresponding subgradient of $\mathcal{Q}_{t+1}\big(x_t\big)$ is

$$g_{t+1} = (1-\lambda_t)\widehat{\gamma}_{t+1} + \lambda_t \left(\gamma_{t+1,\iota} + \frac{1}{\alpha_t N_t}\sum_{j=1}^{N_t} \zeta_{t+1,j} \right), \tag{69}$$

where

$$\zeta_{t+1,j} = \begin{cases} 0 & \text{if} \quad Q_{t+1,j}\big(x_t\big) - Q_{t+1,\iota}\big(x_t\big) < 0, \\ \gamma_{t+1,j} - \gamma_{t+1,\iota} & \text{if} \quad Q_{t+1,j}\big(x_t\big) - Q_{t+1,\iota}\big(x_t\big) \geq 0. \end{cases} \tag{70}$$

The above approach is simpler than the one suggested in [34], and seems to be working as well.

4.4.3 Forward step

The constructed lower approximations $\mathfrak{Q}_t(\cdot)$ of the cost-to-go functions define a feasible policy and hence can be used in the forward step procedure in the same way as it was discussed in section 3.4. That is, for a given scenario (sample path), starting with a feasible first stage solution $\bar{x}_1$, decisions $\bar{x}_t$, $t = 2,...,T$, are computed recursively going forward with $\bar{x}_t$ being an optimal solution of

$$\underset{x_t}{\text{Min}}\, c_t^{\mathsf{T}} x_t + \mathfrak{Q}_{t+1}(x_t) \;\; \text{s.t. } A_t x_t = b_t - B_t \bar{x}_{t-1},\; x_t \geq 0, \tag{71}$$

for $t = 2,...,T$. These optimal solutions can be used as trial decisions in the backward step of the algorithm.

Unfortunately there is no easy way to evaluate the risk-adjusted cost

$$c_1^{\mathsf{T}}\bar{x}_1 + \rho_{2|\xi_1}\left[c_2^{\mathsf{T}}\bar{x}_2(\xi_{[2]}) + \cdots + \rho_{T|\xi_{[T-1]}}\left(c_T^{\mathsf{T}}\bar{x}_T(\xi_{[T]})\right)\right] \tag{72}$$

of the obtained policy, and hence to construct an upper bound for the optimal value of the corresponding risk-averse problem (47). Therefore a stopping criterion based on stabilization of the lower bound was used in numerical experiments. Of course, the expected value (33) of the constructed policy can be estimated in the same way as in the risk neutral case by the averaging procedure.

4.4.4 Generic description of the risk averse SDDP

An algorithmic description for the Mean-AV@R risk averse SDDP algorithm with M trial points per iteration is presented in Algorithm 3.

4.5 Computational results

The numerical experiments are performed on an aggregated representation of the Brazilian Interconnected Power System operation planning problem with historical data as of January 2012. The study horizon is of 60 stages and the total number of considered stages is 120.

We implement two versions of the risk averse SDDP algorithm, one with the mean-AV@R and one with the mean-upper-semideviation risk measures both applied to solve the problem with the model described in chapter 2.

The SAA tree, generated in both cases, has 100 realizations in every stage with a total number of scenarios $1 \times 100 \times \cdots \times 100 = 100^{119}$. In the following experiments we run the SDDP algorithm with 1 trial solution per iteration for 5000 iterations. The individual stage costs and policy value are evaluated using 2000 randomly generated scenarios. Both implementations were written in C++ and using Gurobi 5.0. The codes were run on 1 core of (2 quad-core Intel E5520 Xeons 2.26GHz, and 24GB RAM) machine. Dual simplex was used as a default method for the LP solver.

Algorithm 3 Risk averse SDDP algorithm (Mean-AV@R)

Require: $\left\{\mathfrak{Q}_t^0\right\}_{t=2,...,T+1}$(Init. lower approx.), $\{\alpha_t, \lambda_t\}_{t=2,...,T+1} \in [0,1]$ and i_{max}(max. iterations)

Initialize: $i \leftarrow 0$, $\underline{z} = -\infty$ (Lower bound)
while $i < i_{max}$ **do**
  Sample M scenarios: $\left\{\{c_{tk}, A_{tk}, B_{tk}, b_{tk}\}_{2\leq t\leq T}\right\}_{1\leq k\leq M}$

  (Forward step)
  for $k = 1 \rightarrow M$ **do**
    for $t = 1 \rightarrow T$ **do**
      $\bar{x}_t^k \leftarrow \arg\min_{x_t\in\mathbb{R}^{n_t}} \left\{ \begin{array}{l} c_{tk}^\top x_t + \mathfrak{Q}_{t+1}^i(x_t) : \\ B_{tk}x_{t-1} + A_{tk}x_t = b_{tk}, x_t \geq 0 \end{array} \right\}$
    end for
  end for

  (Backward step)
  for $k = 1 \rightarrow M$ **do**
    for $t = T \rightarrow 2$ **do**
      for $j = 1 \rightarrow N_t$ **do**
        $\left[\widetilde{Q}_{tj}(\bar{x}_{t-1}^k), \widetilde{\pi}_{tj}^k\right] \leftarrow \min_{x_t\in\mathbb{R}^{n_t}} \left\{ \begin{array}{l} c_{tj}^\top x_t + \mathfrak{Q}_{t+1}^i(x_t) : \\ B_{tj}\bar{x}_{t-1} + A_{tj}x_t = b_{tj}, x_t \geq 0 \end{array} \right\}$
      end for
      $\iota \in \{1, ..., N_t\} = (1-\alpha_t)$ sample quantile of $\left\{\widetilde{Q}_{tj}(\bar{x}_{t-1}^k)\right\}_{j\in\{1,...,N_t\}}$
      $\widehat{Q}_t(\bar{x}_{t-1}^k) := \frac{1}{N_t}\sum_{j=1}^{N_t} \widetilde{Q}_{t,j}(\bar{x}_{t-1}^k)$, $g_{tj}^k := -\tilde{\pi}_{tj}^k \widetilde{B}_{t,j}$,$\widehat{g}_t^k := \frac{1}{N_t}\sum_{j=1}^{N_t} g_{tj}^k$
      $S_{t,j}^k := \left[Q_{t,j}\left(\bar{x}_{t-1}^k\right) - Q_{t,\iota}\left(\bar{x}_{t-1}^k\right)\right]_+$
      $\widetilde{\mathcal{Q}}_t\left(\bar{x}_{t-1}^k\right) = (1-\lambda_{t-1})\widehat{Q}_t\left(\bar{x}_{t-1}^k\right) + \lambda_t\left(Q_{t,\iota}\left(\bar{x}_{t-1}^k\right) + \frac{1}{\alpha_t N_t}\sum_{j=1}^{N_t} S_{t,j}^k\right)$
      $\tilde{g}_t^k = (1-\lambda_t)\widehat{g}_t^k + \lambda_t\left(g_{t\iota}^k + \frac{1}{\alpha_t N_t}\sum_{j=1}^{N_t}\left[g_{tj}^k - g_{t\iota}^k\right] \times \mathbf{1}_{Q_{t,j}(\bar{x}_{t-1}^k)\geq Q_{t,\iota}(\bar{x}_{t-1}^k)}\right)$
      $\mathfrak{Q}_t^{i+1} \leftarrow \{x_{t-1} \in \mathfrak{Q}_t^i : -\tilde{g}_t^k x_{t-1} \geq \widetilde{\mathcal{Q}}_t(\bar{x}_{t-1}^k) - \tilde{g}_t^k \bar{x}_{t-1}^k\}$
    end for
  end for

  (Lower bound update)
  $\underline{z} \leftarrow \min_{x_1\in\mathbb{R}^{n_1}} \left\{c_1^\top x_1 + \mathfrak{Q}_2(x_1) : A_1x_1 = b_1, x_1 \geq 0\right\}$

  $i \leftarrow i + 1$
end while

4.5.1 Mean-AV@R risk measures

In this section, we investigate computational results related to the mean-AV@R risk averse SDDP applied to the hydrothermal operation planning problem with the time series model of the energy inflows suggested in chapter 2.

Figure 28 shows the total policy value for 120 stages at iteration 5000 for $\alpha \in \{0.05, 0.1\}$ and $\lambda \in \{0, 0.05, 0.1, \ldots, 0.55\}$. The line with triangles corresponds to $\alpha = 0.1$ and the line with circles corresponds to $\alpha = 0.05$. The average, the 95% and 99% quantiles of the policy value are plotted. As λ increases the average of the policy value for 120 stages increases when compared to the risk neutral case (i.e. $\lambda = 0$). The rate of increase for $\alpha = 0.1$ is lower than the rate of increase for $\alpha = 0.05$. This is expected since $\alpha = 0.1$ targets minimizing lower quantile value than $\alpha = 0.05$. A reduction in the 95% quantile is observed for $\lambda \in [0, 0.3]$ when compared with the risk neutral approach and a similar behaviour occurs for the 99% quantile when $\lambda \in [0, 0.5]$.

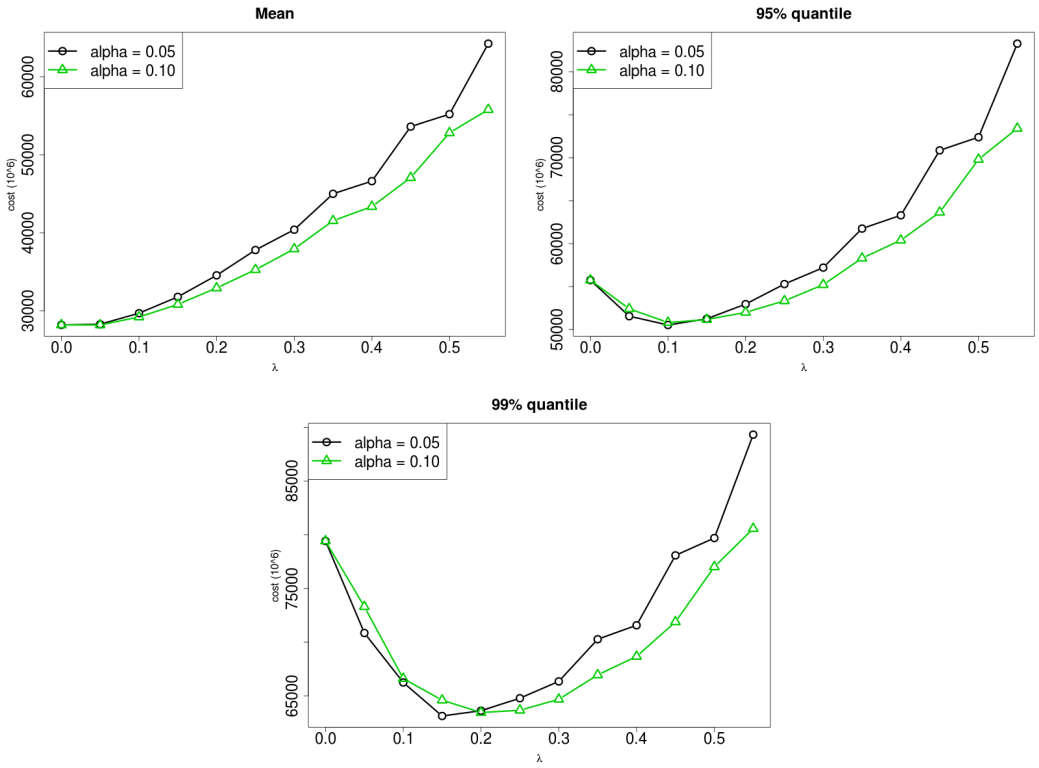

Figure 28: Mean-AV@R approach: Total policy value for 120 stages for $\alpha \in \{0.05, 0.1\}$ as function of λ

Table 12 summarizes the change in percentage of the average, 95% and 99% quantiles of the policy value. The highest reduction in the 99% quantile was achieved by

$\lambda = 0.15$ and $\alpha = 0.05$ (20.53% reduction when compared to the risk neutral case). For $\alpha = 0.05$, the 95% quantile was decreased the most by 9.37% when compared to the risk neutral method for $\lambda = 0.1$. When $\lambda = 0.1$, the recorded loss on average for $\alpha = 0.05$ is 5.30% and for $\alpha = 0.10$ is 3.58%. From these results, it seems that a reasonable choice of the parameters for the risk averse approach is $\alpha = 0.10$ and $\lambda = 0.10$. This choice implies a very moderate loss on average of 3.58% and a reasonable reduction in the 95% and 99% quantiles (8.85% and 16.14% respectively). This choice is also reasonable when we consider the study horizon of 60 stages (cf. Figure 29 and Table 13).

Table 12: Mean-AV@R approach: 120 stages policy value change in %

	$\alpha = 0.05$				$\alpha = 0.10$			
λ	0.05	0.10	0.15	0.20	0.05	0.10	0.15	0.20
Mean	0.30	5.30	12.73	22.52	-0.05	3.58	9.30	16.76
95% quantile	-7.53	-9.37	-8.08	-5.01	-6.00	-8.85	-8.23	-6.74
99% quantile	-10.79	-16.60	-20.53	-19.91	-7.71	-16.14	-18.68	-20.13

Since the study horizon of our problem is the first 60 stages, we plot in Figure 29 the total policy value for 60 stages at iteration 5000 for $\alpha \in \{0.05, 0.1\}$ and $\lambda \in \{0, 0.05, 0.1, \ldots, 0.55\}$. The line with triangles corresponds to $\alpha = 0.1$ and the line with circles corresponds to $\alpha = 0.05$. The figure plots the average and the 95% and 99% quantiles of the policy value. Table 13 shows the change in percentage of the average, 95% and 99% quantiles of the policy value for 60 stages.

Table 13: Mean-AV@R approach: 60 stages policy value change in %

	$\alpha = 0.05$				$\alpha = 0.10$			
λ	0.05	0.10	0.15	0.20	0.05	0.10	0.15	0.20
Mean	3.87	12.41	22.73	35.27	2.93	9.79	17.79	27.61
95% quantile	-6.85	-8.64	-5.61	-2.11	-6.12	-7.52	-7.58	-5.52
99% quantile	-13.57	-19.49	-22.68	-22.92	-10.73	-18.34	-22.39	-22.88

Figure 30 shows the individual stage costs at iteration 5000 for the risk averse

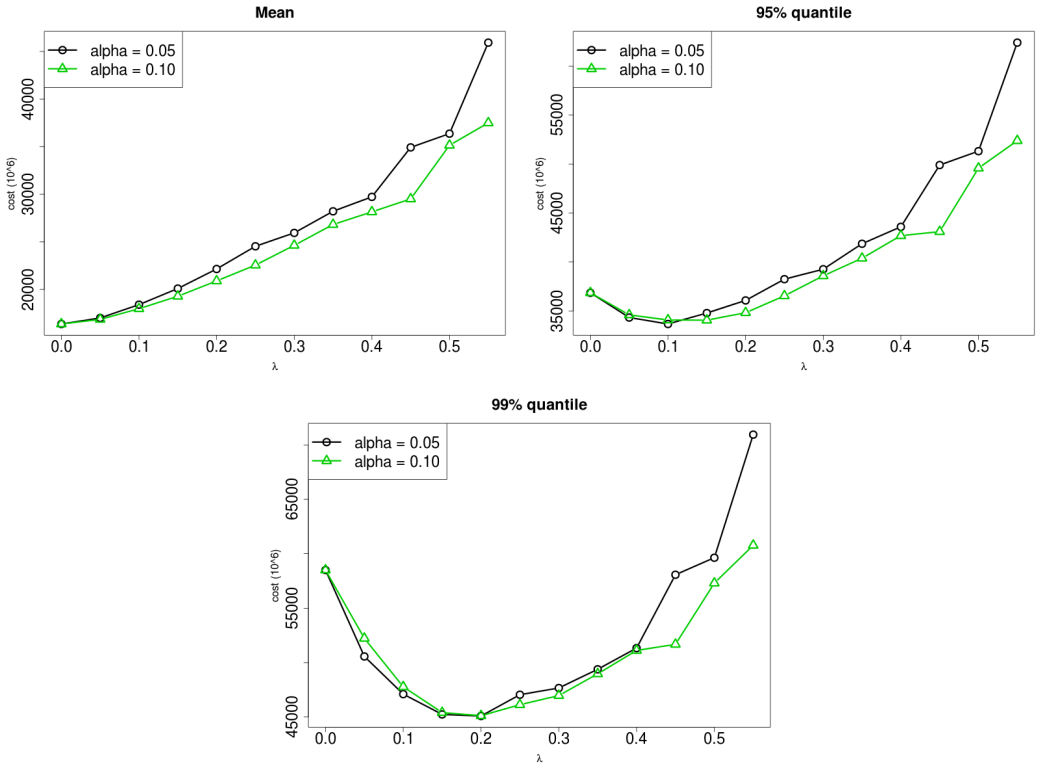

Figure 29: Mean-AV@R approach: Total policy value for 60 stages for $\alpha \in \{0.05, 0.1\}$ as function of λ

approach (with $\lambda = 0.1$ and $\alpha = 0.1$) and the risk neutral approach. The dotted line represents the risk neutral approach and the continuous line represents the risk averse approach. In this figure, we compare the average, 95% and 99% quantiles of individual stage costs. The average costs increase in the first stages and decrease in the final stages. Typically, the increase on average compared to the risk neutral case is observed during rainy seasons. This is due to the risk aversion strategy that consists in consuming less of the hydro resources during rainy seasons so later is could be used in dry seasons. This implies also a reduction in the value of peak average costs during dry seasons. The 95% and 99% quantiles are significantly reduced in the risk averse approach when compared to the risk neutral approach. In other words, the constructed policy is less sensitive to extreme scenarios.

Figure 31 plots the boxplot of individual stage costs for 120 stages. For each stage,

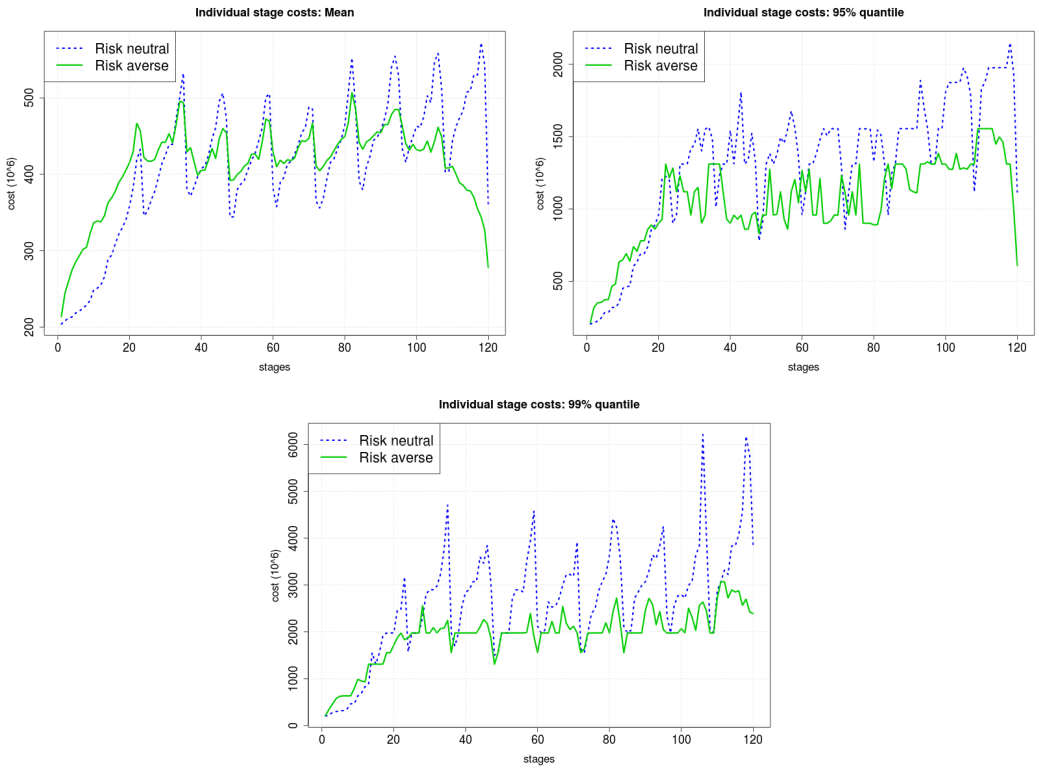

Figure 30: Mean-AV@R approach: Individual stage costs for $\lambda = 0.1$ and $\alpha = 0.1$

the thick line within the white box is the median cost for that stage. The lower end of the white box is the 25% quantile and the upper end of the white box is the 75% quantile. Finally, the lower end of the dotted line is the minimum individual stage cost and the upper end of the dotted line is the maximum individual stage cost. The purpose of such plot is to look at the cost distribution at each stage. We can see the significant reduction in high extreme value when compared to the risk neutral case (cf. Figure 23). Similarly, we can observe the increase in the 25%-75% range.

Figure 32 plots the average deficit in each of the four systems for the risk neutral approach and the risk averse approach with $\alpha = \lambda = 0.1$. The dotted line represents the risk neutral approach and the continuous line represents the risk averse approach. We can observe that the risk averse approach allows a significant reduction in the deficit when compared to the risk neutral method.

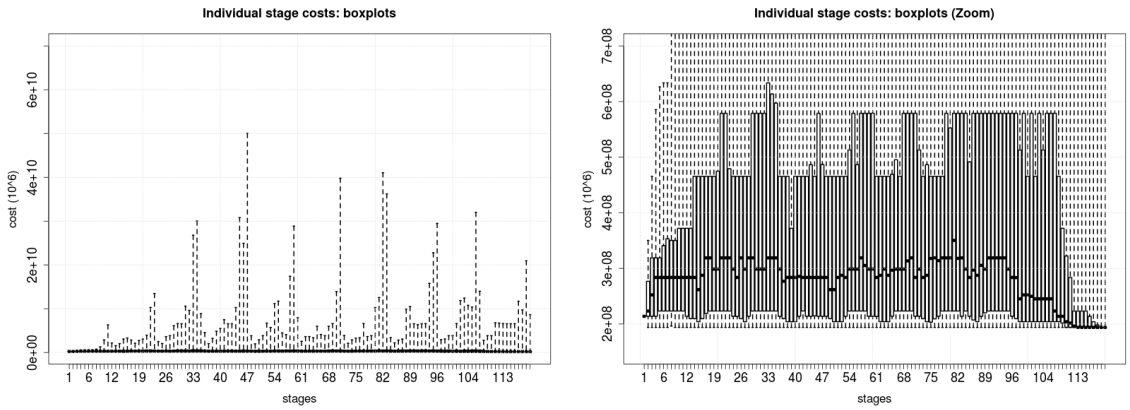

Figure 31: Mean-AV@R approach: boxplot of individual stage costs for $\lambda = 0.1$ and $\alpha = 0.1$

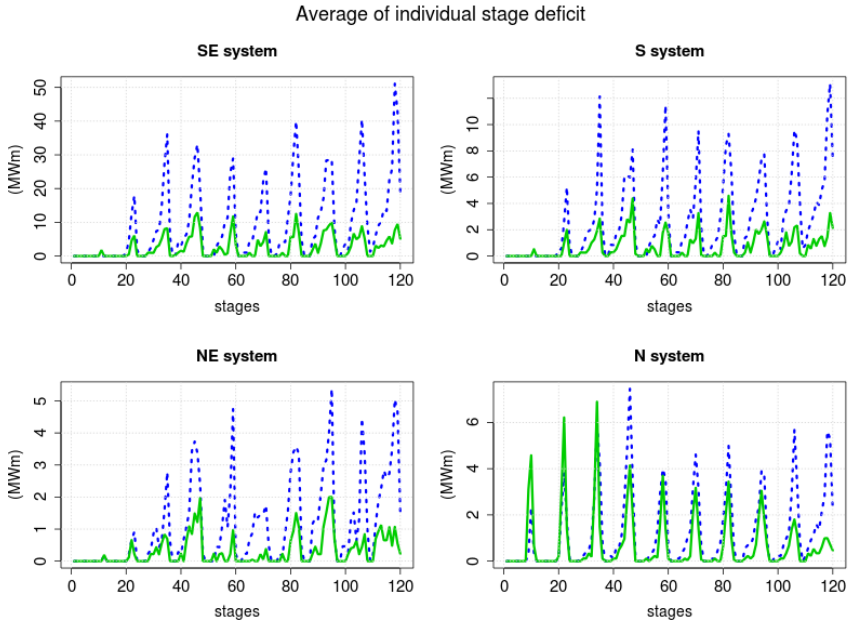

Figure 32: Mean-AV@R approach: Average of individual stage deficit

Figure 33 plots the average storage in each of the four systems for the risk neutral approach and the risk averse approach with $\alpha = \lambda = 0.1$. The dotted line represents the risk neutral approach and the continuous line represents the risk averse approach. We can observe that the risk averse approach improves the average individual stage storage when compared to the risk neutral method.

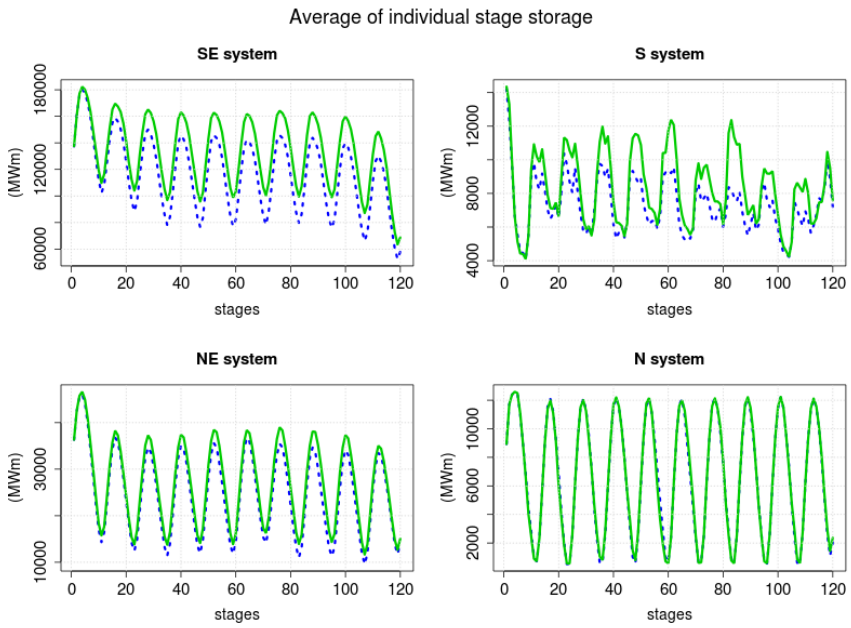

Figure 33: Mean-AV@R approach: Average of individual stage storage

In terms of CPU time, typically there is no loss in CPU time for the risk averse approach when compared to the risk neutral approach. Figure 34 plots the CPU time (in seconds) per iteration for the risk averse approach (continuous,lower line) and risk neutral approach (dotted,upper line). The sudden decreases in CPU time is due to the redundant cutting plane elimination subroutine that is run each 400 iterations in all of our experiments. The risk averse approach spends less CPU time per iteration than the risk neutral approach. This is mainly due to the observation that the risk averse approach has more redundant cutting planes (cf. Figure 35) which the subroutine will remove and allow faster iterations.

Figure 35 plots the percentage of redundant cutting planes for the risk averse approach and risk neutral approach. The risk averse approach has consistently more redundant cutting planes than the risk neutral approach.

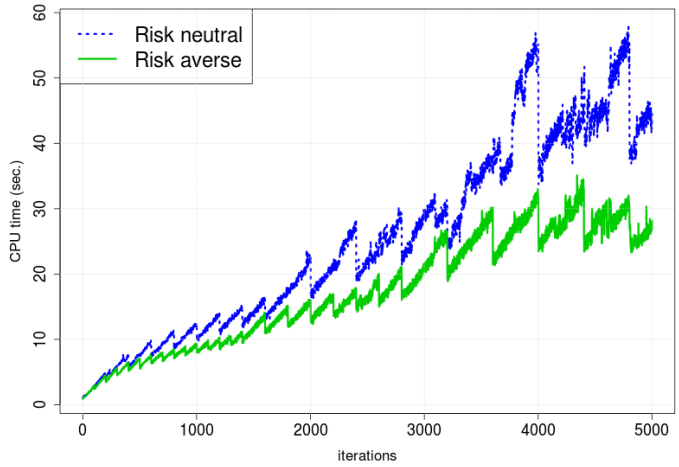

Figure 34: Mean-AV@R approach: CPU time per iteration

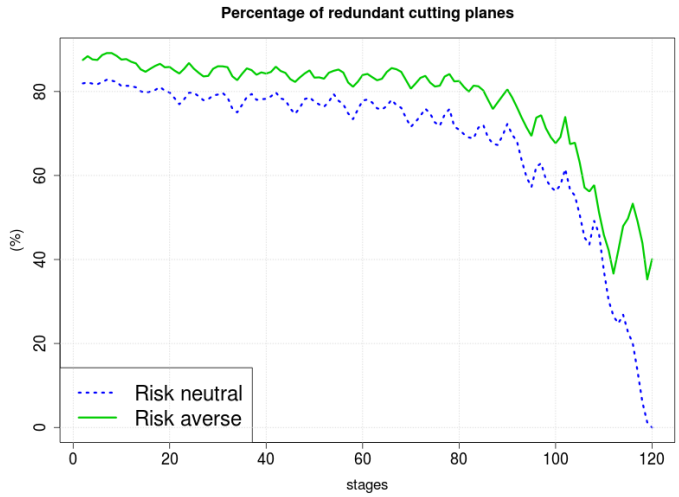

Figure 35: Mean-AV@R approach: Percentage of redundant cutting planes

4.5.2 Mean-upper-semideviation risk measures

In this section, we investigate computational issues related to the mean-upper-semideviation risk averse SDDP discussed in section 4.4.1.

Figure 36 shows the total policy value for 120 stages at iteration 5000 for $p \in \{1, 2, 3\}$ and $\kappa \in \{0, 0.1, 0.2, \ldots, 1\}$. The line with pluses corresponds to $p = 3$, the line with triangles corresponds to $p = 2$ and the one with circles corresponds to

$p = 1$. The average, the 95% and 99% quantiles of the policy value are plotted. As κ increases the average of the policy value for 120 stages increases when compared to the risk neutral case (i.e. $\kappa = 0$). Higher values for p yield higher rate of increase of the average value (i.e. higher loss on average). This is expected since higher values of p is equivalent to a more aggressive strategy toward higher quantile minimization (i.e. more conservative risk averse approach). A reduction in the 99% quantile is observed most of time for $\kappa \in (0, 1]$ and $p \in \{1, 2, 3\}$ when compared with the risk neutral approach and a similar behaviour occurs for the 95% quantile when $p = 1$. Notice that for small values of κ, higher value of p implies higher quantile reduction when compared to the risk neutral approach. However, as κ increases the situation becomes the opposite (i.e. higher value of p implies lower quantile reduction). It is not clear why the higher quantile values explode as κ grows (similar situation happens with the Mean-AV@R risk measure for higher values of λ).

Figure 37 plots the total policy value for 60 stages at iteration 5000 for $p \in \{1, 2, 3\}$ and $\kappa \in \{0, 0.1, 0.2, \ldots, 1\}$. The line with pluses corresponds to $p = 3$, the line with triangles corresponds to $p = 2$ and the one with circles corresponds to $p = 1$. The average, the 95% and 99% quantiles of the policy value are plotted. Similar observations made for the case of 120 stages hold for the 60 stages total cost.

Table 14 shows the change in percentage of the average, 95% and 99% quantiles of the policy value for 60 stages. We can see that the parameter setting of $p = 1$ and $\kappa = 0.3$ allows a moderate loss on average (i.e. 5.61 %) and a reasonable reduction in the 95% and 99% quantiles of the policy value (i.e. 8.5% and 17.72% respectively).

Figure 38 shows the individual stage costs at iteration 5000 for the risk averse approach (with $p = 1$ and $\kappa = 0.3$) and the risk neutral approach. The dotted line represents the risk neutral approach and the continuous line represents the risk averse approach. In this figure, we compare the average, 95% and 99% quantiles of individual stage costs. Similar observations as the mean-AV@R approach hold. The

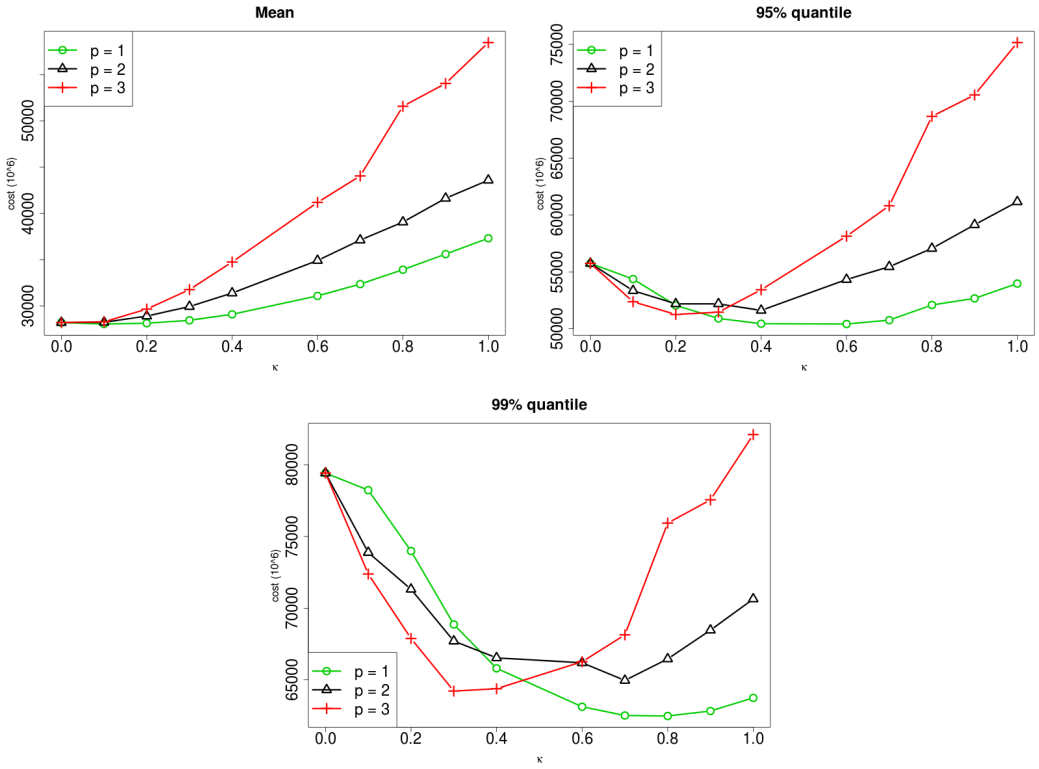

Figure 36: Mean-upper-semideviation approach: Total policy value for 120 stages for $p \in \{1, 2, 3\}$ as function of κ

Table 14: Mean-upper-semideviation approach: 60 stages policy value change in %

	κ	0.1	0.2	0.3	0.4	0.6	0.7
	Mean	0.76	2.59	5.61	9.95	21.22	27.72
$p = 1$	95% quantile	-3.51	-6.85	-8.50	-9.59	-8.23	-6.31
	99% quantile	-7.88	-13.05	-17.72	-18.14	-22.68	-23.92
	Mean	2.25	6.67	12.25	19.12	34.14	43.69
$p = 2$	95% quantile	-4.01	-7.61	-6.66	-6.87	-2.54	0.71
	99% quantile	-9.80	-14.31	-18.55	-19.01	-19.40	-21.94
	Mean	3.40	11.90	22.71	36.49	64.64	77.50
$p = 3$	95% quantile	-6.94	-8.50	-6.16	-1.46	9.23	14.48
	99% quantile	-13.06	-19.22	-21.94	-21.54	-17.86	-14.48

average costs increase in the first stages and decrease in the final stages. Typically, the increase on average compared to the risk neutral case is observed during rainy seasons. This is due to the risk aversion strategy that consists in consuming less of the hydro resources during rainy seasons so later is could be used in dry seasons. This

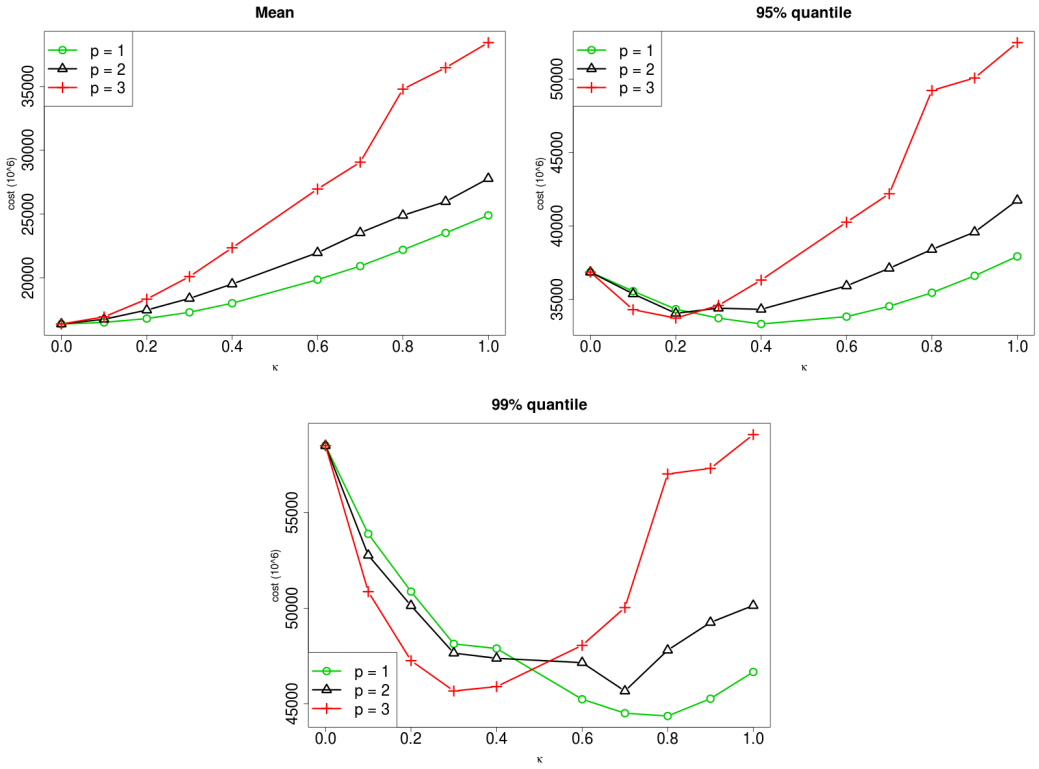

Figure 37: Mean-upper-semideviation approach: Total policy value for 60 stages for $p \in \{1, 2, 3\}$ as function of κ

implies also a reduction in the value of peak average costs during dry seasons. The 95% and 99% quantiles are significantly reduced in the risk averse approach when compared to the risk neutral approach. In other words, the constructed policy is less sensitive to extreme scenarios.

Figure 39 plots the average deficit in each of the four systems for the risk neutral approach and the risk averse approach with $p = 1$ and $\kappa = 0.3$. The dotted line represents the risk neutral approach and the continuous line represents the risk averse approach. We can observe that the risk averse approach allows a significant reduction in the deficit when compared to the risk neutral method.

Figure 40 plots the average storage in each of the four systems for the risk neutral approach and the risk averse approach with $p = 1$ and $\kappa = 0.3$. The dotted line represents the risk neutral approach and the continuous line represents the risk

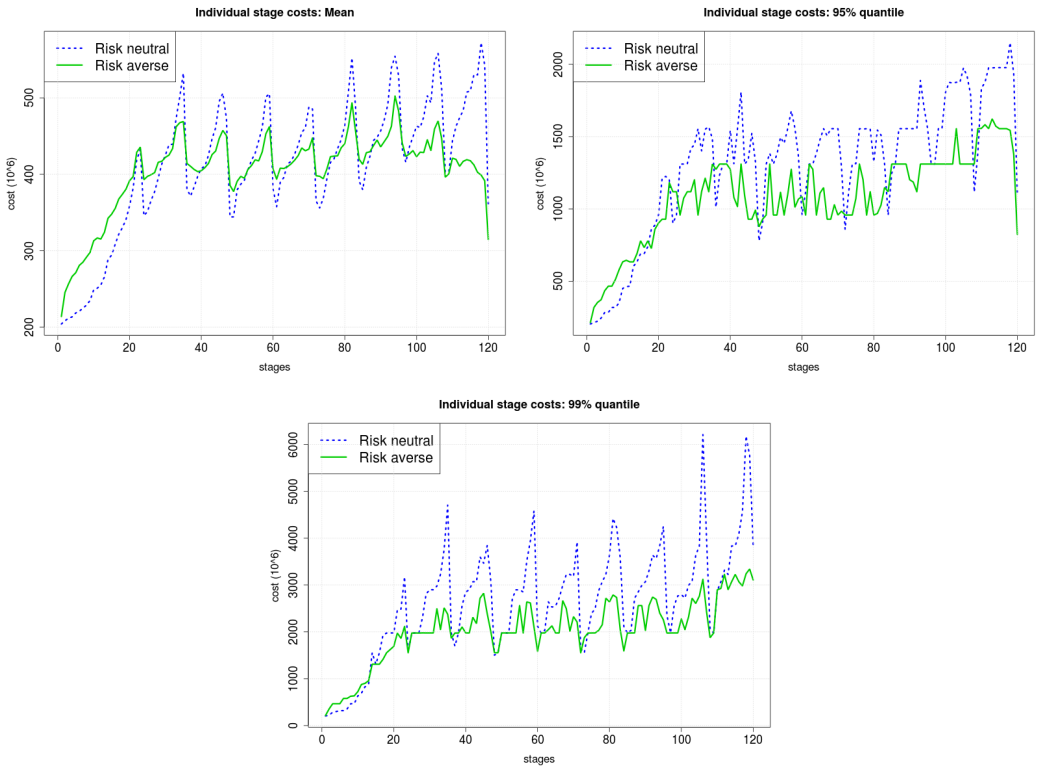

Figure 38: Mean-upper-semideviation approach: Individual stage costs for $p = 1$ and $\kappa = 0.3$

averse approach. We can observe that the risk averse approach improves the average individual stage storage when compared to the risk neutral method.

Similarly to the Mean-AV@R approach, there is no loss in CPU time for the mean-upper-semideviation method when compared to the risk neutral approach. Figure 41 plots the CPU time (in seconds) per iteration for the risk averse approach (continuous,lower line) and risk neutral approach (dotted,upper line). The sudden decreases in CPU time is due to the redundant cutting plane elimination subroutine which is run every 400 iterations. Again, the slightly lower CPU time per iteration at the end of the run time is due to the observation that the mean-upper-semideviation approach has slightly more redundant cutting planes (cf. Figure 42) which the subroutine will remove and allow faster iterations.

Figure 42 plots the percentage of redundant cutting planes for the risk averse

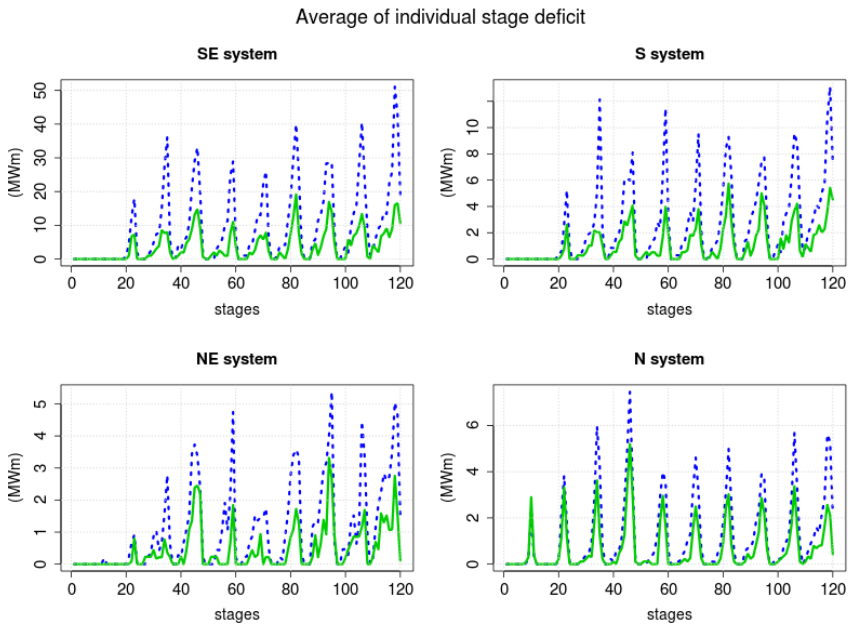

Figure 39: Mean-upper-semideviation approach: Average of individual stage deficit

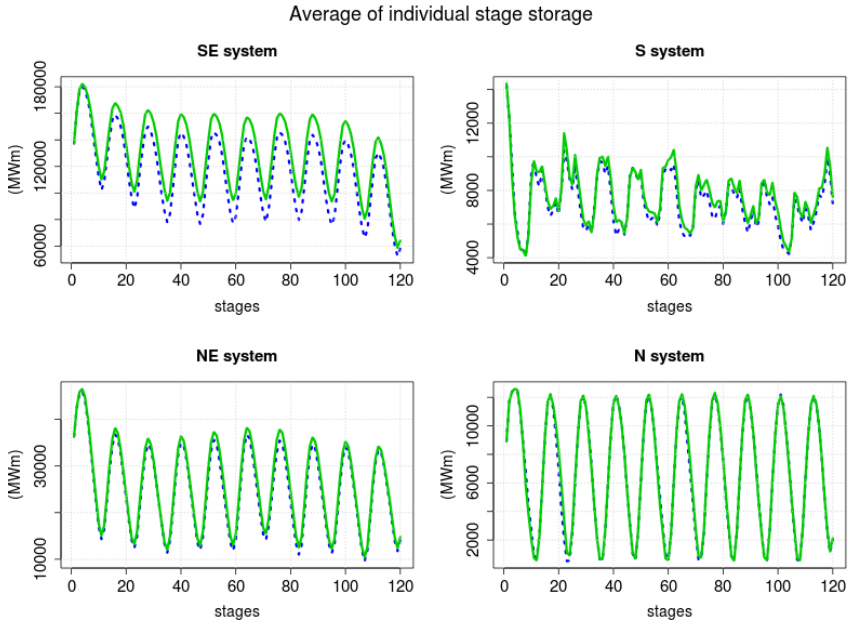

Figure 40: Mean-upper-semideviation approach: Average of individual stage storage

approach and risk neutral approach. The risk averse approach has slightly more redundant cutting planes than the risk neutral approach.

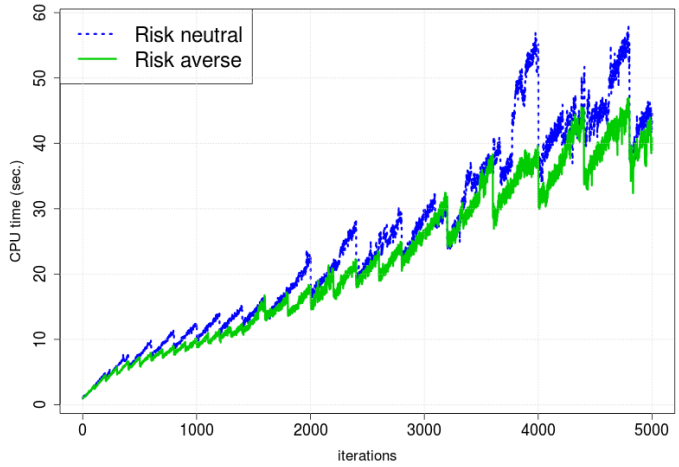

Figure 41: Mean-upper-semideviation approach: CPU time per iteration

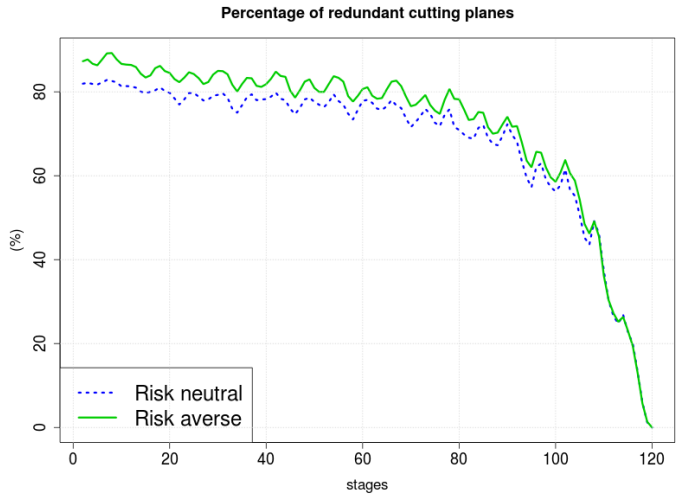

Figure 42: Mean-upper-semideviation approach: Percentage of redundant cutting planes

4.5.3 Variability of SAA problems

Similarly to the risk neutral approach, we discuss the variability of the bounds of optimal values of the SAA problems. Recall that an SAA problem is based on a randomly generated sample, and as such is subject to random perturbations, and in itself is an approximation of the "true" problem.

In this experiment we generate twenty SAA problems where each one having $1 \times 100 \times \cdots \times 100 = 100^{119}$ scenarios. Then we run 5000 iterations of the SDDP algorithm for the mean-AV@R risk averse approach. At the last iteration, we perform a forward step to evaluate the obtained policy with 2000 scenarios and compute the average policy value.

Table 15 shows the 95% confidence interval for the lower bound and average policy value at iteration 5000 over a sample of 20 SAA problems. Each of the policy value observations was computed using 2000 scenarios. The last 2 columns of the table shows the range divided by the average of the lower bound (where the range is the difference between the maximum and minimum observation) and the standard deviation divided by the average value. This problem has relatively low variability (approx. 4%) for both of the lower bound and the average policy value.

Table 15: Mean-AV@R approach: SAA variability

	95% C.I. left ($\times 10^9$)	Average ($\times 10^9$)	95% C.I. right ($\times 10^9$)	range/mean	sdev./mean
Lower bound	48.049	48.920	49.790	14.45%	4.06%
Average policy	28.056	28.581	29.106	16.38%	4.19%

Similarly to the risk neutral method, the mean-AV@R approach shows lower variability of the lower bound and the average policy value.

4.6 Conclusion

In this chapter, an analysis of the risk averse framework and its application to the hydrothermal operation planning problem were presented. In section 4.2, we presented an overview of some mathematical notions that we will be used in later sections namely coherent and conditional risk measures. A general problem statement for multistage stochastic problems with coherent risk measures and an overview of its different formulations were given in section 4.3. A generic description of the risk averse SDDP algorithm was outlined in section 4.4. The adaptive risk averse approach

was discussed under two different perspectives: one through the mean-AV@R and the other using the mean-upper-semideviation risk measures. Finally, computational aspects for the hydrothermal system operation planning problem of the Brazilian interconnected power system were analyzed and the contributions of the risk averse methodology when compared to the risk neutral approach were presented. We have seen that the risk averse approach ensures a reduction in the high quantile values of the individual stage costs. This protection comes with an increase of the average policy value - the price of risk aversion. Furthermore, both of the risk averse approaches come with practically no extra computational effort and, similarly to the risk neutral method, there was no significant variability of the SAA problems.

CHAPTER V

WORST-CASE-EXPECTATION APPROACH

5.1 Introduction

There are basically two popular approaches to optimization under uncertainty. One is the approach of robust optimization where one optimizes a worst possible case of a considered problem. The other approach, of stochastic programming, models uncertain parameters as random variables with a specified probability distribution and optimization is applied to the expected value of the objective function. We may refer to the recent books [4] and [30] where these approaches are discussed in details. Both approaches have advantages and disadvantages and can be applied in different situations. The robust approach could be too conservative especially in cases where uncertain parameters have a large range of variability.

As it was discussed in chapter 2, the hydrothermal operation planning problem has several sources of uncertainty. Some are due to natural conditions, such as the energy inflows of the hydro power plants, and others are due to economic factors, such as the demand. So far we have considered only the energy inflows of the hydro plants as uncertain data. Typically, energy inflows are characterized by a large variability (cf. chapter 2, section 2.3) which justifies the use of stochastic programming framework to tackle the problem.

The national power operator in Brazil runs the SDDP algorithm once a month to compute cost-to-go functions for five years ahead. Uncertain data like the demand process are considered deterministic based on an up to five years forecast. Clearly, it is not possible to predict accurately such data and unforeseen events that imply sudden demand increase can occur (such as higher than expected temperatures or

higher economic activity). The purpose of the methodology that we suggest here is to construct policies that are robust toward such events.

In many situations, such as the operation planning problem, the involved uncertain parameters can be naturally divided into two groups, for one group the robust approach (i.e. demand) makes sense while for the other the stochastic programming approach is more appropriate (i.e. energy inflows). In this chapter, we discuss how the robust and stochastic programming approaches can be combined together. The content of this chapter can be found in a working paper [33].

This Chapter is organized as follows. In section 5.2, we present the worst-case-expectation formulation of the linear multistage problem and the underlying assumptions. An overview of the algorithm tackling such problems is detailed in section 5.3. Finally, we illustrate the contribution of the methodology through computational experiments in section 5.4.

5.2 General problem statement and assumptions

5.2.1 Problem statement

Let $\xi_1, ..., \xi_T$ be the uncertainty process underlying the corresponding multistage problem with ξ_1 being deterministic. Suppose that the data vectors $\xi_t \in \mathbb{R}^{d_t}$, $t = 2, ..., T$, are decomposed into two parts. That is $\xi_t = (\xi_t^1, \xi_t^2)$, with $(\xi_2^1, ..., \xi_T^1) \in \Xi^1$ and $\xi_2^2, ..., \xi_T^2$ being a random process with a specified probability distribution. The set Ξ^1 is nonempty and compact. We refer to $\xi_2^1, ..., \xi_T^1$ as the *uncertain* parameters and to $\xi_2^2, ..., \xi_T^2$ as the *random* parameters of the model.

The extensive formulation of the worst-case-expectation multistage problem is as follows.

$$\begin{aligned} \operatorname*{Min}_{x_1, x_2(\cdot), ..., x_T(\cdot)} \quad & \sup_{(\xi_2^1, ..., \xi_T^1) \in \Xi^1} \quad \mathbb{E}\left\{c_1^\mathsf{T} x_1 + c_2^\mathsf{T} x_2(\xi_{[2]}) + ... + c_T^\mathsf{T} x_T(\xi_{[T]})\right\} \\ & \text{s.t.} \qquad A_1 x_1 = b_1,\ x_1 \geq 0, \\ & \qquad\quad B_t x_{t-1}(\xi_{[t-1]}) + A_t x_t(\xi_{[t]}) = b_t,\ x_t(\xi_{[t]}) \geq 0,\ t = 2, ..., T, \end{aligned} \tag{73}$$

where $\xi_1 = (c_1, A_1, b_1)$, $\xi_t = (c_t, A_t, B_t, b_t)$, $t = 2, ..., T$, $\xi_{[t]} = (\xi_1, ..., \xi_t)$ denotes history of the process up to time t and the expectation is taken with respect to the probability distribution of the random process $\xi_2^2, ..., \xi_T^2$. The optimization is performed over functions $x_t(\xi_{[t]})$, $t = 1, ..., T$, of the history of the data process and the feasibility constraints should be satisfied for all $(\xi_2^1, ..., \xi_T^1) \in \Xi^1$ and almost every (a.e.) realization of the random process.

We have that

$$\begin{aligned} &\mathbb{E}\left\{c_1^\mathsf{T} x_1 + c_2^\mathsf{T} x_2(\xi_{[2]}) + c_3^\mathsf{T} x_3(\xi_{[3]}) + ... + c_T^\mathsf{T} x_T(\xi_{[T]})\right\} = \\ &\quad c_1^\mathsf{T} x_1 + \mathbb{E}\Big\{c_2^\mathsf{T} x_2(\xi_{[2]}) + \left\{\mathbb{E}_{|\xi_{[2]}^2} c_3^\mathsf{T} x_3(\xi_{[3]}) + ... + \mathbb{E}_{|\xi_{[T-1]}^2}\left[c_T^\mathsf{T} x_T(\xi_{[T]})\right]\right\}\Big\}, \end{aligned}$$

where $\mathbb{E}_{|\xi_{[t]}^2}$ denotes the conditional expectation with respect to $\xi_{[t]}^2$. Thus

$$\begin{aligned} \sup_{(\xi_2^1, ..., \xi_T^1) \in \Xi^1} \quad & \mathbb{E}\left\{c_1^\mathsf{T} x_1 + c_2^\mathsf{T} x_2(\xi_{[2]}) + c_3^\mathsf{T} x_3(\xi_{[3]}) + ... + c_T^\mathsf{T} x_T(\xi_{[T]})\right\} \leq \\ & c_1^\mathsf{T} x_1 + \sup_{(\xi_2^1, ..., \xi_T^1) \in \Xi^1} \mathbb{E}\Big\{c_2^\mathsf{T} x_2(\xi_{[2]}) + \sup_{(\xi_2^1, ..., \xi_T^1) \in \Xi^1} \mathbb{E}_{|\xi_{[2]}^2}\left\{c_3^\mathsf{T} x_3(\xi_{[3]}) + ... \right. \\ & \left. + \sup_{(\xi_2^1, ..., \xi_T^1) \in \Xi^1} \mathbb{E}_{|\xi_{[T-1]}^2}\left[c_T^\mathsf{T} x_T(\xi_{[T]})\right]\right\}\Big\}. \end{aligned} \tag{74}$$

The inequality (74) can be strict. The nested formulation of the worst-case-expectation multistage problem is as follows.

$$\operatorname*{Min}_{\substack{A_1 x_1 = b_1 \\ x_1 \geq 0}} c_1^\mathsf{T} x_1 + \rho_{2|\xi_1}\left[\min_{\substack{B_2 x_1 + A_2 x_2 = b_2 \\ x_2 \geq 0}} c_2^\mathsf{T} x_2 + \cdots + \rho_{T|\xi_{[T-1]}}\Big[\min_{\substack{B_T x_{T-1} + A_T x_T = b_T \\ x_T \geq 0}} c_T^\mathsf{T} x_T\Big]\right], \tag{75}$$

where

$$\rho_{t|\xi_{[t-1]}}[\,\cdot\,] = \sup_{(\xi_2^1, ..., \xi_T^1) \in \Xi^1} \mathbb{E}_{|\xi_{[t-1]}^2}[\,\cdot\,], \quad t = 2, ..., T. \tag{76}$$

The extensive and nested formulation of the worst-case-expectation multistage problem are not equivalent (cf., (74)).

For the nested problem it is possible to write the following dynamic programming equations (cf., [27],[35])

$$Q_t(x_{t-1}, \xi^1_{[t]}, \xi^2_{[t]}) = \inf_{B_t x_{t-1} + A_t x_t = b_t,\, x_t \geq 0} \left\{ c_t^{\mathsf{T}} x_t + \mathcal{Q}_{t+1}(x_t, \xi^1_{[t]}, \xi^2_{[t]}) \right\}, \tag{77}$$

$t = 2, ..., T$, with $\mathcal{Q}_{T+1}(\cdot) \equiv 0$ and

$$\mathcal{Q}_{t+1}(x_t, \xi^1_{[t]}, \xi^2_{[t]}) = \sup_{(\xi^{1'}_2, ..., \xi^{1'}_T) \in \Xi^1} \mathbb{E}_{|\xi^2_{[t]}} \left\{ Q_{t+1}(x_t, \xi^{1'}_{[t+1]}, \xi^2_{[t+1]}) : \xi^{1'}_{[t]} = \xi^1_{[t]} \right\}. \tag{78}$$

5.2.2 Assumptions

We make the following assumptions. The set Ξ^1 is nonempty and compact. It is given by a direct product of individual uncertainty sets (i.e. $\Xi^1 = \Xi^1_2 \times \cdots \times \Xi^1_T$). We assume that the data process $\xi_2, ..., \xi_T$ is *stagewise independent*, that is random vector ξ^2_t is independent of $(\xi^2_2, ..., \xi^2_{t-1})$, $t = 3, ..., T$.

Under the stagewise independence assumption, the dynamic equations (77)–(78) simplify to

$$Q_t(x_{t-1}, \xi^1_t, \xi^2_t) = \inf_{B_t x_{t-1} + A_t x_t = b_t,\, x_t \geq 0} \left\{ c_t^{\mathsf{T}} x_t + \mathcal{Q}_{t+1}(x_t) \right\}, \tag{79}$$

$t = 2, ..., T$, with $\mathcal{Q}_{T+1}(\cdot) \equiv 0$ and

$$\mathcal{Q}_{t+1}(x_t) = \sup_{\xi^1_{t+1} \in \Xi^1_{t+1}} \mathbb{E} \left\{ Q_{t+1}(x_t, \xi^1_{t+1}, \xi^2_{t+1}) \right\}, \tag{80}$$

where the expectation is taken with respect to ξ^2_{t+1}. Note that under the above assumptions of stagewise independence the cost-to-go functions $\mathcal{Q}_{t+1}(x_t)$ do not depend on the data process. Note also that functions $Q_t(x_{t-1}, \xi^1_t, \xi^2_t)$ are convex in x_{t-1}, and hence functions $\mathcal{Q}_t(x_{t-1})$ are convex.

5.3 Description of the worst-case-expectation algorithm

In this section, we suggest an (SDDP) type algorithm to solve the worst-case-expectation problem introduced in the previous section. We may refer the reader for a detailed discussion to [33].

In order to apply the SDDP algorithm we need to compute subgradients of the cost-to-go functions $\mathcal{Q}_{t+1}(x_t)$. Consider function

$$q_t(x_{t-1}, \xi_t^1) = \mathbb{E}\left\{Q_t(x_{t-1}, \xi_t^1, \xi_t^2)\right\}, \quad t = 2, ..., T,$$

where the expectation is taken with respect to the distribution of ξ_t^2. This function is convex in x_{t-1} and, as it was assumed, is finite valued and hence by the Strassen Theorem (cf., [37])

$$\partial q_t(x_{t-1}, \xi_t^1) = \mathbb{E}\left\{\partial Q_t(x_{t-1}, \xi_t^1, \xi_t^2)\right\}, \tag{81}$$

where all subgradients are taken with respect to x_{t-1}. We have that

$$\mathcal{Q}_t(x_{t-1}) = \sup_{\xi_t^1 \in \Xi_t^1} q_t(x_{t-1}, \xi_t^1),$$

and by the Levin-Valadier Theorem (cf., [14, p.213])

$$\partial \mathcal{Q}_t(x_{t-1}) = \operatorname{conv}\left\{\cup_{\xi_t^1 \in \bar{\Xi}_t^1(x_{t-1})} \partial q_t(x_{t-1}, \xi_t^1)\right\}, \tag{82}$$

where $\operatorname{conv}(A)$ denotes convex hull of set A and

$$\bar{\Xi}_t^1(x_{t-1}) := \arg\max_{\xi_t^1 \in \Xi_t^1} q_t(x_{t-1}, \xi_t^1).$$

Therefore a subgradient of $\mathcal{Q}_{t+1}(x_t)$ is given by

$$\nabla \mathcal{Q}_t(x_{t-1}) = \mathbb{E}\left\{\nabla Q_t(x_{t-1}, \bar{\xi}_t^1, \xi_t^2)\right\}, \tag{83}$$

for some $\bar{\xi}_t^1 \in \bar{\Xi}_t^1(x_{t-1})$.

The first step of numerical solution is to discretize the data process. The random process ξ_t^2, $t = 2, ..., T$, is discretized using the Sample Average Approximation (SAA) method. Discretization of the uncertainty sets Ξ_t^1 will be discussed in section 5.3.3.

5.3.1 Backward step

Suppose for the sake of simplicity that only the right hand sides b_t, $t = 2, ..., T$, are uncertain. That is, $\xi_t = b_t$ and $\xi_t^1 = b_t^1$, $\xi_t^2 = b_t^2$, $b_t = (b_t^1, b_t^2)$. Let b_{tj}^2, $j = 1, ..., N$, be the respective random sample, $t = 2, ..., T$. Let $\bar{x}_t$, $t = 1, ..., T-1$, be trial points (we can use more than one trial point at every stage of the backward step, an extension to that will be straightforward). Let $\mathcal{Q}_t(\cdot)$ be the cost-to-go functions of dynamic programming equations associated with the considered multistage problem, and $\mathfrak{Q}_t(\cdot)$ be a current approximation of $\mathcal{Q}_t(\cdot)$ given by the maximum of a collection of *cutting* planes

$$\mathfrak{Q}_t(x_{t-1}) = \max_{k \in \mathcal{I}_t} \left\{ \alpha_{tk} + \beta_{tk}^{\mathsf{T}} x_{t-1} \right\}, \ t = 1, ..., T-1. \tag{84}$$

For a given b_T^1 and $b_{Tj} = (b_T^1, b_{Tj}^2)$ at stage $t = T$ we solve N problems

$$\operatorname*{Min}_{x_T \in \mathbb{R}^{n_T}} c_T^{\mathsf{T}} x_T \ \text{ s.t. } B_T \bar{x}_{T-1} + A_T x_T = b_{Tj}, \ x_T \geq 0, \ j = 1, ..., N. \tag{85}$$

The optimal value of problem (85) is $Q_{Tj}(\bar{x}_{T-1}, b_T^1)$. We should compute value of the cost-to-go function $\mathcal{Q}_T(x_{T-1})$ at trial point $\bar{x}_{T-1}$. We have

$$\mathcal{Q}_T(\bar{x}_{T-1}) = \max_{b_T^1 \in \Xi_T^1} q_T(\bar{x}_{T-1}, b_T^1), \tag{86}$$

where

$$q_T(\bar{x}_{T-1}, b_T^1) = N^{-1} \sum_{j=1}^{N} Q_{Tj}(\bar{x}_{T-1}, b_T^1). \tag{87}$$

Now going one stage back $Q_{T-1,j}(\bar{x}_{T-2}, b_{T-1}^1)$ is equal to the optimal value of problem

$$\operatorname*{Min}_{x_{T-1} \in \mathbb{R}^{n_{T-1}}} c_{T-1}^{\mathsf{T}} x_{T-1} + \mathcal{Q}_T(x_{T-1}) \ \text{ s.t. } B_{T-1} \bar{x}_{T-2} + A_{T-1} x_{T-1} = b_{T-1,j}, \ x_{T-1} \geq 0. \tag{88}$$

However, function $\mathcal{Q}_T(\cdot)$ is not available. Therefore we replace it by $\mathfrak{Q}_T(\cdot)$ and hence consider problem

$$\operatorname*{Min}_{x_{T-1} \in \mathbb{R}^{n_{T-1}}} c_{T-1}^{\mathsf{T}} x_{T-1} + \mathfrak{Q}_T(x_{T-1}) \ \text{ s.t. } B_{T-1} \bar{x}_{T-2} + A_{T-1} x_{T-1} = b_{T-1,j}, \ x_{T-1} \geq 0. \tag{89}$$

Recall that $\mathfrak{Q}_T(\cdot)$ is given by maximum of affine functions (see (84)). Therefore we can write problem (84) in the form

$$\begin{array}{ll} \underset{x_{T-1}\in\mathbb{R}^{n_{T-1}},\theta\in\mathbb{R}}{\text{Min}} & c_{T-1}^{\mathsf{T}}x_{T-1}+\theta \\ \text{s.t.} & B_{T-1}\bar{x}_{T-2}+A_{T-1}x_{T-1}=b_{T-1,j},\ x_{T-1}\geq 0 \\ & \theta\geq \alpha_{Tk}+\beta_{Tk}^{\mathsf{T}}x_{T-1},\ k\in\mathcal{I}_T. \end{array} \tag{90}$$

Then we have to solve the problem

$$\max_{b_{T-1}^1\in\Xi_{T-1}^1} q_{T-1}(\bar{x}_{T-2},b_{T-1}^1), \tag{91}$$

where

$$q_{T-1}(\bar{x}_{T-2},b_{T-1}^1)=N^{-1}\sum_{j=1}^{N}Q_{T-1,j}(\bar{x}_{T-2},b_{T-1}^1),$$

and so on.

Let us consider the following approach. Suppose that we can sample from sets Ξ_t^1. For example if sets Ξ_t^1 are finite, probably with large cardinality, we can sample an element of Ξ_t^1 with equal probability. Consider the cost-to-go function $\mathcal{Q}_T(x_{T-1})$. Sample L points $b_{T\ell}^1$, $\ell=1,...,L$, from Ξ_T^1. The number L can be small, even $L=1$. For $\ell=1,...,L$, compute subgradient (at $\bar{x}_{T-1}$)

$$\gamma_{T\ell}=N^{-1}\sum_{j=1}^{N}\nabla Q_{Tj}(\bar{x}_{T-1},b_{T\ell}^1). \tag{92}$$

Note that by (83) the subgradient $\nabla Q_{Tj}(\bar{x}_{T-1},b_{T\ell}^1)$ can be computed by solving the dual of problem (85) for $b_{Tj}=(b_{T\ell}^1,b_{Tj}^2)$. Add the corresponding cutting planes

$$q_T(\bar{x}_{T-1},b_{T\ell}^1)+\gamma_{T\ell}^{\mathsf{T}}(x_{T-1}-\bar{x}_{T-1}),\ \ell=1,...,L,$$

to the collection of cutting planes of $\mathfrak{Q}_T(\cdot)$. By (86) we have that $\mathcal{Q}_T(\bar{x}_{T-1})\geq q_T(\bar{x}_{T-1},b_T^1)$ for any $b_T^1\in\Xi_T^1$, and hence

$$\mathcal{Q}_T(x_{T-1})\geq q_T(\bar{x}_{T-1},b_{T\ell}^1)+\gamma_{T\ell}^{\mathsf{T}}(x_{T-1}-\bar{x}_{T-1}), \tag{93}$$

i.e., $q_T(\bar{x}_{T-1},b_{T\ell}^1)+\gamma_{T\ell}^{\mathsf{T}}(x_{T-1}-\bar{x}_{T-1})$ is indeed a cutting plane for $\mathfrak{Q}_T(\cdot)$.

And so on for stages $t=T-1,...,2$.

5.3.2 Forward step

The forward step of the algorithm is done in the standard way. The computed approximations $\mathfrak{Q}_2(\cdot), ..., \mathfrak{Q}_T(\cdot)$ (with $\mathfrak{Q}_{T+1}(\cdot) \equiv 0$ by definition) and a feasible first stage solution $\bar{x}_1$ can be used for constructing an implementable policy as follows. For a realization $\xi_t = (c_t, A_t, B_t, b_t)$, $t = 2, ..., T$, of the data process, decisions $\bar{x}_t$, $t = 1, ..., T$, are computed recursively going forward with $\bar{x}_1$ being the chosen feasible solution of the first stage problem, and $\bar{x}_t$ being an optimal solution of

$$\operatorname*{Min}_{x_t} c_t^{\mathsf{T}} x_t + \mathfrak{Q}_{t+1}(x_t) \ \text{ s.t. } A_t x_t = b_t - B_t \bar{x}_{t-1}, \ x_t \geq 0, \tag{94}$$

for $t = 2, ..., T$. These optimal solutions can be used as trial decisions in the backward step of the algorithm.

The forward step of the standard SDDP algorithm has two purposes: (i) to generate trial points, and (ii) to estimate value of the constructed policy and hence to provide an upper bound for the optimal value of the considered problem. Unfortunately the second function of the forward step cannot be reproduced in the present case.

5.3.3 Sampling from the uncertainty set

Following the general methodology of robust optimization (see [4]), suppose that the uncertainty set Ξ_t^1, $t = 2, ..., T$, is an ellipsoid, centered at a point $\bar{\xi}_t$. That is,

$$\Xi_t^1 := \{\xi : (\xi - \bar{\xi}_t)^{\mathsf{T}} A (\xi - \bar{\xi}_t) \leq r\}, \tag{95}$$

where A is a positive definite matrix and $r > 0$. Consider the set of points of Ξ_t^1 which are not dominated by other points of Ξ_t^1,

$$D := \left\{\xi \in \Xi_t^1 : \text{does not exist } \xi' \in \Xi_t^1 \text{ such that } \xi' \neq \xi \text{ and } \xi \leq \xi'\right\}.$$

In applications which we have in mind it makes sense to restrict our sampling to the set $D \subset \Xi_t^1$, i.e., in fact we consider the uncertainty set given by boundary points of the ellipsoid Ξ_t^1 which are "larger" than the reference value $\bar{\xi}_t$.

The set D can be represented in the following form

$$D = \bigcup_{a \geq 0,\, \|a\|=1} \arg\max \left\{ a^{\mathsf{T}} \xi : (\xi - \bar{\xi}_t)^{\mathsf{T}} A (\xi - \bar{\xi}_t) \leq r \right\}.$$

The maximizer of $a^{\mathsf{T}}\xi$, subject to $(\xi - \bar{\xi}_t)^{\mathsf{T}} A (\xi - \bar{\xi}_t) \leq r$, is obtained by writing the optimality condition

$$a - \lambda A (\xi - \bar{\xi}_t) = 0,$$

with $\lambda > 0$. Hence such maximizer is given by $\xi^* = \lambda^{-1} A^{-1} a + \bar{\xi}_t$.

We can generate the required sample as follows. Generate $Z_i \sim N(0, I)$, where I is the identity matrix of an appropriate dimension. Take $\xi_i = cA^{-1}|Z_i| + \bar{\xi}_t$, where the absolute value $|Z_i|$ of vector Z_i is taken componentwise, and c is the calibration constant such that

$$c^2 (A^{-1}|Z_i|)^{\mathsf{T}} A (A^{-1}|Z_i|) = r,$$

i.e., $c = \sqrt{r / \left(|Z_i|^{\mathsf{T}} A^{-1} |Z_i| \right)}$.

5.3.4 Generic description of the worst-case-expectation algorithm

In this section, we present an algorithmic description for the worst-case-expectation SDDP algorithm with one trial point per iteration.

5.4 Computational results

We consider the following construction for the uncertainty sets, discussed in section 5.3.3, for $t \geq 2$:

$$\begin{cases} r_t &= \left(\|\bar{\xi}_t^1\|_2 \times u \right)^2 \\ A &= \Sigma^{-1} \end{cases}$$

where Σ denotes the demand correlation matrix for the 4 systems estimated using historical demand data (60 observations), u, the uncertainty parameter, denotes the percentual increment on the demand and $\bar{\xi}_t^1$ denotes the demand forecast at stage t.

Figure 43 plots the average discounted total cost of 120 stages as a function of the demand increase for both risk neutral and worst-case-expectation approaches. As

Algorithm 4 Worst-case-expectation SDDP algorithm

Require: $\left\{\mathfrak{Q}_t^0\right\}_{t=2,\ldots,T+1}$(Init. Lower approx.) and i_{max}(max. iterations)

Initialize: $i \leftarrow 0$, $\underline{z} = -\infty$ (Lower bound)
while $i < i_{max}$ **do**
    Sample 1 scenario: $\left\{c_t, A_t, B_t, (\bar{b}_t^1; b_t^2)\right\}_{2 \leq t \leq T}$

    (Forward step)
    for $t = 1 \rightarrow T$ **do**
        $\bar{x}_t \leftarrow \arg\min_{x_t \in \mathbb{R}^{n_t}} \left\{c_t^\top x_t + \mathfrak{Q}_{t+1}^i(x_t) : B_t x_{t-1} + A_t x_t = (\bar{b}_t^1; b_t^2), x_t \geq 0\right\}$
    end for

    (Backward step)
    for $t = T \rightarrow 2$ **do**
        for $j = 1 \rightarrow N_t$ **do**
            $\left[\widetilde{Q}_{tj}(\bar{x}_{t-1}, \bar{b}_t^1), \widetilde{\pi}_{tj}\right] \leftarrow \min_{x_t \in \mathbb{R}^{n_t}} \left\{ \begin{array}{l} c_t^\top x_t + \mathfrak{Q}_{t+1}^i(x_t) : \\ B_t \bar{x}_{t-1} + A_t x_t = (\bar{b}_t^1; b_{tj}^2), x_t \geq 0 \end{array} \right\}$
        end for
        $\widetilde{\mathcal{Q}}_t(\bar{x}_{t-1}, \bar{b}_t^1) := \frac{1}{N_t} \sum_{j=1}^{N_t} \widetilde{Q}_{t,j}(\bar{x}_{t-1}, \bar{b}_t^1)$; $\tilde{g}_t := -\frac{1}{N_t} \sum_{j=1}^{N_t} \tilde{\pi}_{tj} B_t$
        $\mathfrak{Q}_t^{i+1} \leftarrow \{x_{t-1} \in \mathfrak{Q}_t^i : -\tilde{g}_t x_{t-1} \geq \widetilde{\mathcal{Q}}_t(\bar{x}_{t-1}, \bar{b}_t^1) - \tilde{g}_t \bar{x}_{t-1}\}$
    end for

    (Lower bound update)
    $\underline{z} \leftarrow \min_{x_1 \in \mathbb{R}^{n_1}} \left\{c_1^\top x_1 + \mathfrak{Q}_2(x_1) : A_1 x_1 = b_1, x_1 \geq 0\right\}$

    $i \leftarrow i + 1$
end while

the demand increases, the average policy value increases for both the risk neutral and (WCE) approaches. However, the rate of increase for the (WCE) approach is lower than for the risk neutral approach. Furthermore, the difference is reduced after the threshold of a demand increase of 3%. Intuitively, this observation is expected since we considered a value of $u = 3\%$.

Figure 44 plots the average and 99% quantile for the stage costs with 2% demand increase for the risk neutral and (WCE) approaches. In both cases (i.e. for the average and the 99% quantile), we can notice the reduction in peak values and a modest increase for the lower costs period for the (WCE) approach.

Table 16 summarizes the CPU time required to perform 5000 iterations for the risk neutral approach and the (WCE) approach. There was no significant extra CPU

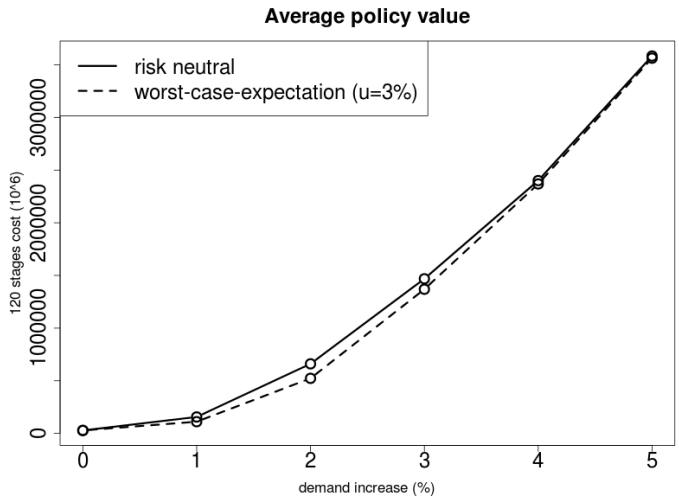

Figure 43: (WCE) approach: 120 stages policy values for risk neutral and (WCE) ($u = 3\%$)

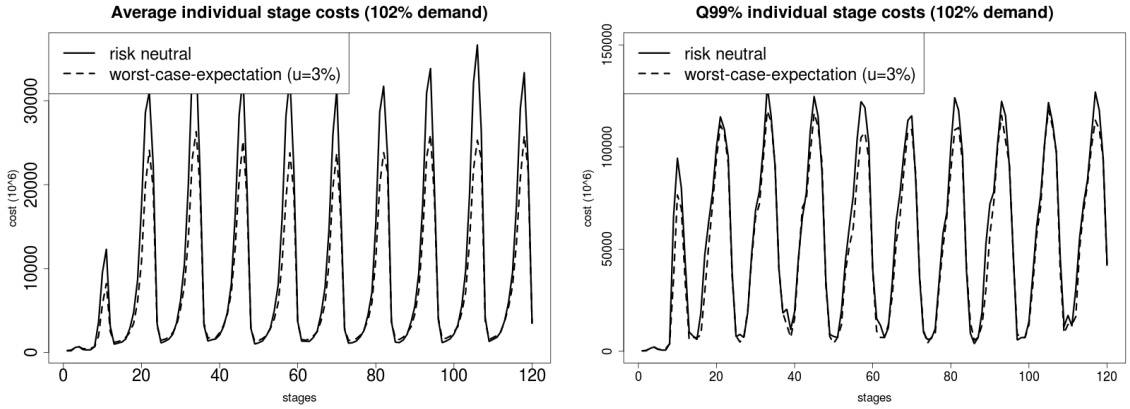

Figure 44: (WCE) approach: average individual stage costs for risk neutral and (WCE) ($u = 3\%$)

time required for the (WCE) approach when compared to the risk neutral approach.

Table 16: Worst-case-expectation approach: Total CPU time

Case Study	dd:hh:mm:ss
Risk Neutral	01:06:57:40
$u = 1.00\%$	01:06:50:30
$u = 3.00\%$	01:07:02:59

5.4.1 Risk averse vs. Worst-case-expectation approaches

In this section, we compare the risk averse approach, discussed in the previous chapter, and the worst-case-expectation method suggested in this chapter. We run the mean-AV@R risk averse approach with $\lambda = 0.15$ and $\alpha = 0.05$ for 5000 iterations and evaluate the policy using 2000 randomly generated scenarios. This value of λ achieves a significant reduction for the 99% quantile among candidates with 0.05 increments (i.e. $0.05, 0.10, 0.15, \dots$) for $\alpha \in \{0.05, 0.1\}$. We consider the worst-case-expectation method with $u = 3\%$.

Figure 45 plots the average, 95% and 99% quantiles of the total cost as function of the demand increase for the worst-case-expectation and the risk averse approach. When the forecast demand data is used (i.e. demand increase = 0%), the worst-case-expectation approach has lower average and almost similar 95% and 99% quantiles when compared with the risk averse method. The worst-case-expectation approach has considerably lower average policy value consistently as the demand increases. Furthermore, it outperforms the risk averse method with lower 95% and 99% quantiles when the demand increase is greater than 2%.

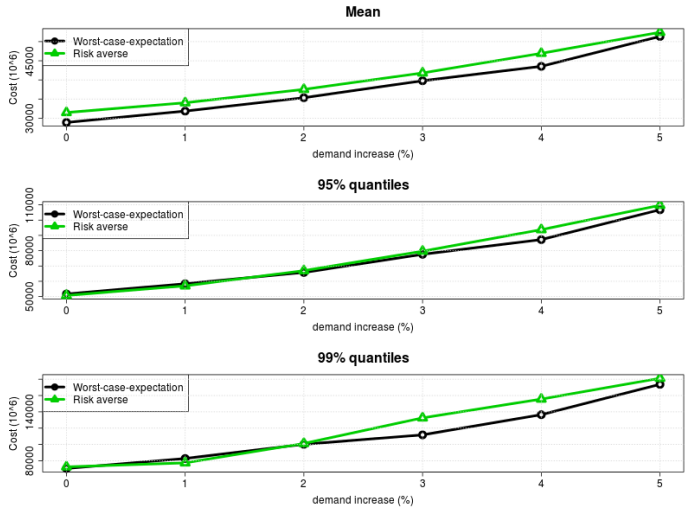

Figure 45: (WCE) approach: 120 stages discounted cost as function of demand increase

Figure 46 shows the average individual stage costs with 0% and 1% demand increase for the worst-case-expectation and the risk averse approach. In most of the first 100 stages, the worst-case-expectation approach has lower average value when compared to the risk averse method. However, in final stages, higher costs occur for the former method. The worst-case-expectation approach allows a smoother average individual costs across stages than the risk averse approach. An increase of 1% in the demand process shifts up approximately in similar manner the average costs for both methods.

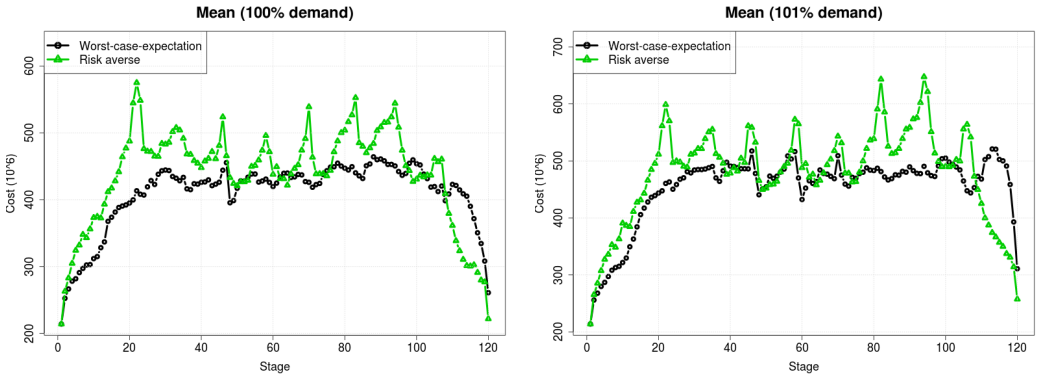

Figure 46: (WCE) approach: average individual stage costs with 0% and 1% demand increase

Figure 47 plots the 99% quantile of the individual stage costs with 0% and 1% demand increase for the worst-case-expectation and the risk averse approach. The worst-case-expectation approach has higher 99% quantile value most of the time with 0% and 1% demand increase. In some sense, a better performance at this level is expected for the risk averse method, especially under low demand increase.

Figure 48 plots the average and 99% quantile of the individual stage costs with 3% demand increase for the worst-case-expectation and the risk averse approach. The worst-case-expectation approach has lower average individual stage costs than the risk averse method for most of the stages. Furthermore, the latter method exhibits significantly higher 99% quantile peaks.

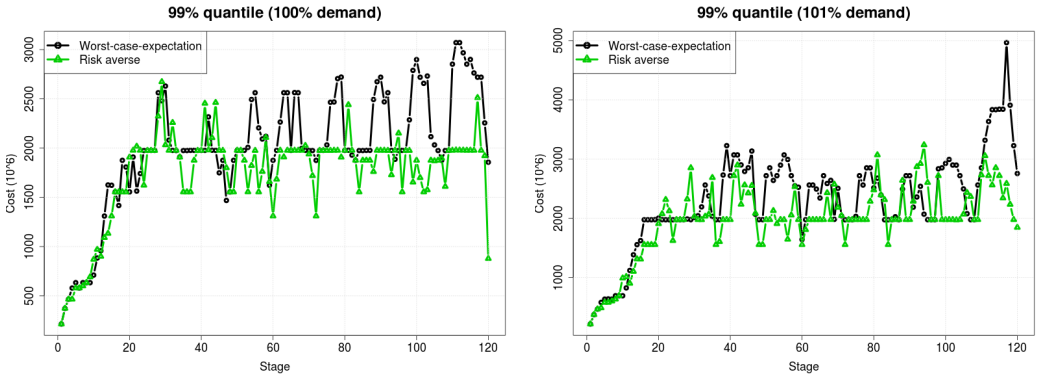

Figure 47: (WCE) approach: 99% quantile individual stage costs with 0% and 1% demand increase

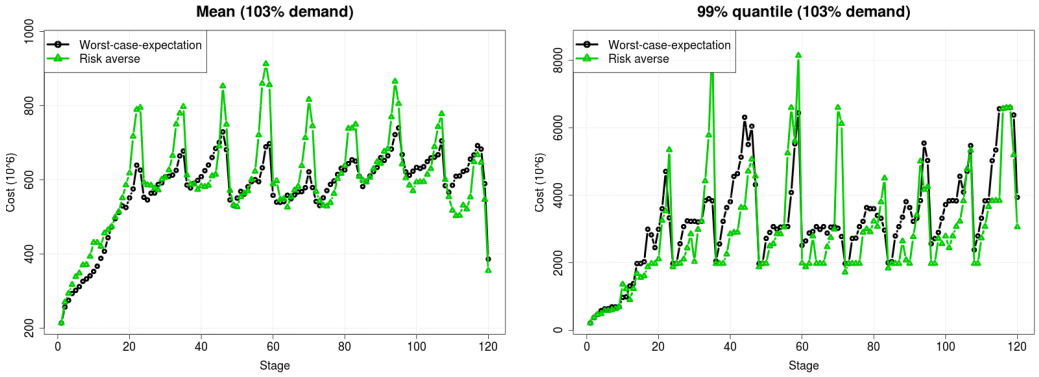

Figure 48: (WCE) approach: 99% quantile individual stage costs with 0% and 1% demand increase

5.5 Conclusion

In this chapter, we investigated a multistage stochastic programming problem where the data process can be naturally separated into two components, one can be modeled as a random process, with a specified probability distribution, and the other one can be treated from a robust point of view. In section 5.2, the basic ideas were discussed in the multistage setting and a formulation with the corresponding dynamic programming equations is presented.

In order to solve the obtained multistage problem an approach based on the Stochastic Dual Dynamic Programming method is suggested in section 5.3.

Finally, in section 5.4, we discussed numerical experiments with this approach applied to Brazilian operation planning of hydro plants. The worst-case-expectation approach constructs a policy that is less sensitive to unexpected demand increase with a reasonable loss on average when compared to the risk neutral method. Also, we compared the suggested method with a risk averse approach based on coherent risk measures. On the one hand, the idea behind the risk averse method is to allow a trade off between loss on average and immunity against unexpected extreme scenarios. On the other hand, the worst-case-expectation approach consists in a trade off between a loss on average and immunity against unanticipated demand increase. In some sense, there is a certain equivalence between the policies constructed using each of these methods.

REFERENCES

[1] Artzner, P., Delbaen, F., Eber, J.-M., and Heath, D., "Coherent measures of risk," *Mathematical Finance*, vol. 9, no. 3, pp. 203–228, 1999.

[2] Arvanitidits, N. and Rosing, J., "Composite representation of a multireservoir hydroelectric power system," *Power Apparatus and Systems, IEEE Transactions on*, vol. PAS-89, pp. 319 –326, feb. 1970.

[3] Beale, E. M. L., "On minimizing a convex function subject to linear inequalities," *Journal of the Royal Statistical Society. Series B (Methodological)*, vol. 17, no. 2, pp. pp. 173–184, 1955.

[4] Ben-Tal, A., Ghaoui, L. E., and Nemirovski, A., *Robust Optimization*. Princeton University Press, Princeton, 2009.

[5] Benders, J. F., "Partitioning procedures for solving mixed-variables programming problems," *Numerische Mathematik*, vol. 4, pp. 238–252, 1962. 10.1007/BF01386316.

[6] Birge, J. R., "Decomposition and partitioning methods for multistage stochastic linear programs," *Operations Research*, vol. 33, no. 5, pp. pp. 989–1007, 1985.

[7] Birge, J. R. and Louveaux, F., *Introduction to Stochastic Programming*. Springer Series in Operations Research and Financial Engineering, Springer, July 1997.

[8] Birge, J. R. and Louveaux, F. V., "A multicut algorithm for two-stage stochastic linear programs," *European Journal of Operational Research*, vol. 34, no. 3, pp. 384 – 392, 1988.

[9] Chen, Z. L. and Powell, W. B., "Convergent cutting-plane and partial-sampling algorithm for multistage stochastic linear programs with recourse," *Journal of Optimization Theory and Applications*, vol. 102, pp. 497–524, 1999. 10.1023/A:1022641805263.

[10] Dantzig, G. B., "Linear programming under uncertainty," *Management Science*, vol. 1, no. 3-4, pp. 197–206, 1955.

[11] Donohue, C. and Birge, J., "The abridged nested decomposition method for multistage stochastic linear programs with relatively complete recourse," *Algorithmic Operations Research*, vol. 1, no. 1, 2006.

[12] Eichhorn, A. and Rmisch, W., "Polyhedral risk measures in stochastic programming," *SIAM Journal on Optimization*, vol. 16, no. 1, pp. 69–95, 2005.

[13] Guigues, V. and Rmisch, W., "Sampling-based decomposition methods for multistage stochastic programs based on extended polyhedral risk measures," *SIAM Journal on Optimization*, vol. 22, no. 2, pp. 286–312, 2012.

[14] Ioffe, A. D. and Tikhomirov, V. M., *Theory of extremal problems*, vol. 6. Elsevier Science, 1979.

[15] Kelley, J. E., J., "The cutting-plane method for solving convex programs," *Journal of the Society for Industrial and Applied Mathematics*, vol. 8, no. 4, pp. pp. 703–712, 1960.

[16] Linowsky, K. and Philpott, A. B., "On the convergence of sampling-based decomposition algorithms for multistage stochastic programs," *Journal of Optimization Theory and Applications*, vol. 125, pp. 349–366, 2005. 10.1007/s10957-004-1842-z.

[17] Louveaux, F. V., "A solution method for multistage stochastic programs with recourse with application to an energy investment problem," *Operations Research*, vol. 28, no. 4, pp. pp. 889–902, 1980.

[18] Nemirovski, A. and Shapiro, A., "Convex approximations of chance constrained programs," *SIAM Journal on Optimization*, vol. 17, no. 4, pp. 969–996, 2007.

[19] Pereira, M. V. F. and Pinto, L. M. V. G., "Stochastic optimization of a multireservoir hydroelectric system: A decomposition approach," *WATER RESOURCES RESEARCH*, vol. 21, pp. 779–792, 1985.

[20] Pereira, M. V. F. and Pinto, L. M. V. G., "Multi-stage stochastic optimization applied to energy planning," *Mathematical Programming*, vol. 52, pp. 359–375, 1991. 10.1007/BF01582895.

[21] Philpott, A. and de Matos, V., "Dynamic sampling algorithms for multi-stage stochastic programs with risk aversion," *European Journal of Operational Research*, vol. 218, no. 2, pp. 470 – 483, 2012.

[22] Philpott, A. and Guan, Z., "On the convergence of stochastic dual dynamic programming and related methods," *Operations Research Letters*, vol. 36, no. 4, pp. 450 – 455, 2008.

[23] Rich, J. L., "Brazil to end rationing of electricity," *The New York Times*, February 2002.

[24] Rockafellar, R. T. and Wets, R. J. B., *Variational Analysis*. Springer, 1998.

[25] Rother, L., "Electricity rationing in brazil inflames regional animosities," *The New York Times*, November 2001.

[26] Ruszczyski, A., "Decomposition methods," in *Stochastic Programming* (Ruszczynski, A. and Shapiro, A., eds.), vol. 10 of *Handbooks in Operations Research and Management Science*, pp. 141 – 211, Elsevier, 2003.

[27] Ruszczyski, A. and Shapiro, A., "Conditional risk mappings," *Mathematics of Operations Research*, vol. 31, no. 3, pp. 544–561, 2006.

[28] Ruszczyski, A. and Shapiro, A., "Optimization of convex risk functions," *Mathematics of Operations Research*, vol. 31, no. 3, pp. 433–452, 2006.

[29] Shapiro, A., *Topics in Stochastic Programming*. Philadelphia: Universite Catholique de Louvain, core lecture series ed., 2011.

[30] Shapiro, A., Dentcheva, D., and Ruszczyński, A., *Lectures on Stochastic Programming: Modeling and Theory*. Philadelphia: SIAM, 2009.

[31] Shapiro, A. and Tekaya, W., "Report for technical cooperation between georgia institute of technology and ons - operador nacional do sistema eletrico - time series model," tech. rep., Georgia Institute of Technology, 2011.

[32] Shapiro, A., Tekaya, W., Paulo da Costa, J., and Pereira Soares, M., "Report for technical cooperation between georgia institute of technology and ons - operador nacional do sistema eletrico - phase 1," tech. rep., Georgia Institute of Technology, 2011.

[33] Shapiro, A., Tekaya, W., Pereira Soares, M., and Paulo da Costa, J., "Worst-case-expectation approach to optimization under uncertainty," tech. rep., 2012.

[34] Shapiro, A., "Analysis of stochastic dual dynamic programming method," *European Journal of Operational Research*, vol. 209, no. 1, pp. 63 – 72, 2011.

[35] Shapiro, A., "Minimax and risk averse multistage stochastic programming," *European Journal of Operational Research*, vol. 219, no. 3, pp. 719 – 726, 2012.

[36] Shapiro, A., Tekaya, W., da Costa, J. P., and Soares, M. P., "Risk neutral and risk averse stochastic dual dynamic programming method," *European Journal of Operational Research*, vol. 224, no. 2, pp. 375 – 391, 2013.

[37] Strassen, V., "The existence of probability measures with given marginals," *The Annals of Mathematical Statistics*, pp. 423–439, 1965.

[38] Terry, L. A., Pereira, M. V. F., Neto, T. A. A., Silva, L. F. C. A., and Sales, P. R. H., "Coordinating the energy generation of the brazilian national hydrothermal electrical generating system," *Interfaces*, vol. 16, no. 1, pp. pp. 16–38, 1986.

[39] Van Slyke, R. and Wets, R., "L-shaped linear programs with applications to optimal control and stochastic programming," *SIAM Journal on Applied Mathematics*, vol. 17, no. 4, pp. 638–663, 1969.

[40] Walkup, D. W. and Wets, R. J.-B., "Stochastic programs with recourse," *SIAM Journal on Applied Mathematics*, vol. 15, no. 5, pp. pp. 1299–1314, 1967.

[41] Walkup, D. W. and Wets, R. J.-B., "Stochastic programs with recourse ii: On the continuity of the objective," *SIAM Journal on Applied Mathematics*, vol. 17, no. 1, pp. pp. 98–103, 1969.

[42] Wets, R. J. B., "Programming under uncertainty: The equivalent convex program," *SIAM Journal on Applied Mathematics*, vol. 14, no. 1, pp. pp. 89–105, 1966.